THREE DIMENSIONAL FINITE ELEMENT MODELING FOR THE LATERALLY LOADED PASSIVE PILE BEHAVIOR

A THESIS SUBMITTED TO
THE GRADUATE SCHOOL OF NATURAL AND APPLIED SCIENCES
OF
MIDDLE EAST TECHNICAL UNIVERSITY

BY

ANIL EKİCİ

IN PARTIAL FULFILLMENT OF THE REQUIREMENTS
FOR
THE DEGREE OF THE MASTER OF SCIENCE
IN
CIVIL ENGINEERING

JUNE 2013

Approval of the thesis:

THREE DIMENSIONAL FINITE ELEMENT MODELING FOR THE LATERALLY LOADED PASSIVE PILE BEHAVIOR

submitted by **ANIL EKİCİ** in partial fulfillment of the requirements for the degree of **Master of Science in Civil Engineering Department, Middle East Technical University** by,

Prof.Dr. Canan Özgen
Dean, Gradute School of **Natural and Applied Sciences** ____________

Prof.Dr. Ahmet Cevdet Yalçıner
Head of Department, **Civil Engineering** ____________

Asst. Prof. Dr. Nejan Huvaj Sarıhan
Supervisor, **Civil Engineering Dept., METU** ____________

Examining Committee Members:

Prof. Dr. Ufuk Ergun
Civil Engineering Dept., METU ____________

Asst. Prof. Dr. Nejan Huvaj Sarıhan
Civil Engineering Dept., METU ____________

Prof. Dr. Sadık Bakır
Civil Engineering Dept., METU ____________

Inst. Dr. Onur Pekcan
Civil Engineering Dept., METU ____________

Dr. Özgür Kuruoğlu
Civil Engineer, Yüksel Proje ____________

Date: 11.06.2013

I hereby declare that all information in this document has been obtained and presented in accordance with academic rules and ethical conduct. I also declare that, as required by these rules and conduct, I have fully cited and referenced all material and results that are not original to this work.

Name, Last name	: Anıl, EKİCİ
Signature	:

ABSTRACT

THREE DIMENSIONAL FINITE ELEMENT MODELING FOR THE LATERALLY LOADED PASSIVE PILE BEHAVIOR

Ekici, Anıl
M.Sc., Department of Civil Engineering
Supervisor: Asst. Prof. Dr. Nejan Huvaj Sarıhan

June 2013, 116 pages

In this study, some of the factors affecting the slope stabilizing pile response have been investigated by means of three dimensional finite element solution using PLAXIS 3D software. Three full scaled field experiments were modeled for the verification of the proposed 3D models. It was concluded that PLAXIS 3D can successfully predict the measured pile deflection and force distributions. Afterwards, a parametric study was carried out. Two series of analyses (i) studying the effect of the pile embedment depth and (ii) studying the effect of pile spacing were performed. Some of the conclusions of this study are: (1) There is a critical pile embedment depth necessary to provide sufficient pile resistance, and this depth depends on unstable soil properties and strength ratio of stable soil to unstable soil. (2) As piles get closer (smaller s/d), load on each pile decreases and soil arching increases (i.e. less flowing of the soil between the piles). So there is an optimum pile spacing by considering soil arching and group reduction phenomena. (3) For sandy soils, effect of soil arching significantly decreases for pile spacing ratios (s/d) larger than 6. Piles in group start to behave like individual piles approximately at s/d=8. Stronger soil arching develops at pile spacing ratios (s/d) between 2 and 4. (4) Significant group reduction develops when piles are closely spaced. Approximately 30% reduction was observed in lateral loads exerted to piles in group for s/d=2. Therefore, s/d=4 was seen to be more optimum value for an effective pile design.

Keywords: Passive piles, slope stabilization, soil arching, group reduction, finite element method, PLAXIS 3D

ÖZ

ÜÇ BOYUTLU SONLU ELEMANLAR YÖNTEMİYLE YANAL YÜKLÜ PASİF KAZIK DAVRANIŞININ MODELLENMESİ

Ekici Anıl
Yüksek Lisans, İnşaat Mühendisliği Bölümü
Tez Yöneticisi: Yard. Doç. Dr. Nejan Huvaj Sarıhan

Haziran 2013, 116 sayfa

Bu çalışmada, heyelan kazığı davranışını etkileyen faktörlerden bazıları PLAXIS 3D yazılımı kullanılarak üç boyutlu sonlu elemanlar yöntemiyle incelenmiştir. Önerilen 3D modellerin doğruluğu üç tam ölçekli saha deneyi modellenmesiyle kontrol edilmiştir. Sonuç olarak PLAXIS 3D'nin ölçülmüş kazık deplasman ve yük dağılımlarını başarılı bir şekilde tahmin edebildiği görülmüştür. Sonrasında parametrik bir çalışma gerçekleştirilmiştir. (i) kazık gömme derinliğinin ve (ii) kazıklar arası mesafe etkilerinin çalışılması amacıyla 2 seri analiz yürütülmüştür. Bu çalışmanın sonuçlarının bazıları: (1) Kazığın uç kısmının hareketsizliğini sağlamak için gerekli kritik bir kazık gömme derinliği vardır ve bu derinlik hareketli zemin özellikleri ile hareketli ve hareketsiz zemin mukavemetlerinin oranına bağlıdır. (2) Kazıklar birbirine yaklaştıkça (daha küçük s/d) kazıklara etki eden yük azalmakta ve zemin kemerlenmesi artmaktadır (zeminin kazıkların arasından daha az akması). Bu sebeple zemin kemerlenmesi ve grup etkisi azalımı açısından optimum bir kazıklar arası mesafe vardır. (3) Kumlu zeminler için, zemin kemerlenmesi 6'dan büyük kazık mesafe oranları (s/d) için önemli ölçüde azalmaktadır. Gruptaki kazıklar yaklaşık olarak s/d=8 kazık mesafe oranından sonra tekil kazık olarak hareket etmeye başlamaktadır. 2 ve 4 kazık mesafe oranları (s/d) arasında güçlü zemin kemerlenmesi meydana gelmektedir. (4) Kazıklar sık aralıklarla yerleştirildiğinde önemli ölçüde grup etkisi oluşmaktadır. s/d=2 için gruptaki kazıklara gelen yanal yüklerde yaklaşık olarak %30 azalım görülmüştür. Bu sebeple s/d=4 kazık mesafe oranının etkili bir kazık tasarımı için daha optimum bir değer olduğu gözlenmiştir.

Anahtar Kelimeler: Pasif kazıklar, şev stabilizasyonu, zemin kemerlenmesi, grup etkisi azalımı, sonlu elemanlar yöntemi, PLAXIS 3D

To My Family

ACKNOWLEDGMENTS

I would like to express my deepest gratitude to my advisor, Asst. Prof. Dr. Nejan Huvaj Sarıhan for her invaluable supervision and continuous support in every stage of this study. Her sincere friendship and belief in me always gave encouragement and motivation throughout this research. I am extremely grateful for the opportunity to work with her.

I would also like to thank Prof. Dr. Ufuk Ergun for his comments and guidance throughout this study. I am grateful to him for sharing his invaluable experience in every stage.

I would like to thank my all but especially in geotechnical engineering division instructors in METU. I learned all from them throughout my undergraduate and graduate study.

I would like to express my special gratitude to my parents; my mother Nalan Ekici and my father Aygün Ekici for their continuous support and encouragement. I am grateful for their understanding and patience in every level of my research.

Finally, I would like to thank my close friends who endured me and gave courage especially in difficult times. Their continuous support and friendship are deeply appreciated.

TABLE OF CONTENTS

LIST OF TABLES

TABLES

LIST OF FIGURES

FIGURES

CHAPTER 1

INTRODUCTION

Landslide is a worldwide natural hazard which frequently causes loss of life and significant damages to buildings and lifelines. A landslide can be considered as the movement of an unstable soil layer above a stationary layer due to the gravitational and other forces. There are many stabilization methods for slopes that are moving. These can be categorized into reducing the driving forces and increasing the resisting forces of the slope. Flattening of the slope, reducing the weight of the unstable soil by excavation are some examples of ways to reduce the driving forces. To increase the resisting forces, soil nailing, stone columns, bio-chemical ground improvement and other methods are available. Use of passive piles in slope stabilization has become extremely popular among all these remedial measures in the last decades (Figure 1.1). Estimation of the lateral loads coming from the sliding of unstable soil, resultant stresses and bending moments developed in the pile shaft are crucial for an economical and safe design. There are numerous factors and parameters that affect the response of piles under lateral soil movements. There exist some studies in the literature that looks into this topic however three dimensional finite element methodology is not widely used. In this study, some of the factors that govern the passive pile behavior in response to ground movements are investigated by three dimensional finite element approach.

Figure 1.1 Lanslide stabilization with passive piles for a freeway in Tokat

1.1 Problem Statement

Passive pile usage for potential landslides is one of the most common slope stabilization methods in geotechnical engineering practice. Numerous successful applications have been reported by several researchers (De Beer and Wallays 1972, Esu and D’Elia 1974, Sommer 1977, Kalteziotis 1993). There are also unsuccessful cases that structural failure has been reported (Fukuoka 1977, Finno et al. 1991). Although there have been attempts for the establishment of a general calculation procedure (Ito Matsui and Hong 1981, 1982, Chen and Poulos 1997, Nalcakan 1999, Ergun 2000, Kourkoulis 2012 etc.), there is a lack of comprehensive and widespread design guideline in this topic. Because the interaction between the passive piles and soil is quite a complex mechanism, it involves significant number of variables in the nature of the problem. Pile spacing, pile embedment depth, pile rigidity, strength properties of unstable and stable soils, pile head fixity conditions, location of the piles in the slope are some of them. Investigation of these factors and revealing the interrelation between them has a vital importance for the understanding of the actual pile behavior.

1.2 Research Objectives

The main objective of this study is to investigate the slope stabilizing passive piles and their behavior by using three dimensional finite element method. Other objectives are:

(1) Determination of the geometrical and boundary constraints for three dimensional finite element modeling (such as the size of the finite element model, boundary conditions, and finite element mesh properties) of passive pile response.

(2) Verification of the accuracy of three dimensional finite element model used and investigation of compatibility with the full scale field tests.

(3) Investigation of the required pile embedment depth and interrelation of this with the unstable soil properties and strength ratios between unstable and stable soil layers.

(4) Determination of the optimum pile spacing by considering two of the most important factors of slope stabilizing pile design (i) soil arching and (ii) group reduction phenomena.

In order to better understand the relationships between the factors, several of them are aimed to be revealed for the purpose of understanding the actual mechanism. Findings in this study can be useful for developing a better understanding of the passive pile behavior in moving soils and for developing a practical design procedure of slope stabilizing piles.

1.3 Scope

This study investigates the laterally loaded passive pile behavior by using three dimensional finite element software Plaxis 3D 2010. A literature review is presented in Chapter 2. In the scope of this research, three dimensional shear box models have been developed to be able to control the number of variables for the simulation of actual pile response. In Chapter 3, the geometry and boundary conditions of the 3D finite element model of passive piles were studied. A number of case studies have been analyzed to verify the accuracy of the proposed models (Chapter 4). Afterwards, in Chapter 5, a parametric study is carried out to investigate the factors affecting the passive pile behavior.

CHAPTER 2

LITERATURE REVIEW

Use of slope stabilizing piles has become extremely popular for several decades in various kinds of projects worldwide (Figure 2.1 and Figure 2.2). Piles are designed to withstand the vertical and lateral loads in geotechnical engineering projects. Lateral load carrying capacity is one of the most important functions of the pile as a retaining structure. As Vesic (1975) indicated; laterally loaded piles can be considered in two different groups according to their behavior. Piles can be loaded laterally at some point of their shaft or, most probably, at the pile head. These loads are transmitted to the soil by the pile and consequently horizontal soil deformations develop. These types of piles are called *active piles*. On the other hand, piles can be loaded laterally throughout their shaft because of the horizontal movement of the surrounding soil. These types of piles are called *passive piles* (Figure 2.3). In a landslide, lateral movement of the soil is tried to be prevented by the resistance of a row, or multiple rows of piles. Therefore, slope stabilizing piles are called as passive piles.

Figure 2.1 a) Landslide stabilization with reinforced concrete piles in Güzelyalı, Bursa

Figure 2.2 b) Landslide stabilization with reinforced concrete piles in Güzelyalı, Bursa

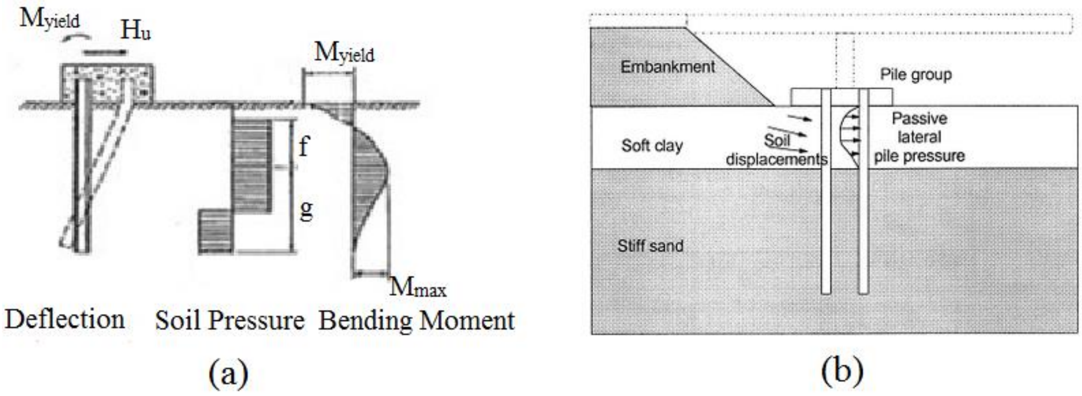

Figure 2.3 a) Illustration for active loading of piles (Broms 1964) b) Illustration for passive loading of piles under an embankment construction (Bransby and Springman 1994)

An example of a landslide movement, as measured by inclinometers, can be seen in Figure 2.4 for one of the most widely referenced, slow-moving landslide cases in literature, San Martino landslide in Italy (Bertini 1984). The slope is composed of a colluvial layer (about 20 m thick) which overlies a weathered marine marly clay bedrock, which in turn overlies the unweathered marly clay bedrock. In this landslide, as in many other landslides, a uniform movement with depth is observed indicating that the material moved approximately as a rigid body without having much internal shear deformations. The movements of the slope have been related to the water level fluctuations, for example, high water level in March 1981 resulted in a higher displacement rate, and low water level in September 1980 showed almost unnoticeable movements (Bertini et al. 1984).

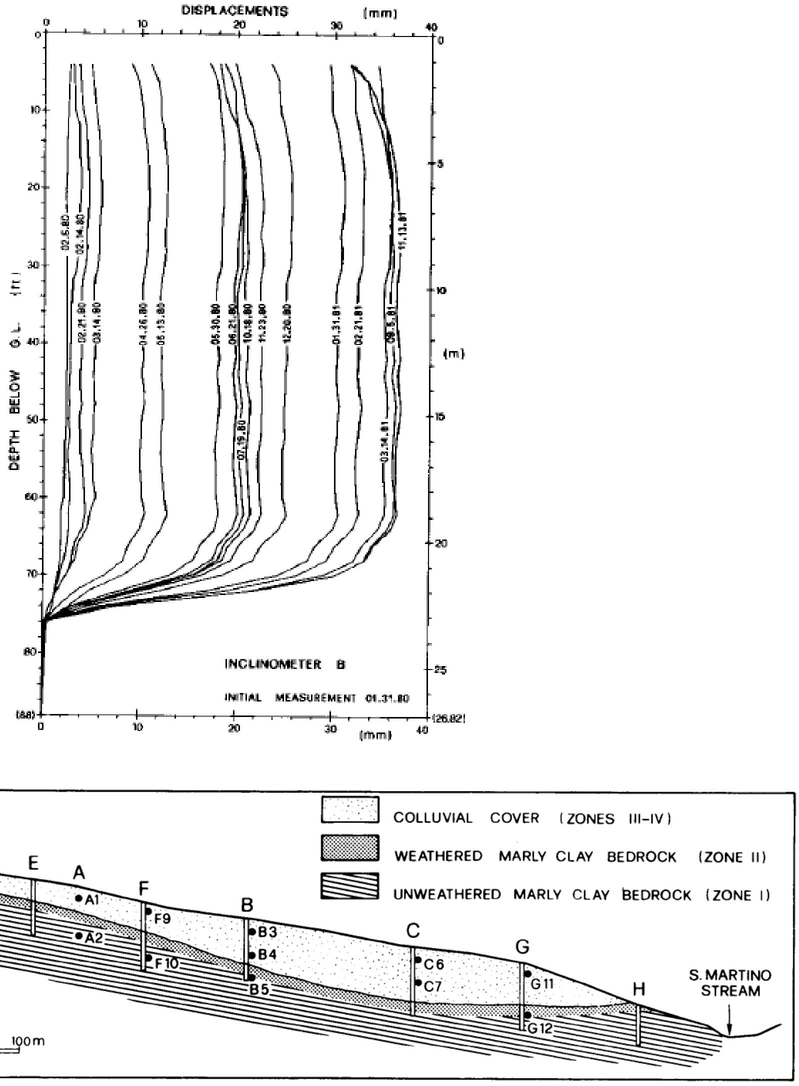

Figure 2.4 Displacements measured by inclinometers at the San Martino landslide (Bertini et al. 1984)

The landslides for which slope stabilization can be realistically considered as a solution are the "slow" to "extremely slow"-moving landslides with typical rate of movements given as in the table below:

Table 2.1 Velocity Classification (Cruden and Varnes 1996)

Velocity Class	Velocity Description	Typical Velocity Limits	in mm/day
7	Extremely rapid	> 5 m/s	$> 4.3\times10^{8}$
6	Very rapid	3 m/min – 5 m/s	$4.3\times10^{6} – 4.3\times10^{8}$
5	Rapid	1.8 m/hr – 3 m/min	$4.3\times10^{4} – 4.3\times10^{6}$
4	Moderate	13 m/mo – 1.8 m/hr	$433 – 4.3\times10^{4}$
3	Slow	1.6 m/yr – 13 m/mo	4 – 433
2	Very slow	16 mm/yr – 1.6 m/yr	$4.4\times10^{-2} – 4$
1	Extremely slow	< 16 mm/yr	$< 4.4\times10^{-2}$

Slope stabilization by using passive piles is one of the most common and practical remedial solution to an unstable slope. Passive piles are generally used for relatively slow movement of an unstable layer above a sliding plane in geotechnical engineering practice. Even though passive pile use in slopes has become increasingly popular, well established and widely accepted design procedure has not yet been developed. This can be caused by the variety of the number of factors affecting the problem. For a reasonable engineering design, accurate estimation of lateral loads coming to a passive pile row from deforming ground has a vital importance. Therefore, significant number of studies has been made for this purpose by several researchers (Broms 1964, Ito and Matsui 1975, Ingold 1977, Fukuoka 1977, Viggiani 1981). Research on laterally loaded passive piles can be divided into two categories as theoretical and experimental studies.

2.1 Theoretical Studies

As De Beer (1977) indicated, the theoretical studies can be classified as (1) modulus of subgrade reaction method considering the pile as an elastic beam on a foundation, (2) elastic continuum methods assuming the soil to be a linear elastic or elastic-plastic material, (3) finite element methods simulating the stress-strain behavior of soil with multilinear or hyperbolic approximations and some other empirical methods.

2.1.1 Modulus of Subgrade Reaction Method

Hetenyi (1946) assumed piles as beams on an elastic foundation and soil reaction represented by Winkler springs. Equation 2.1 was proposed by Hetenyi (1946) for the solution of loaded piles in soils as long as both pile and soil stays in elastic limits (Oztürk 2009).

$$\frac{d^2M}{dz^2} + Q\frac{d^2y}{dz^2} - p = 0 \tag{2.1}$$

Where;

M: Bending moment

Q: Axial load on the pile

z: Depth along the pile

y: Lateral deflection of pile at point z

p: Lateral resistance of soil per unit length of pile

In case of slope stabilizing laterally loaded passive piles, axial loading on pile (Q), can be ignored and Equation 2.1 can be transformed into the following equation with some modifications as:

$$E_P I\frac{d^4y_p}{dz^4} = K_S(y_p - y_s) \tag{2.2}$$

Where;

E_p: Deformation modulus of pile

I: Moment of inertia of pile

y_p: Lateral displacement of the pile at depth z

y_s: Lateral displacement of the soil at depth z if no pile was placed in the slope

K_s: Subgrade reaction modulus of soil

In Equation 2.2, subgrade reaction modulus, (K_s) is variable with depth and relative displacement (y_p-y_s). De Beer (1977) indicated that there may be uncertainties of the solution of Equation 2.2 because of the difficulties of determining lateral displacement of the soil if no pile exists in the slope, (y_s).

Fukuoka (1977) studied lateral resistance of passive piles subjected to creep type of soil movement. Subgrade reaction methodology was used to estimate pile response against laterally moving slope. Unbalanced force and resistance force values were evaluated as a function of the inclination of the slope and displacement velocity of the soil mass. For this reason, careful monitoring of moving slopes was recommended by Fukuoka (1977). Especially for soils where ground water level fluctuations may occur, determination of the relationship between displacement velocity and these fluctuations could be essential.

Poulos and Davis (1980) investigated the subgrade reaction modulus of soils and its variability with depth. Solutions of the Equation 2.2 were developed by considering the subgrade reaction modulus constant or properly distributed with depth for different pile head fixity conditions and pile rigidities.

Viggiani (1981) studied lateral loads on piles due to the moving cohesive soil by using subgrade reaction theory. In his approach, rectangular stress distribution through the pile shaft was assumed instead of trapezoidal stress distribution. Possible failure mechanisms that a pile can undergo were investigated for the calculation of total lateral force applied to the pile. Yield soil pressure on piles due to the moving cohesive soils in undrained condition was predicted by the equation similar to other researchers (Brinch Hansen, 1961; Broms, 1964) as

$$\mathrm{p} = \mathrm{k}.\,c_u.\,\mathrm{d} \tag{2.3}$$

Where;

p: Yield soil pressure along the pile

c_u: Undrained shear strength

d: Pile diameter

k :Bearing capacity factor

Several researchers (Brinch Hansen 1961, Broms 1964, De Beer 1977, Ito and Matsui 1975) proposed different ranges of bearing capacity factor for cohesive soils. It was suggested that k values should be different for piles in non-displaced soil (active pile) and piles in moving soil (passive pile). Besides, k values should also be different above and below the slip surface. It is well known that most of the time, soil movement stops before ultimate pile capacities are not reached (Ergun 2000). Therefore selection of appropriate bearing capacity factor has vital importance when using this equation, because calculated pressures are ultimate soil pressures at failure condition.

Ingold (1977) used modulus of subgrade reaction method for a theoretical example of one row steel pipe pile in a sliding ground. In his solution, pile deflection, shear force and bending moment distributions through the pile length were estimated. Calculations of these parameters for different pile head fixity conditions (free, unrotated, hinged and fixed) were studied. Safety factors against bending moment and shear force failure were determined. It was concluded that as pile head becomes more rigid, safety factor of pile against failure is increased. Therefore, Ingold (1977) emphasized the importance of preventing the deflection of the pile head for the effective usage of piles for slope stabilization.

Magueri and Motta (1992) investigated the variation of subgrade reaction modulus of soils. They proposed a non-linear hyperbolic function for the estimation of the lateral load on passive piles. Subgrade reaction modulus depends on the relative pile soil displacement and initial value of the subgrade reaction modulus.

2.1.2 Elastic Continuum Methods

Oteo (1977) applied the methodology of Begemaan and De Leeuw (1972) for the estimation of soil pressures and bending moments on passive piles. In this method, piles are exposed to soil pressure because of the surcharge load at the surface. Horizontal pressures are obtained by considering the effect of the relative flexibility of the pile which is reasonable to adapt because Oteo (1977) specified that stiff piles may have a restrictive field of application. Soil was considered as linearly elastic material in his analyses. It was concluded that if the pile is stiff, maximum pressure methods can be applied; however if the pile is flexible, methods using the pile-soil interaction is needed.

Poulos (1973) proposed a calculation method to obtain horizontal pressure and displacements affecting a pile-soil system. Soil was considered to be an elastic-plastic material. In this approach, pile displacements were calculated from the bending equation of a thin strip and soil displacements were evaluated from the Mindlin (1936) equation for horizontal displacements caused by horizontal loads within a semi-infinite mass (Nalcakan 1999).

Banerjee and Davies (1978) used point load solution for the calculation of displacement and bending moment distributions of single pile in both homogenous and non-homogeneous soils. Linearly increasing soil deformation modulus was introduced in the analyses. As a result of analyses, higher bending moments in non-homogenous soils were calculated than those predicted for homogenous soils for both free and fixed head piles.

2.1.3 Finite Element Method

Concept of slope stabilization by using passive piles has been investigated by researchers for a long period of time. However, considerable number of variables in the problem made it difficult and complex to analyze the factors affecting the real pile-soil interaction. In this manner, numerical studies and finite element approaches were developed and applied to this concept to understand the phenomena more accurately (Rowe and Poulos 1979, Chen and Poulos 1993, 1997). Especially for the last three decades, advances in computer programs made it possible to evaluate complex geometries and multilayered soil strata. Two and three dimensional finite element modeling of the problem has been recently used by several researchers (Chow 1996, Pan et al. 2002, Kahyaoglu et al. 2007, Liang and Yamin 2009**,** Kourkoulis et al. 2011, 2012) to capture actual pile-soil interaction behavior and to propose a feasible design guideline. Accuracy and relatively short calculation time make numerical methods through softwares an inevitable part of the future of this study.

Rowe and Poulos (1979) used two dimensional (2D) finite element technique to evaluate undrained soil behavior of slopes reinforced by multi-row pile groups. Effect of piles on the deformation and stability of slope investigated for different pile head fixity and pile stiffness conditions. It was concluded that very stiff piles should be used in slopes to get a considerable effect on slope stability. Increase in pile stiffness, restraints at the top and tip of the pile enhance the efficiency of the pile. In addition, pile arrangement and soil profile has a significant effect on pile-soil interaction behavior.

Chen and Poulos (1993) studied passive pile behavior by using finite element methods. In two dimensional (2D) analyses, group reductions in pile capacities were observed and compared with single pile results.

Chow (1996) suggested a numerical solution which piles were modeled with beam elements, soil was modeled using subgrade reaction modulus and pile soil interaction was considered according to the theory of elasticity. Chow (1996) compared his proposed solution with two field cases: Esu and D'Elia (1974) and Kalteziotis et. al (1993); one of these cases is for single pile and the other is for pile groups. Pile deflections, pile rotations, bending moment and shear force distributions throughout pile length were evaluated in this study. It was concluded that results show significantly good agreement with the measured values.

Pan et al. (2002) used three dimensional (3D) finite element analysis program ABAQUS to investigate the behavior of single pile subjected to lateral soil movement. In analyses, pile was assumed as linearly elastic material. Von Mises constitutive model was used to simulate non-linear stress-strain behavior of moving soil. Pile was modeled as width of 1 m square cross section and 15 m length. Undrained behavior of cohesive soil was considered in all analyses. Normalized p-y curves and variations of ultimate soil pressures with depth were evaluated for stiff and flexible piles. Consequently, maximum ultimate soil pressures for stiff piles were computed as $10s_u$ and for flexible pile as $10.8s_u$; where s_u is undrained shear strength of moving soil. It was emphasized that these values agrees well with the literature.

Kahyaoglu et al. (2009) used three dimensional (3D) finite element analysis program PLAXIS 3D Foundation to investigate single pile and group of free head pile behavior in horizontally deforming soils. Laboratory setup that Poulos et al. (1995) used was modeled three dimensionally and it was concluded that bending moment distributions show pretty good agreement with the measured values. In addition, a parametric study was conducted to investigate the effect of pile spacing and internal friction angle of cohesionless materials in soil arching. It was concluded that when the soil movement reaches a certain value of 1.2 times pile diameter (1.2d) in cohesionless soils, soil arching fully develops. In addition, no arching effect was observed for pile spacing larger than 8d.

Kelesoglu and Cinicioglu (2009) proposed a methodology to find soil stiffness degradation in soft soils for laterally loaded passive piles beneath an embankment. Authors emphasize that because stresses are calculated from the free field deformation values, nonlinearity and inhomogeneity of the soil behavior can be captured with this analysis procedure. Three dimensional (3D) modeling of a case study was performed for the verification of the proposed methodology by using PLAXIS 3D Foundation software.

Liang and Zeng (2002) performed a numerical study for the investigation of soil arching development in drilled shaft systems. Effect of pile spacing, pile diameter, pile shape, internal friction angle of cohesionless soils and cohesion value of clayey materials on soil arching were studied by finite element simulations. It was concluded that most important factor affecting the soil arching is pile spacing variation. In addition, cohesionless soils having higher friction angles are more likely to build stronger soil arching. Authors emphasize that parametric analysis results significantly matched with the experimental results.

Liang and Yamin (2009) constructed three dimensional (3D) models using finite element analysis program ABAQUS for the investigation of soil arching in drilled shafts socketed into a stable stratum. Soil arching was evaluated with a defined dimensionless load transfer factor, (η)

$$\eta = \frac{F'}{F} \tag{2.4}$$

In Equation 2.4, F' is total force acting on the vertical plane at the interface between the drilled shaft and the soil just on the downslope side, where F is total force acting on upslope side. Illustration of the calculation of dimensionless load transfer factor was presented in Figure 2.5. Results of parametric analyses conclude that in the case of passive piles, when piles are socketed in a stable layer for a sufficient depth, s/d=2-4 pile spacing provides significant improvement in factor of safety of the slope.

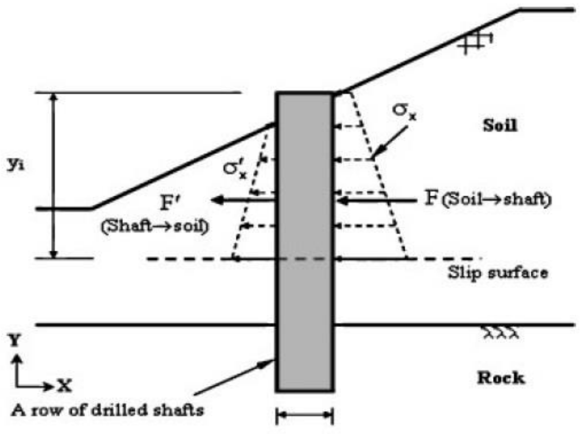

Figure 2.5 Estimation of load transfer factor from geometric model (Liang and Yamin 2009)

Kourkoulis et al. (2011, 2012) proposed a hybrid method for the design of piles used for slope stabilization. Method consists of mainly two steps. First step includes traditional slope stability analyses. To increase the safety factor of the slope to a desired value, additional resisting lateral force to be provided by piles is calculated. In the second step, pile configurations are estimated by 3D FEM modeling for a prescribed deformation level. Optimum pile design that gives the required resisting force is determined by this way. Kourkoulis et al. (2011, 2012) performed parametric model studies to verify the feasibility of their methodology (Figure 2.6). Prescribed displacements were assumed as uniformly distributed in the unstable sliding mass. Pile influence distance is accepted as 5d (5 times of pile diameter) and the geometry of the finite element model is constructed this way to save some calculation time. Both cohesive and granular soils were modeled as unstable layer with a sliding height (H_u) varying within 4 to 12 m. Besides, influence of pile spacing on soil arching, pile embedment depth into stable layer and stiffness of the stable layer effects were also studied.

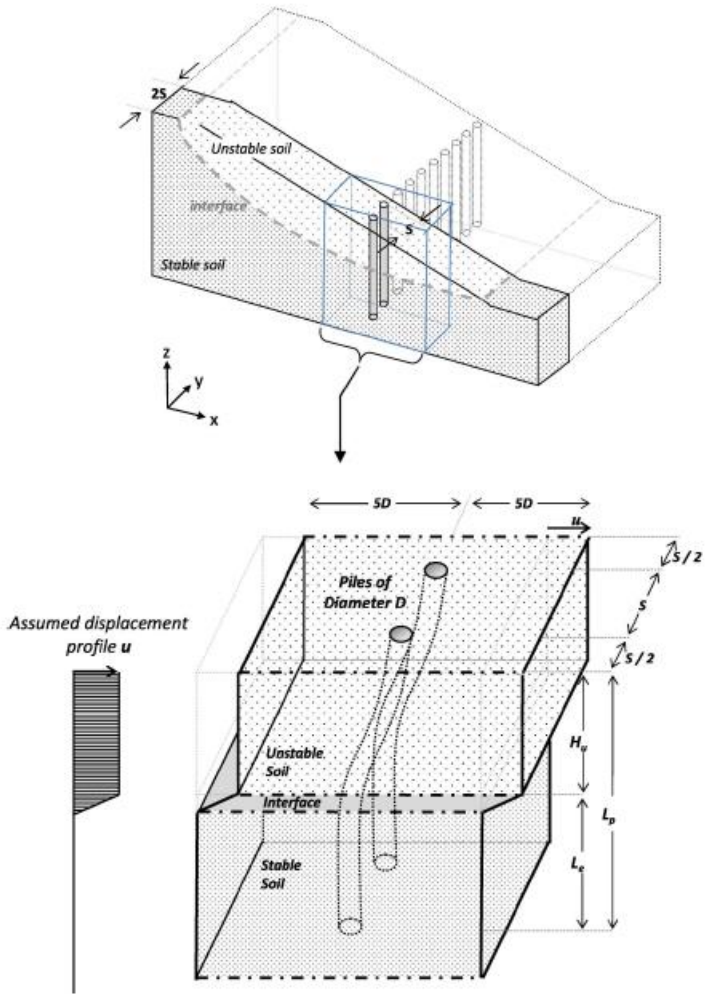

Figure 2.6 (a) Illustration of the slope where the focus of the model was defined (b) 3D geometric figure of the simplified decoupled model (Kourkoulis et al. 2012)

In simplified geometric models, design charts were generated for different pile spacing ratios. Relations between resisting force with pile deflection and bending moment were evaluated in these charts. Kourkoulis et al. (2011, 2012) suggested that different design charts could be formed for different pile configuration and soil profile at any depth. After several analyses, it was concluded that most economical and optimum pile spacing that cause to produce soil arching in the ground is s/d=4. Piles began to behave like single pile for spacings larger than 4d. Moreover, field cases and comparison with theoretical solutions were studied. According to authors, predictions of the soil and pile displacements as well as pile lateral loads are quite satisfactory. Consequently, method provides effective design tool for slope stabilizing piles. However, full bonding between the pile and the soil has been assumed in 3D FEM models. Therefore, method may not give accurate results in surfaces which are smooth in respect of pile-soil interaction.

Dao (2011) studied validation of the recently developed “embedded pile” option in Plaxis 3D software for lateral loading. In this study, detailed comparison between modeling of the embedded pile (as a beam element) and modeling of mass volume pile was made for piles located near the toe of an embankment. It was concluded that embedded pile option in Plaxis 3D is a good tool to model actual laterally loaded pile behavior. However, Dao (2011) emphasized that modeling smooth surfaces may not give desirable results because embedded pile option does not consider relative pile soil displacement in lateral direction.

2.1.4 Other Studies

Chen and Poulos (1997) used boundary element method to evaluate vertical pile response subjected to lateral soil movements. Both pile and soil were assumed to behave elastically in the analyses. They emphasized the importance of accurate determination of limiting pile soil pressure. For this purpose, dimensionless group factor, f_p was defined as;

$$f_p = \frac{p_{ui}}{p_{us}} \tag{2.5}$$

Where, p_{ui} is limiting soil pressure in pile in a group and p_{us} is limiting soil pressure in isolated single pile. Dimensionless group factors were listed for several pile configurations and pile spacing. Moreover, design charts were formed for uniform and linearly increasing soil stiffness properties, uniform and linearly decreasing lateral soil movements. Maximum bending moment of pile groups were evaluated in these design charts according to the different relative pile stiffness values. The design chart method was compared with reported field case results. It was concluded that design charts generally give overestimation of maximum bending moments and pile head deflections. However, method gives more convenient results with the decrease of lateral soil movement. Authors pointed out that proposed design chart methodology could be useful for preliminary design especially if there is a lack of detailed site information.

Ito and Matsui (1975) developed a theory to estimate lateral loads on passive piles in plastically deforming ground. According to Ito and Matsui (1975) two possible plastic states can occur in the soil around the piles. One of them assumes plastic deformation of soil satisfying Mohr-Coulomb yield criterion. The other one treats the surrounding ground as a visco-plastic solid (plastic flow mechanism) which is applicable for mud type of soil layers. In theory of plastic deformation, lateral load on a pile row was estimated in plain strain analysis (plain strain condition is in the direction of depth) as shown in Figure 2.7.

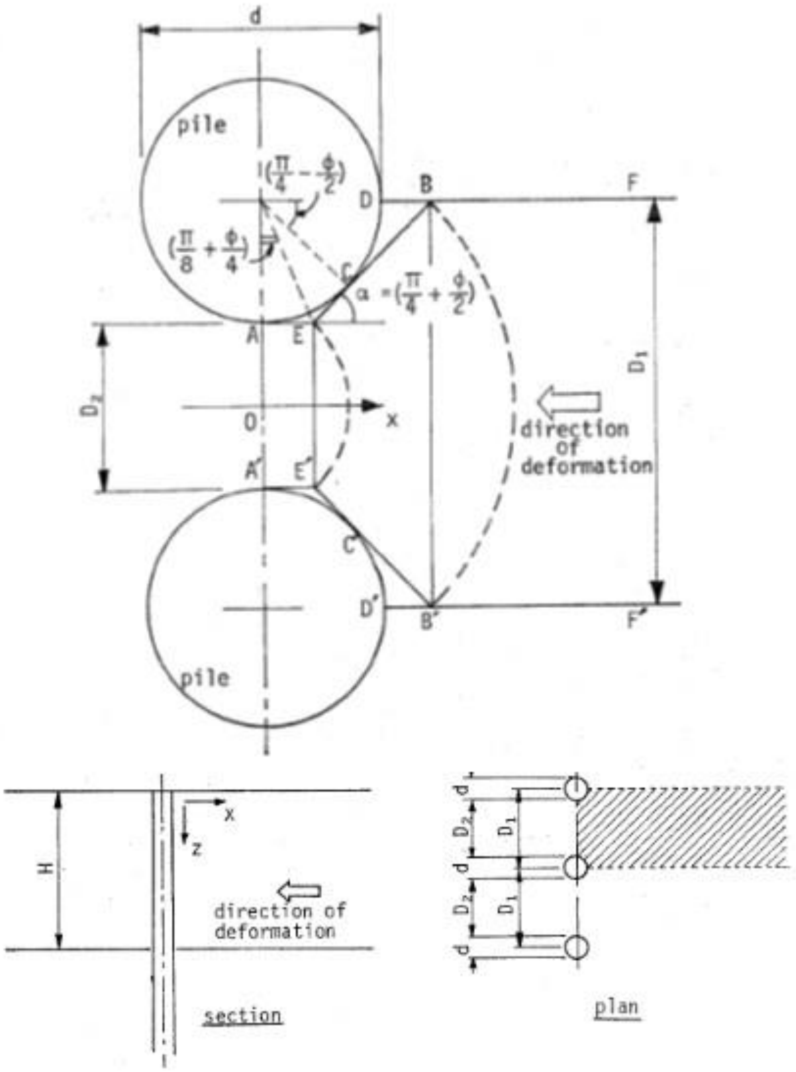

Figure 2.7 Plastic deformation of soil squeezed between two piles in a row
(Ito and Matsui 1975)

Ito and Matsui (1975) assumed that no reduction in the shear resistance occur along the sliding surface caused by moving soil which means that only the soil around the piles undergoes to plastic state. Therefore, lateral load predictions on piles were made by ignoring the state of equilibrium changes in moving slope. Besides, piles are accepted as rigid piles. According to these assumptions, they developed an equation calculating the lateral load on piles in plastically deforming ground. Lateral pressure distribution in unstable layer along the pile length is trapezoidal shape. Ito and Matsui (1975) emphasized that comparison between load estimations from established theory and field measurements show satisfactory resemblance.

Broms (1964) proposed empirical equations for the estimation of ultimate soil pressure acting on piles. Soil pressure and bending moment distributions for short, intermediate and long piles in both cohesive and cohesionless soils were determined according to free and restrained head fixity conditions (Figure 2.8 and Figure 2.9). As pile length changes failure mechanism of the pile also changes and this will affect the pressure and bending moment distributions. According to Broms (1964), there is no soil pressure from the ground surface to a depth of 1.5 times of pile diameter in cohesive soils. Below this level, soil exerts a pressure equal to 9 times of undrained shear strength of cohesive soil ($9c_u$). In cohesionless case, soil exerts a pressure equal to 3 times of Passive Rankine Earth Pressure at all depths.

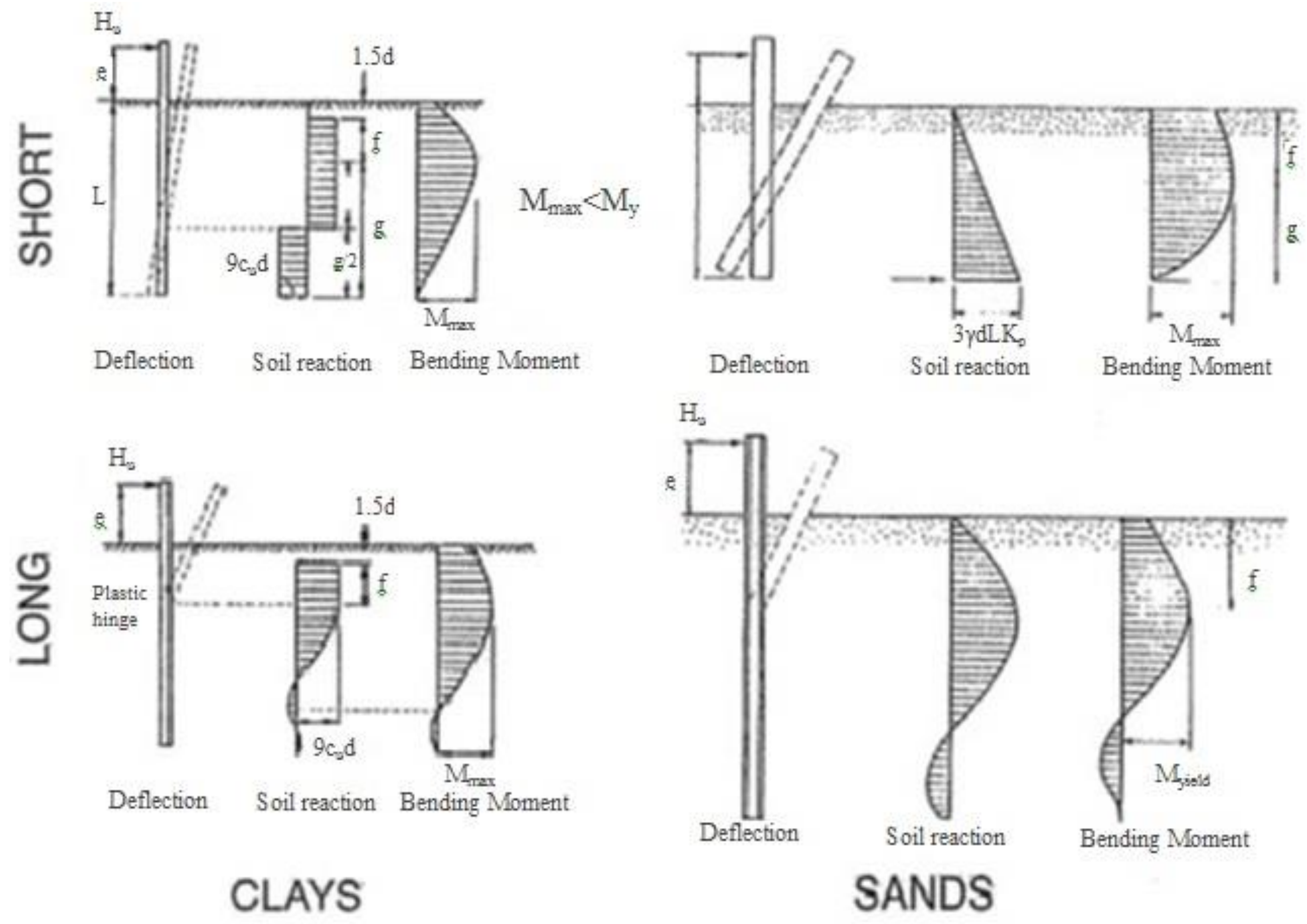

Figure 2.8 Ultimate lateral capacities of free head piles (Broms 1964)

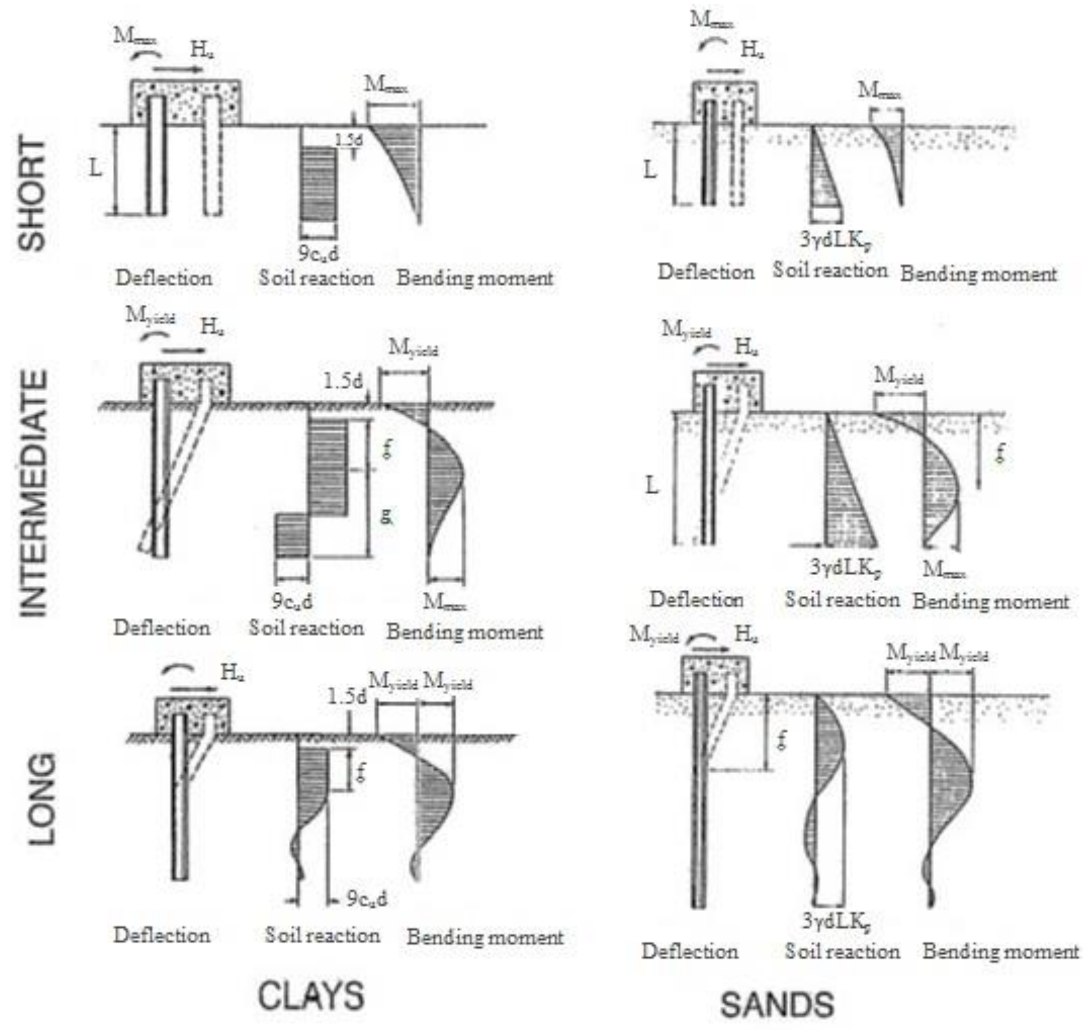

Figure 2.9 Ultimate lateral capacities of fixed head piles (Broms 1964)

Wang and Yen (1974) developed a method to investigate soil arching in passive piles placed in infinitely long slopes. One row of rigid piles socketed into a stable stratum was used in the analyses. Optimum pile spacing that cause soil arching was tried to be determined at the potential failure condition of the slope.

Reese et al. (1992) proposed a method to estimate the stress and deformation distribution of a laterally loaded passive pile embedded in a firm stratum. In this approach, driving force of moving soil and resulting moment were considered to act on pile at the point of unstable to stable soil layer transition. After the estimation of total driving force and moment coming from horizontally deforming soil, these values were used for the calculation of load deformation curve of the pile.

2.2 Experimental Studies

Some experimental studies have been conducted to understand the actual behavior of laterally loaded single pile or pile groups. Not only these studies give ideas about complex behavior of soil and pile systems, but also they provide a reliable comparison tool for the development of theoretical approaches in this concept. Experimental studies can be grouped into two, such as laboratory model tests and in-situ field tests.

2.2.1 Laboratory Tests

Fukuoka (1977) explained the laboratory experiment made by Fukumoto (1975) to investigate the laterally loaded passive pile behavior in a model study. Soil was placed in a rectangular iron box and lateral load applied to the rectangular shape of model piles which was made of iron plates and cedar planks. As a result of the test, it was concluded that deformation profile of the pile is closely related with the flexural rigidity of the pile.

Ilyas et al. (2004) conducted series of centrifuge model tests to investigate laterally loaded pile group behavior in cohesive soils. Different pile groups (2x2, 2x3, 3x3, 4x4) interconnected with the pile head were studied. Scaled models were rotated about a vertical axis until exerted forces to the system reaches to gravitational forces. Test results were evaluated in terms of graphs of lateral load with pile head deflection and load deflection graph of individual piles in group. As an important outcome, authors emphasize that taking average performance of piles in a group may be inappropriate because results show that laterally loaded piles in a row do not show same behavior. Outer piles were observed to take significantly more loads and bending moments than inner piles in a row.

Dao (2011) explained the centrifuge model study performed by Stewart (1992) to investigate laterally loaded single pile and pile group behavior adjacent to an embankment construction. Model piles were inserted into soft clay layer underlined by dense sand. Bending moment measurements were obtained during the test from the measurements of strain gages. Bending moment increase was seen at the pile head and interface of soft clay to dense sand layer. It was concluded that centrifuge testing results show very good agreement with the actual field test results.

Dagistani (1992) and Kin (1993) studied on laterally loaded passive pile behavior in a shear box model. Shear box with 30x30 cm cross section, maximum depth of 60 cm and movable part of 15 cm were used in analyses. Pressure distribution on passive piles in cohesive soil was measured using miniature stress cells. Experiments were conducted for different pile penetration depths and soil consistencies.

Nalcakan (1999) conducted a laboratory experiment to investigate group action reduction in passive pile groups. Same shear box model with Dagistani (1992) and Kin (1993) was used in experiments. Two types of material were investigated in analyses as soft clay and stiff clay with undrained shear strength of 12 kPa and 85 kPa respectively. Model piles having 30 cm length and 1 cm diameter were inserted into the soil inside the shear box in a row. After the model was setup, shear box was loaded laterally with a constant shear rate of 0.37 mm/min. Nalcakan (1999) measured displacement of the shear box, total load applied to the shear box and the load on two selected piles in each test series for different pile spacings. In tests, pile spacing ratios ranged between s/d=15 (single pile) to s/d=2. Graphs of displacement ratio (lateral movement divided by pile diameter, %ε) with total load and displacement ratio with load per pile were presented. It was concluded that load on a single pile mainly depends on undrained shear strength of moving material. Load on a pile decreases as pile spacing decreases because group action reduction develops when piles are closely spaced. In addition, single pile load and group reduction also depend on the amount of displacement ratio (%ε). During initial stage of loading (low displacement ratios) lower values of group reduction was observed.

Ozturk (2009) investigated bending moment distributions of single and group of piles in cohesionless soil using model piles. Strain gages attached to the pile shafts were used to measure bending moments during the test. Maximum bending strain was observed approximately at the depth of 0.7L (L: Pile length) and maximum negative bending strain measured at the depth of 0.3L for both single pile and pile groups. It was concluded that even if the amount of loading change general behavior of the bending moment distribution remains same especially for single piles.

2.2.2 Field Tests

De Beer and Wallays (1972) reported a field test in Belgium to investigate embankment construction influence on adjacent pile foundations. For this purpose two different cases were studied. A steel pipe pile having 28 m length, 0.9 m diameter and 1.5 cm wall thickness was used in one of the cases. In the other case, 23.2 m length and 0.6 m diameter reinforced concrete pile was used. In both cases pile deflections, bending moments and lateral soil movements in the ground were measured. There is not much information about the properties of sliding soil however it was indicated that soil profile mainly consists of sandy materials.

Esu and D'Elia (1974) conducted a field case to investigate the behavior of slope stabilizing reinforced concrete pile. The test pile was 30 m in length, 0.79 m in diameter and had a flexural rigidity (E_pI_p) of 360 MNm^2. It was reported that depth of sliding soil is 7.5 m. Not much information was given about the soil properties of the ground except that it was considered to consist mainly from cohesive soils. Test pile was instrumented with pressure cells at the depth of 5 m, 10 m and 15 m along its shaft. Bending moment, shear force and pile deflection distributions of the pile were presented in the report.

Sommer (1977) reported a field investigation on a sliding slope under an embankment. 15 m depth of highly plastic preconsolidated clay movement with an inclination of 5°-8° stopped with 3 m diameter reinforced concrete piers embedding to stable layer into 5m (Figure 2.10). Earth pressure distributions on piles were recorded with pressure cells. It was observed that measured soil pressures were much smaller than the (only %30) design pressure which had been calculated according to the Brinch Hansen formula.

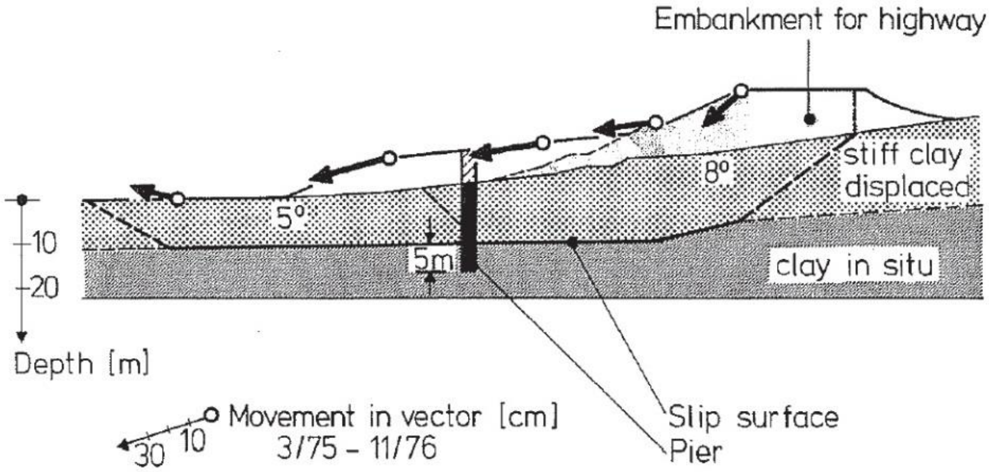

Figure 2.10 Cross section of the sliding slope (Sommer 1977)

Kalteziotis et al. (1993) reported a field case where cracks had appeared in the road pavement of a semi-bridge structure in Greece. Moving soil formation consists of mainly neogene lacustrine deposits. Sliding soil depth was reported as 4 m. Two rows of concrete piles having 1 m diameter and 12 m length with pile spacing of 2.5 m were used to stabilize this landslide. Two of the piles were replaced with steel pipe piles having the same flexural rigidity with the concrete piles. These steel piles were monitored by using strain gages and inclinometers. Bending moment, shear force, pile deflection and pile rotation distributions were presented according to these measurements.

As indicated before, concept of slope stabilization by using passive piles is a complex problem involving significant number of variables. In Table 2.2 and Table 2.3, some of these variables and affected properties by them are summarized for understanding the actual pile-soil interaction behavior in slope stabilization works.

Table 2.2 Summary table of the relationships between the variables related to geometry and boundary conditions and their effect

Affecting parameter	**Affected property**	**Conclusion**	**Reference**
Boundary sizes	Pile influence distance	Influence zone of each pile does not exceed 5 times of pile diameter, 5d. (d: Pile diameter)	Kourkoulis et al. (2011,2012), Reese and Van Impe (2001)
Material mesh generation	Lateral displacement, pile head deformation and calculation time	Finer mesh gives more displacement and bending moment. Deformations at pile head could differ up to %20 when mesh changes from very fine to very coarse. In addition, calculation time significantly increases from coarse mesh to finer mesh.	Dao (2011)
Differences between modeling in 2D and 3D	Factor of safety	Three dimensional models tend to estimate higher factors of safety values compared to two dimensional models.	Albataineh (2006), Gilson et al. (2008)

Table 2.3 Summary table of the relationships between the factors that affect the design of piles used in slope stabilization

Affecting parameter	Affected property	Conclusion	Reference
Factor of safety of moving slope	*Horizontal soil movements*	Horizontal soil deformations are much larger if the factor of safety (F) of slope is lower than 1.4. Deformations decrease substantially above this value.	Marche and Chapuis (1973), De Beer and Wallays (1972)
Pile spacing/pile diameter (s/d)	*Soil arching*	As piles are closely spaced, soil arching develops between the piles. In fact, most economical and optimum pile spacing can be chosen as s/d=4.	Kourkoulis et al. (2011)
		No arching effect is observed for pile spacing larger than 8d.	Liang and Zeng (2002), Kahyaoglu et al. (2009)
	Group action reduction	As pile spacing (s) decreases, piles in a group take less load compared to a single pile. Group action reduction develops.	Broms (1964), Nalcakan (1999), Pan et al. (2002)
		No significant group effect occurs if pile spacing is larger than 4d for cohesive soils.	Chen (2001)
	Single pile load	As pile spacing (s) increases lateral load per pile also increases.	Nalcakan (1999), Ergun (2000)
	Factor of safety of slope	As pile spacing (s) increases factor of safety of slope against failure decreases.	Wei (2008)
		In case of passive piles are socketed in a stable layer enough, s/d=2-4 pile spacing provides significant improvement in factor of safety of the slope.	Liang and Yamin (2009)
Material properties of unstable ground	*Lateral pile load*	Lateral force per pile increases as internal friction (ϕ) and cohesion (c) parameters increases	Ito and Matsui (1975)
		Yield soil pressure on piles due to the moving cohesive soils increase as undrained shear strength (c_u) of soil increases.	Brinch Hansen (1961), Broms (1964), De Beer (1977), Viggiani (1981)
Material properties of stable ground	*Pile deflection and bending moment*	If piles are embedded in a relatively soft stratum, larger pile deflections are required to reach same level of ultimate resistance as embedded in a stiff stratum. Additionally, when the stable ground is stiff, the flexural distortion of the pile is more localized (close to the sliding interface) and give larger bending moments.	Kourkoulis et al. (2011)

Table 2.3 (Continued)

Affecting parameter	Affected property	Conclusion	Reference
Relative pile stiffness, H/Le $L_e = \sqrt[4]{\frac{E_p I_p}{G}}$ ***H= Thickness of soft soil*** ***L_e= Elastic length of pile soil system*** ***E_pI_p= Flexural rigidty of the pile*** ***G= Elastic shear modulus of soil***	*Degree of rigidity*	If H/Le≤4-5 Stiff piles If H/Le≥4-5 Flexible piles	Begemann and De Leeuw (1972), Oteo (1977)
$K_r = \frac{EI}{E_S L^4}$ ***EI= Flexural rigidity of pile*** ***E_s=Average soil deformation modulus*** ***L= Pile length***	*Pile deflection*	Deflection of flexible pile (smaller Kr) is much greater than stiff pile (higher Kr).	Pan et al. (2002)
	Degree of rigidity	If Kr>10^{-2} Rigid pile If Kr>10^{-3} Medium flexible pile If Kr<10^{-5} Very flexible pile	Davis and Poulos (1980)
Embedment depth of pile into stable layer	*Slope stability*	Appropriate embedment depth should be the depth point where bending moment and shear forces approaches to zero. This can be determined by infinite pile length analysis.	Nalcakan (1999), Ergun (2000)
		Critical embedment depth of pile into a stable stratum can be considered as $L_{em(critical)}$=1H_u for $P_{u(stable)}$=2$P_{u(unstable)}$	Poulos (1999)
		$L_{em(critical)}$=1.5H_u for $P_{u(stable)}$=$P_{u(unstable)}$ $L_{em(critical)}$=0.7H_u for $P_{u(stable)}$=3$P_{u(unstable)}$ H_u= Thickness of unstable soil $P_{u(stable)}$= Ultimate passive soil pressure provided by stable layer $P_{u(unstable)}$= Ultimate passive soil pressure provided by unstable layer	Kourkoulis et al. (2011)
Pile head fixity conditions	*Safety factor against pile failure*	As pile head becomes more rigid, safety factors of pile against shear and bending moment failure are increased.	Ingold (1977), Ito and Matsui (1981), Rowe and Poulos (1979),
Pile location	*Safety factor of the slope*	For a desired factor of safety value, pile rows should be located at a point where distribution of horizontal internal forces (obtained from slope stability analyses) is greater in the slope.	Nakamura (1984), Yamagami et al. (1992)

CHAPTER 3

GEOMETRY AND BOUNDARY CONDITIONS OF THE 3D FINITE ELEMENT MODEL OF PASSIVE PILES

3.1 Introduction

In this thesis study, numerical models have been formed to investigate the factors affecting the passive pile behavior used in slope stabilization works. Case studies with measured field data were used to control the accuracy of the numerical model results (Chapter 4). After verification of finite element analysis solution, a parametric study has been conducted (Chapter 5). Variations in the factors such as the embedment depth of the pile, material properties of unstable ground, pile spacing, amount of lateral soil movement, and their affects were studied. Three dimensional geotechnical finite element package PLAXIS 3D 2010 was used in all analyses for this purpose. Properties and main functions of the 3D finite element methodology are presented briefly for better understanding of the model designs.

Plaxis 3D 2010 consists of two parts which are input and output program. Input program is used for the definition of the model and assignment of analysis properties. At the beginning of the input program, project properties are asked from the user. Model boundaries in two horizontal directions (x and y) and unit system used in analyses are defined in this part.

Input program includes five main components that are soil, structures, mesh, water levels and staged construction. In soil mode, soil stratigraphy is assigned to the model by creating boreholes. In addition, ground water level of a specific point is defined also with boreholes. Multiple boreholes can be defined in any number at any point. Plaxis 3D interpolates layer thicknesses and ground water levels that are assigned in every borehole. Desired non-uniform three dimensional soil profiles and water level can be obtained with this way. In structures mode, all kinds of geometric entities, structural elements and their configurations are assigned. In addition, boundary conditions; predefined displacement or loading of a point, line or a surface can be defined in this part. Both soil and structure modes include material sets option which is used for the definition of material properties of soil and structural elements. In mesh mode, geometry is divided into mesh elements with desired amount of fineness. Plaxis 3D has five default mesh element distributions. These are very coarse, coarse, medium, fine and very fine mesh generations. In addition, desired amount of local fineness of a specific volume or geometric entity can be achieved with fineness factor option. In water levels mode, water levels outside of the model can be defined for the simulation of external water pressures. Additionally, it can be used as phreatic level for partially saturated soils. After finalization of all geometric entries, calculation stages are arranged in staged construction mode according to the purpose of the analysis. All geometric elements can be activated or deactivated for every stage. Besides, analysis properties of each stage such as calculation type, maximum number of iteration and error tolerance can be defined separately. After setup of all stages, analysis can be conducted.

Plaxis 3D provides extensive ways for the documentation of the analysis results. Output program presents all numerical analysis results in variety of forms including curves, diagrams and tables. It mainly consists of the results of deformations and stresses. In addition, force results are presented for structural elements.

3.2 Model Properties

Finite element analysis software Plaxis 3D were used for the investigation of laterally loaded pile behavior. In order to carry out a parametric study, other properties should be kept constant while the effect of the change in a certain property is being investigated. The two possible options to use for the geometry of the problem were (i) to use a real slope geometry having a certain ground surface angle, or (ii) to use a simple shear box model to represent the movement of the upper soil relative to the lower soil. In a real slope geometry, as the soil and geometrical properties are changed, the critical failure surface, the mechanism of movement, the amount and distribution of movement in the unstable soil zone may change. Therefore, the interpretation of parametric study results will be more complex, since the effect of several factors will interfere with each other. In addition, real landslide model with all external boundaries will require much more 3D mesh elements which cause longer calculation times. Therefore shear box analysis, also used by Kourkoulis et al. (2011, 2012), is adapted for the evaluation of passive pile response in laterally moving soils to simulate the actual slope stability problem (Figure 3.1). Shear box models provide control of the number of variables and it prevents the redundant uncertainties. Unstable ground was modeled by using uniform predefined horizontal displacements and lateral loading of piles were achieved in this way. Stability of bottom soil was provided with surface fixities. Consequently shearing zone was formed between unstable and stable soils just like in real landslide cases. Embedment of pile into stable stratum caused the development of passive resistance in pile.

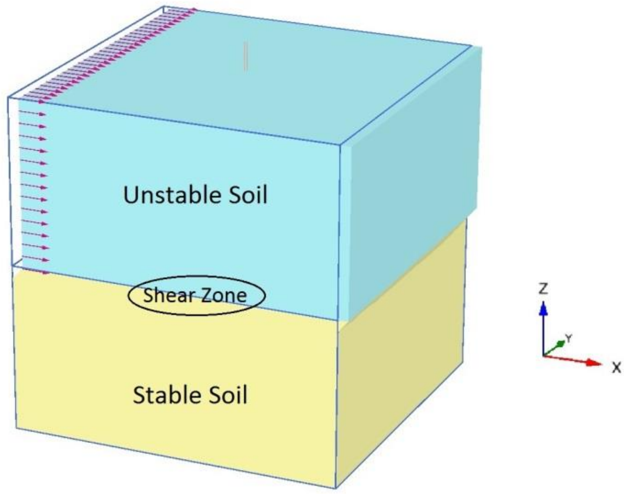

Figure 3.1 Geometric illustration of the shear box model

Elastic-perfectly plastic Mohr Coulomb failure criterion was used in all analyses as material model. Drained and undrained analyses were conducted for sandy and clay type of ground materials. Although it is well known that, the more advanced soil constitutive models can capture the nonlinear stress-strain behavior of soils more accurately, they also require significant number of material model parameters to be input. Therefore Mohr-Coulomb model is considered to be adequate for the content of this parametric study.

Embedded pile option in Plaxis 3D was used to model the vertical pile and its properties in all analyses. Plaxis 3D generates embedded piles like linear beam elements. This option gives the opportunity of modeling piles as structural members with a definite rigidity and mechanical properties. Dao (2011) indicated that embedded pile option is a good tool to model laterally loaded pile behavior and it shows very similar behavior with volume pile modeling, i.e. when the pile is defined as a different material having a certain diameter, length and properties. Nevertheless, 6 edged hexagonal soil elements (having the same diameter as the real pile) are defined and material properties were assigned the same as that of the surrounding soil (Figure 3.2). In this way, the behavior of the soil having interaction with the pile could closely be observed by providing finer mesh generation in that area.

In embedded pile option, special interface elements are automatically defined to model the interaction between the beam and the surrounding soil. Interaction at the pile skin is described by 3 node-line interface elements with pairs of nodes instead of one single node. One node of each pair belongs to the beam element, whereas the other virtual node is created in the soil volume element. Interface builds a connection between those pair of nodes by considering the material stiffness matrices and the amount of relative displacements (Plaxis 3D Reference and Scientific Manuals 2010). In addition, Dao (2011) pointed out that embedded pile option in Plaxis 3D does not consider slide of the soil at the skin of pile in horizontal directions. Therefore, it may not give reliable results for laterally loaded piles having smooth interaction surfaces.

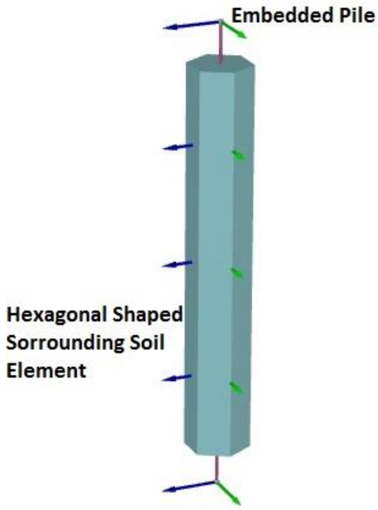

Figure 3.2 Model illustration of the pile and the surrounding soil

Before systematically investigating the factors affecting the pile-soil interaction behavior, the boundary size, surface fixity conditions and mesh generation effects were studied as it is necessary in order to establish correct geometry and model of the problem. In this chapter, shear box model is used to study geometry, shape and boundary conditions of the problem.

3.3 Boundary Size and Surface Fixity Conditions

It is desirable to select the size/geometry of the model large enough so that boundaries are far away from the area where we are making calculations, and that stress-strain distributions in the soil are not affected from the geometrical constraints near the boundaries. However, long calculation times in three dimensional analyses make this procedure inefficient. Therefore, the size/geometry of the model and distance to the boundaries were studied to determine the optimum dimensions sufficient for an accurate model. The deflections in the soil are investigated as a result of pile resistance are not affected or interrupted because of the model boundaries.

For the model size/geometry determination, single pile analyses were performed and same materials were used for unstable and stable soils. Assigned material properties for unstable soil, stable soil and embedded pile are listed in Table 3.1 and Table 3.2.

Table 3.1 Material properties of unstable and stable soil

Parameter			Value	Unit
General	Material model		Mohr Coulomb	-
	Drainage type		Drained	-
	Unit weight	γ_{unsat}	17.5	kN/m^3
		γ_{sat}	18	kN/m^3
Strength parameters	Deformation modulus	E'	15000	kN/m^2
	Poisson's ratio	ν'	0.3	-
	Cohesion	c'	5	kN/m^2
	Internal friction angle	ϕ'	15	°
	Dilatancy angle	Ψ	0	°

Table 3.2 Material properties of embedded pile

Parameter			Value	Unit
Strength parameters	Deformation modulus	E	20x10^6	kN/m^2
	Unit weight	γ	24	kN/m^3
	Predefined pile type	Massive circular pile	-	-
	Pile diameter	d	1	m
Skin resistance	Maximum traction allowed at the pile top	$T_{top,max}$	500	kN/m
	Maximum traction allowed at the pile bottom	$T_{bot,max}$	500	kN/m
	Base resistance	F_{max}	5000	kN

Boundary surface fixities of the model were determined to simulate the behavior of a laterally moving soil above a stable ground. For this purpose, standard surface boundary conditions of Plaxis 3D were applied to the stable soil at the bottom and stability of the soil was sustained with this way. For vertical boundaries, this option provides the fixity of the surface in the direction of axis which the surface is perpendicular to (Plaxis 3D Reference Manual 2010). Bottom surface boundary of the model is fixed in all directions in all cases.

Surface boundaries of unstable ground were redefined with surface prescribed displacement property (Figure 3.3). Movement in y direction is prevented and z direction is allowed for all surfaces. In x direction, an amount of uniformly distributed prescribed displacement (u_x) was defined on the left side surface of the model box. Rear and front side surfaces were allowed for movement in x direction. Right side surface movement was first tried to be freely allowed in x direction however, load increment failure and soil body collapse errors were generally encountered in the vertical model boundary without any constraint (especially in cohesionless materials). For analyses that calculation phases were fully completed, excessive deformations and spilling of soil body from right hand side were observed especially depending on the assigned material properties and the amount of prescribed displacements (Figure 3.3). Additional structural support for right side surface boundary could be a solution but it was observed that they can destroy the nature of the problem by imposing unwanted friction and geometrical constraints. Therefore, it was determined to take right hand side surface of the box model fixed in a very far distance which both pile and soil deformations are not affected from this surface fixity (Table 3.3). In that case, soil in front of the piles does not freely deform or spill to the right hand side. Proposed model geometry simulates landslide stabilization cases where soil in front of the piles is not yielded.

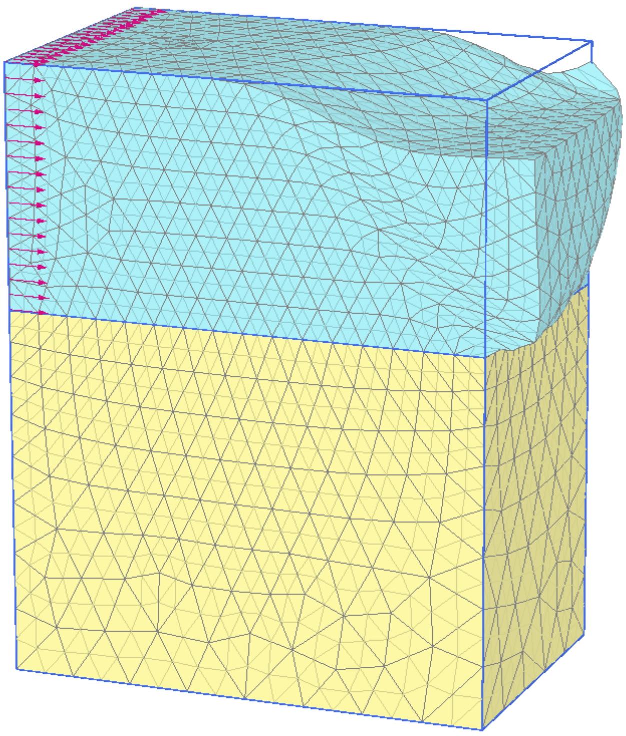

Figure 3.3 Spilling of unstable soil from right hand side when right boundary is free to move in the direction of movement

Validity of the surface boundary fixities were also confirmed in case study modeling (Chapter 4.1 and Chapter 4.2). Effect of different surface boundary conditions was evaluated in models for case studies. Lateral deflection and bending moment behavior of model piles were compared with field measurements of case study piles. Most accurate model boundaries simulating the actual pile behavior were selected same as in parametric study.

Table 3.3 Surface boundary fixities for unstable ground

Surface		**x direction**	**y direction**	**z direction**
Unstable ground	Front side	Free	Fixed	Free
	Rear side	Free	Fixed	Free
	Right side	Fixed	Fixed	Free
	Left side	Prescribed displacement (u_x)	Fixed	Free

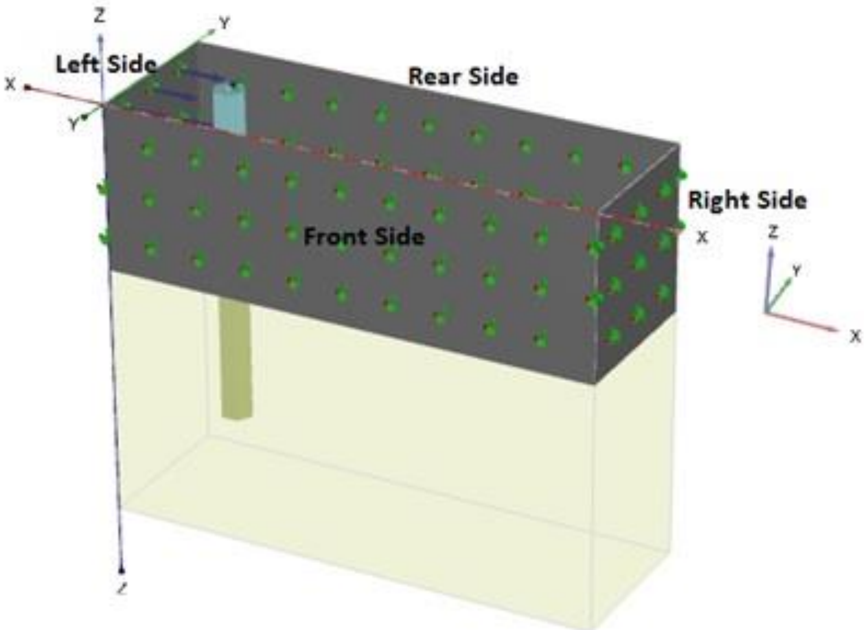

Figure 3.4 Boundary surfaces for unstable soil (movement in y direction is prevented and z direction is allowed for all surfaces, At the left side surface, an amount of uniformly distributed prescribed displacement (u_x) was defined to represent a moving landslide mass. On the right side surface of the box, movement in x-direction is prevented. The rear and front side surfaces were allowed for movement in x-direction)

In all model geometry/size/boundary determination analyses, lateral deformation of the pile head was allowed and full embedment of the pile into stable layer was provided. Because model bottom surface is fixed against movement in all directions, enough distance was remained between the end of the pile and the bottom surface of the box to prevent the development of undesired forces and moments at the end of the pile (Figure 3.4).

Different variations in boundary distances were studied to obtain optimum model size that does not affect the displacement profile of the soil. Schematic illustration of the model dimensions is presented in Figure 3.5. All model dimensions were considered in terms of multipliers of pile diameter (d).

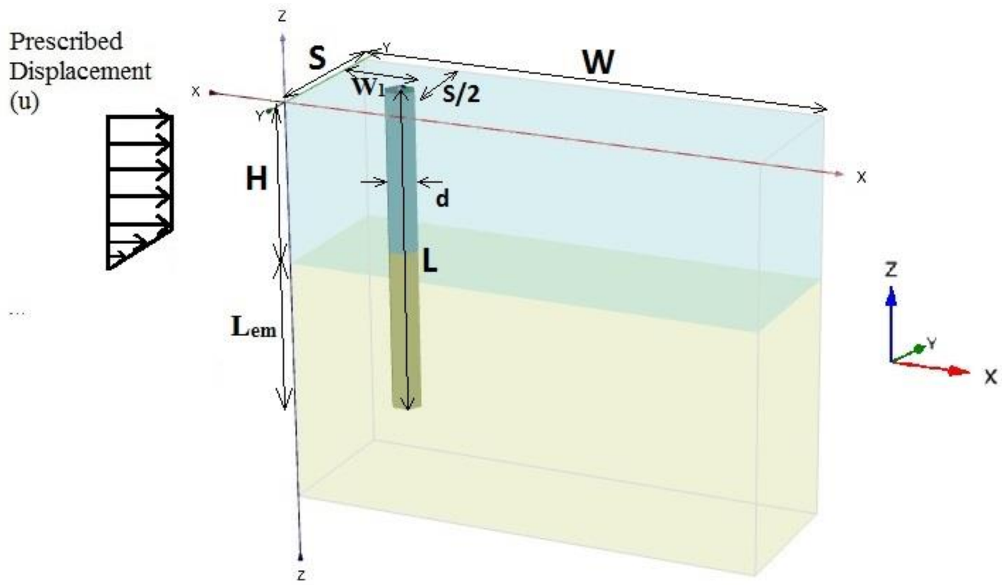

Figure 3.5 Model view of the pile and the surrounding soil

In Figure 3.5,

d: Pile diameter

S: Width of the model

W_1: Distance between left side surface (where prescribed displacement is applied) and the pile

W: Length of the model in x direction

H: Unstable soil depth

L_{em}: Embedded pile depth into the stable layer

L: Pile length ($L=H+L_{em}$)

Displacement ratio ($\varepsilon=u_x/d$) was defined as a function of pile diameter for lateral deformation input. Lateral prescribed movement (u_x) was assigned to the left side surface of upper unstable soil. Analyses in the scope of boundary size evaluation were performed by changing the ratio of the model length in x direction to the unstable soil depth (W/H) as shown in Table 3.4.

Table 3.4 Variation of parameters in boundary size determination analyses

Pile diameter	**Width of the model**	**Distance btw prescribed disp. and pile**	**Pile length**	**Embedded pile depth into stable layer**	**Unstable soil depth**	**Length of the model**	**Dim. Ratio**	**Lateral prescribed movement**	
d (m)	S(m)	W_1(m)	L (m)	L_{em} (m)	H (m)	W (m)	W/H	$\varepsilon=u_x/d$	u_x (cm)
1	10d	5d	20d	10d	10d	10d	1	0.1	10
"	"	"	"	"	"	20d	2	"	"
"	"	"	"	"	"	30d	3	"	"
"	"	"	"	"	"	40d	4	"	"
"	"	"	"	"	"	50d	5	"	"
"	"	"	"	"	"	60d	6	"	"
"	"	"	"	"	"	70d	7	"	"

3.3.1 Discussion of Results

Distribution of horizontal soil deformations in x direction was compared for different model lengths to evaluate boundary effect on lateral soil deflections (Figure 3.6). Ground level deformations were considered in this purpose because maximum lateral deflections were observed at the ground surface.

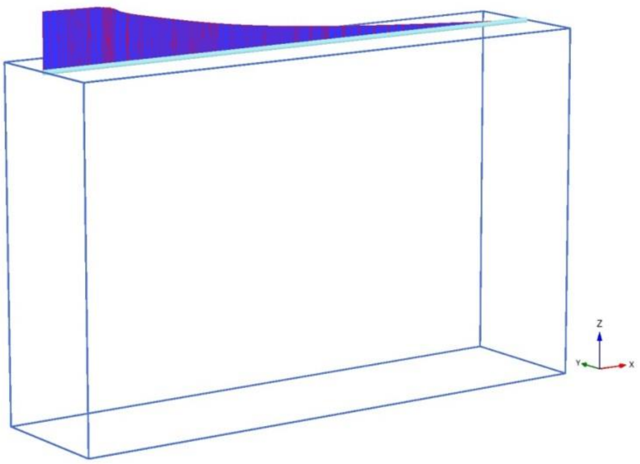

Figure 3.6 Distribution of horizontal soil deformations in x direction at the ground surface

Lateral displacements were evaluated in Figure 3.7 as percentage of residual horizontal soil displacements according to dimension ratio (model length divided by unstable soil depth, W/H). Residual displacements were obtained as the ratio of the deformation of that point to total prescribed deformation assigned to the left surface. This value was considered as an indication of the reduction of lateral deformations through model length. In Figure 3.7, soil deformation distribution is not much affected as model length gets longer. Behavior is seem to be almost same especially for higher model lengths than W=50d. Only less than 15% of horizontal displacements remain at the distance of W=40d for larger model lengths. Therefore, W/H=4 or W=40d could be chosen as sufficient model length in respect of horizontal soil distributions for the assumed boundary fixity conditions.

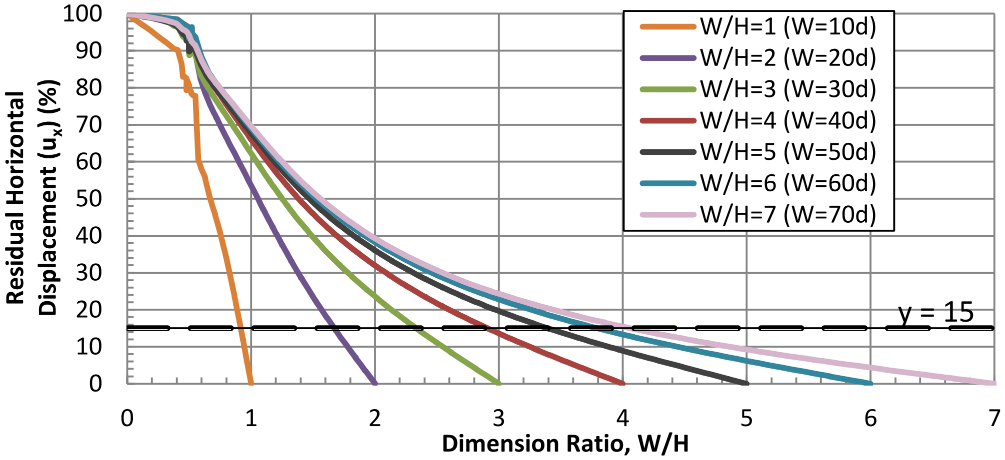

Figure 3.7 Residual horizontal displacements at the ground surface (z=0) in x direction versus dimension ratio

Lateral deflection and bending moment profile of the pile were also compared for different dimension ratios. In Figure 3.8, it can be seen that pile deflection behavior is almost same for larger dimension ratios than W/H=3-4. It can be observed that embedment depth of pile into stable layer (L_{em}=H) is not sufficient to create enough passive resistance for stabilization. Stiffness properties of stable ground were assigned deliberately weaker because boundary conditions became more critical when lateral pile deformations and rotations were higher. Bending moment profile of pile through its length according to different model sizes indicated that bending behavior also becomes same for dimension ratios larger than W/H=4 (Figure 3.9).

Consequently, dimension ratio of W/H=4 or W=40d was chosen as model length in parametric study. In addition, model width of S=10d was observed to be sufficient for single pile modeling. Determined model dimensions and boundary fixities were used in all numerical analyses. Approximation accuracy of the assumed model sizes to real passive pile behavior was also verified in case study models (Chapter 4.1 and Chapter 4.2).

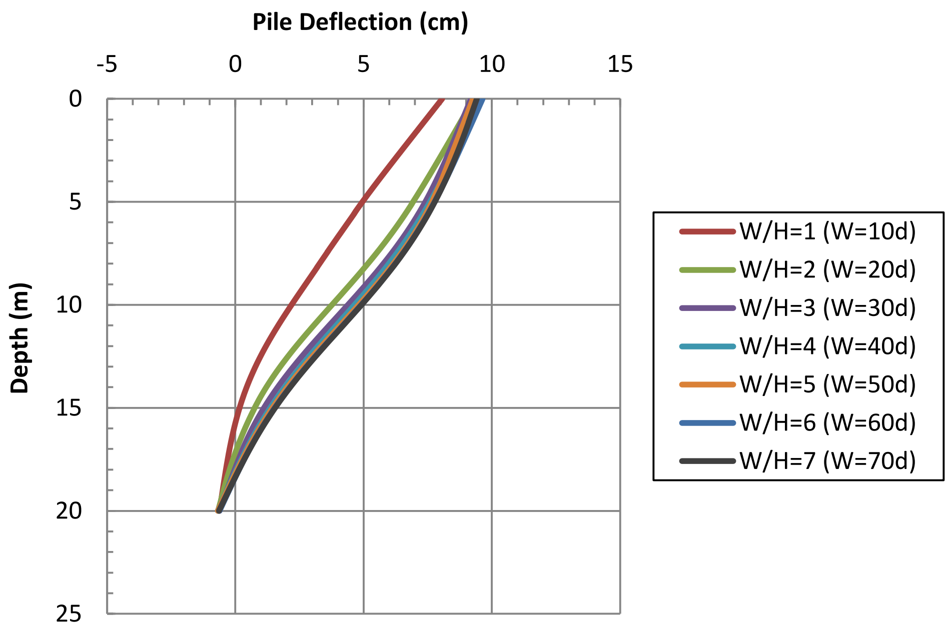

Figure 3.8 Pile deflection versus depth

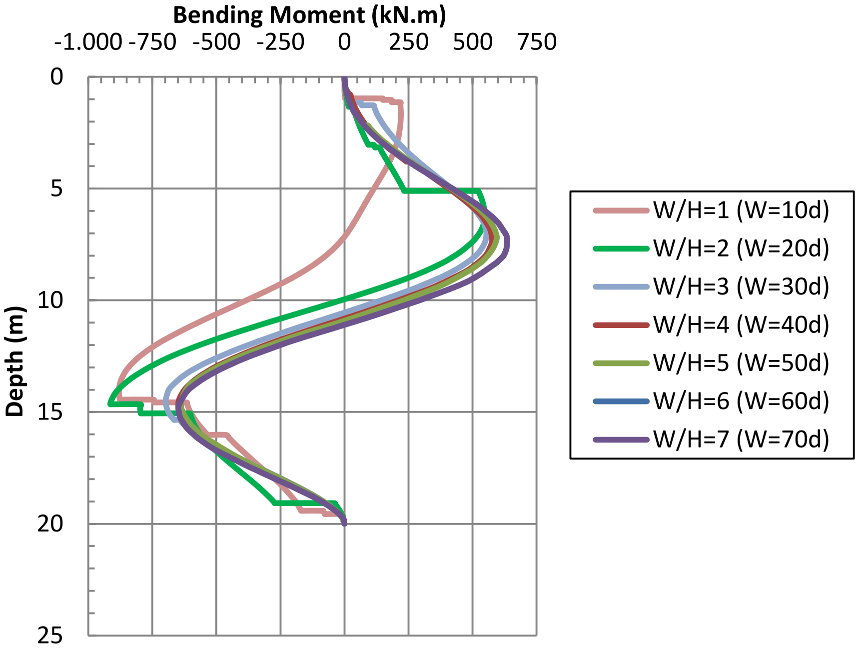

Figure 3.9 Bending moment versus depth

3.4 Evaluation of Mesh Generation

Plaxis 3D software uses 10 noded tetrahedral mesh elements to model soil formations (Figure 3.10). Different mesh elements are used for structural objects and interface elements. Mesh generation is an important part of a finite element calculation. Meshes should be generated fine enough to obtain accurate results and coarse enough to avoid from excessive amount of calculation times.

Plaxis 3D have five standard finite element mesh generation options. These are very coarse, coarse, medium, fine and very fine meshes. Other than these standard options, desired amount of mesh fineness and local refinement for a specific volume or structural object can be provided by changing the fineness factor that is defined for all geometric entries.

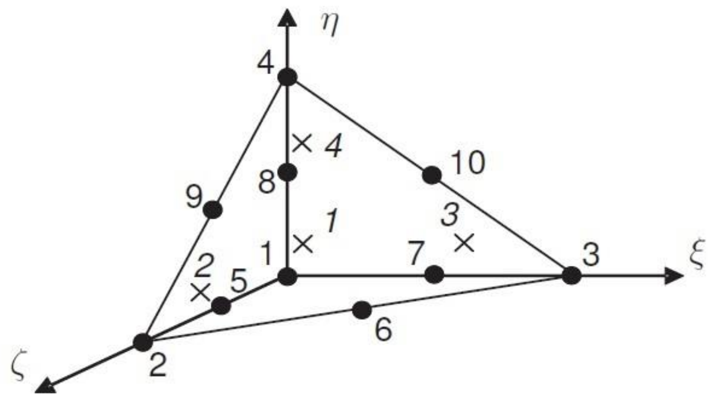

Figure 3.10 10 noded tetrahedral mesh element for soil formations
(Plaxis 3D Reference Manual 2010)

Standard mesh generation alternatives were investigated in this part. Optimum mesh elements were decided by studying their effects on deformations and structural forces for both pile and soil formations. Boundary size and surface fixity conditions determined in Chapter 3.2 were used in analyses. In addition, same material properties used in Chapter 3.2 were assigned to the models for unstable soil, stable soil and the pile (Table 3.1 and Table 3.2).

6 edged hexagonal soil elements were defined just around the piles in previous analyses. This way, pile soil interaction behavior could be investigated clearly by providing finer mesh generation just around the piles (Figure 3.2). However, hexagonal soil elements were not defined only for mesh evaluation analyses to observe general mesh fineness effect on pile in respect of deformations and structural forces (Figure 3.11). Model properties and variation of parameters for the evaluation of mesh generation are presented in Table 3.5.

Table 3.5 Variation of parameters in analyses for the evaluation of mesh generation

Pile diameter d (m)	**Width of the model, S (m)**	**Length of the model, W (m)**	**Lateral prescribed movement**		**Mesh fineness**
			$\varepsilon=u_x/d$	u_x (cm)	
1	10d=10	40d=40	0.1	10	Very coarse
"	"	"	"	"	Coarse
"	"	"	"	"	Medium
"	"	"	"	"	Fine
"	"	"	"	"	Very fine

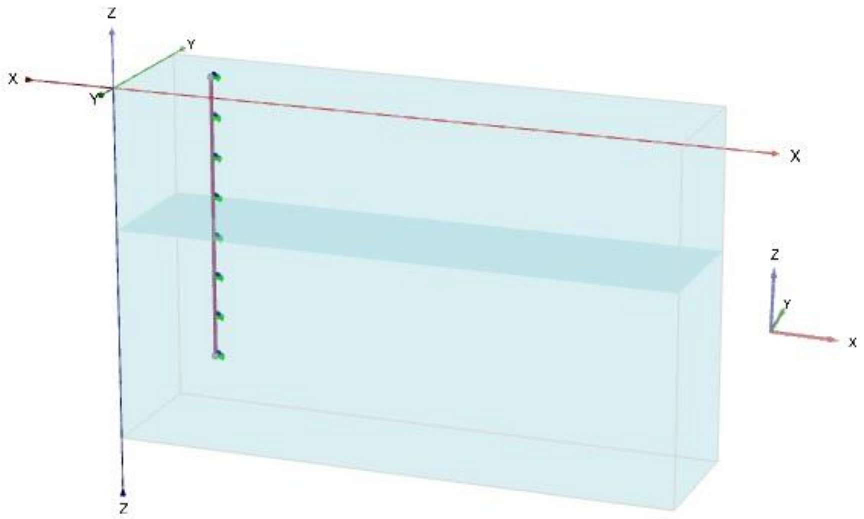

Figure 3.11 Model illustration of embedded pile and soil for mesh evaluation analyses

3.4.1 Discussion of Results

Five general mesh types were analyzed and mesh dependence on some properties were discussed in Table 3.6. It was observed that calculation time of different mesh types is highly variable. It may depend on implemented model sizes, material and interface properties, calculation type, error tolerance and of course the processor capacity of the computer system. However, it is absolute that calculation time drastically increases from coarse meshes to very fine meshes. In mesh evaluation study, very coarse and coarse mesh analyses lasted around 2-6 minutes, medium meshes around 10-15 minutes, fine and very fine meshes around 25-150 minutes for these indicated material types and conditions. However, analyses lasting 8 hours to 2-3 days were encountered for fine and especially very fine mesh generation for different circumstances.

Deformations and structural forces of the pile were compared for implemented mesh generation types. It should be indicated that these values and variations between them depend also on the geometry of the simplified model. In analyses, pile deflection, bending moment and shear force profiles through pile length were almost identical but only their maximum values were different.

Lateral deflection of the pile head was allowed in all cases. Pile head deflection because of the prescribed soil deformation was observed to increase generally from very coarse meshes to very fine meshes (Table 3.6). However, there is no significant variation in values. This may cause from the amount of prescribed deformation level and proximity of the pile to the surface which deformation was assigned. Maximum bending moment and shear force in the pile decreased from coarse to fine meshes. Maximum bending moments differ up to 20%, maximum shear forces differ up to %50 from very coarse mesh to very fine mesh generation.

Lateral soil deformations on the ground surface at the distances of 10d and 20d from left side surface were also compared for different mesh generations. The results indicated that deformation levels slightly decrease from coarse to finer meshes for both distances. However, difference in values may be considered as insignificant.

Table 3.6 Results for different types of mesh generation

Mesh generation	**Pile head deflection (cm)**	**Maximum bending moment in the pile (kN.m)**	**Maximum shear force in the pile (kN)**	**Horizontal soil deformations on the ground surface (cm)**	
				at 10d (10m) distance from left surface	**at 20d (20m) distance from left surface**
Very coarse	9.42	868	464	6.63	3.26
Coarse	9.49	843	428	6.77	3.20
Medium	9.54	802	363	6.61	3.20
Fine	9.60	764	316	6.57	3.14
Very fine	9.50	740	302	6.56	3.13

In conclusion, it is determined that medium mesh generation has sufficient degree of fineness and it gives enough numerical accuracy for the scope of parametric analyses. Displacement and structural forces of both pile and soil generally differ less than 15% with medium mesh generation and very fine mesh generation. Medium mesh could be selected as optimum mesh generation element considering excessive time consumption of very fine meshes. Besides, 6 edged hexagonal shaped surrounding soil element that defined just around the pile provides additional fineness near the pile region in other numerical analyses. Therefore, pile deflections and forces can be calculated with higher numerical accuracy. Medium mesh generation in model view is presented in Figure 3.12.

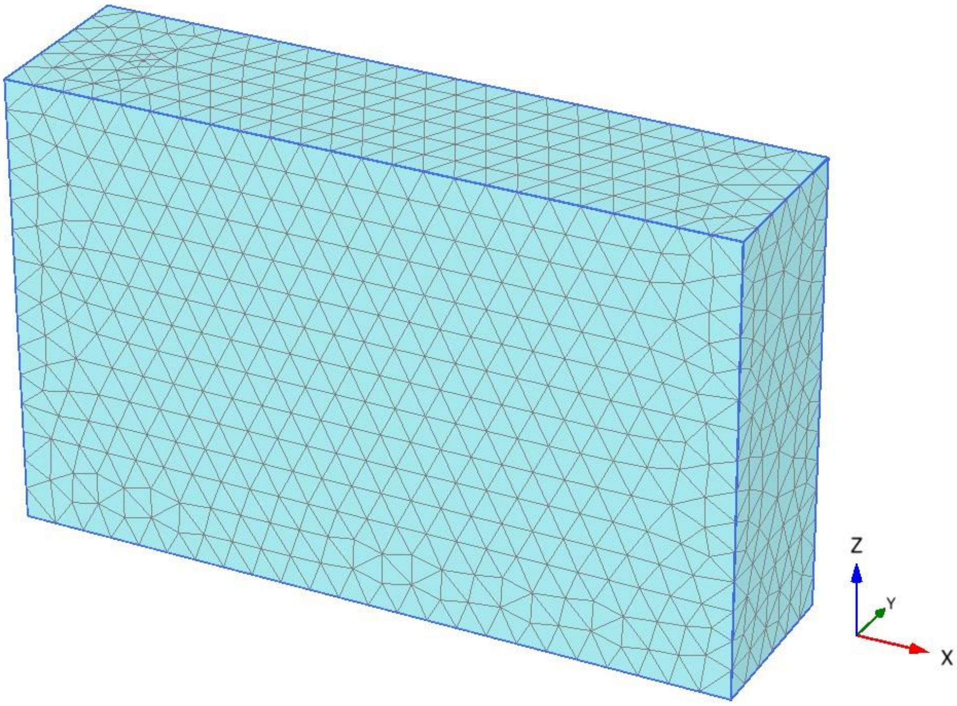

Figure 3.12 Medium type of mesh generation

CHAPTER 4

CASE HISTORIES

In situ field experiments were studied to verify the accuracy of three dimensional numerical modeling approach for real passive pile behavior. Three dimensional models of cases were investigated by comparing their results with measured field data and approximation methods of some other researchers. Two case histories were selected as De Beer and Wallays (1972) and Esu and D’Elia (1974) for this purpose. De Beer and Wallays (1972) investigated embankment construction effects on pile foundations subjected to non-uniform ground movement in sandy soils. Both steel pipe pile and reinforced concrete pile were used in their experiment. On the other hand, Esu and D’Elia (1974) conducted a field experiment to study slope stabilizing reinforced concrete pile in clayey type of soil. Applicability of three dimensional modeling for different pile materials, different soil materials and different lateral soil movement distributions could be investigated by these two cases.

4.1 De Beer and Wallays (1972)

Two case studies were reported by De Beer and Wallays (1972) in Belgium for the investigation of laterally loaded adjacent pile foundations in sandy soils. In one of the cases, a steel pipe pile having 28 m length, 0.9 m diameter and 1.5 cm wall thickness was used. Reinforced concrete pile with 23.2 m length and 0.6 m diameter was used in the other case. Pile top was restrained to move in both cases. Spacing between the adjacent piles has not been indicated and there is not much information given about the stiffness properties of the soil profile. Non-uniform lateral soil movement was measured by using inclinometers as it is seen in Figure 4.1. In addition, deflection and bending moment distribution of piles were measured for both cases.

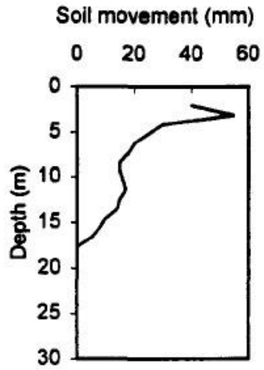

Figure 4.1 Lateral soil movement profile of De Beer and Wallays (1972) case studies (Chen and Poulos 1997)

Chen and Poulos (1997) analyzed case studies of De Beer and Wallays (1972) by using boundary element methodology. They aimed to predict actual laterally loaded pile response by appropriate assessment of lateral soil movement, deformation modulus of soil and limiting soil pressure. Chen and Poulos (1997) made some assumptions about the soil stiffness and pile properties to match their predictions with the measured field data. Information given by De Beer and Wallays (1972) about the case studies and some assumptions of Chen and Poulos (1997) were presented in Table 4.1.

Table 4.1 Given information and some assumptions about the case studies of De Beer and Wallays (1972)

	Information given by De Beer and Wallays (1972)	Additional assumptions of Chen and Poulos (1997)
Soil properties	*- Lateral soil displacement profile was given* *- Soil profile consists of mainly sandy materials.*	*- Deformation modulus (E_s=30 kPa) uniformly distributed and constant with depth* *- Ultimate soil pressure was considered as 2 times of Rankine passive earth pressure* *- Internal friction angle (ϕ= 33.3°)*
Case 1. steel pipe pile	*- 28 m length* *- 0.9 m diameter* *- 1.5 cm wall thickness* *- No lateral movement allowed in pile head* *- Bending moment and pile deflection distributions were presented*	*- Deformation modulus (E_p=210 GPa)* *E_pI_p=858 MN.m^2* *- Pile was considered as single isolated pile*
Case 2. reinforced concrete pile	*- 23.2 m length* *- 0.6 m diameter* *- No lateral movement allowed in pile head* *- Bending moment and pile deflection distributions were presented*	*- Deformation modulus (E_p=20 GPa)* *E_pI_p=127 MN.m^2* *- Pile was considered as single isolated pile*

Both steel pipe pile and reinforced concrete pile cases were modeled by using three dimensional finite element analysis software Plaxis 3D. Piles were considered as single isolated piles in analyses because of the lack of information about the pile spacings.

There is not much information about the geometry of the site. Therefore, model boundaries were determined according to trial and error procedure. Different model length, width and surface fixities were tried to understand the effect of boundary conditions on the results of pile deflections and structural forces in case studies. Minimum boundary size and surface fixity conditions that are not affecting the results were decided same as in Chapter 3.3 for all of the case studies.

Steel pipe pile and reinforced concrete pile were subjected to same amount of lateral soil movement according to De Beer and Wallays (1972). Therefore, same prescribed deformation profile was assigned to the models in both cases. Measured non-uniform lateral soil movement profile of De Beer and Wallays (1972) was simplified as shown in Figure 4.2. Passive loading of piles was sustained with the application of this lateral soil movement to the models.

Lateral deformation of the pile head was prevented by point displacement property. Pile head was fixed to move in lateral directions in Plaxis 3D models.

Medium type of mesh generation was observed to have enough sensitivity for the calculation of deformations and structural forces. Plaxis 3D applies fine mesh generation for the defined prescribed surfaces in models by default. This default property wasn't changed. In addition, 6 edged cylindrical surrounding soil volume defined just around the pile with a diameter equals to the pile as mentioned in previous parts. Therefore, local fine mesh generation was assigned for this specific area (Figure 4.4 and Figure 4.9).

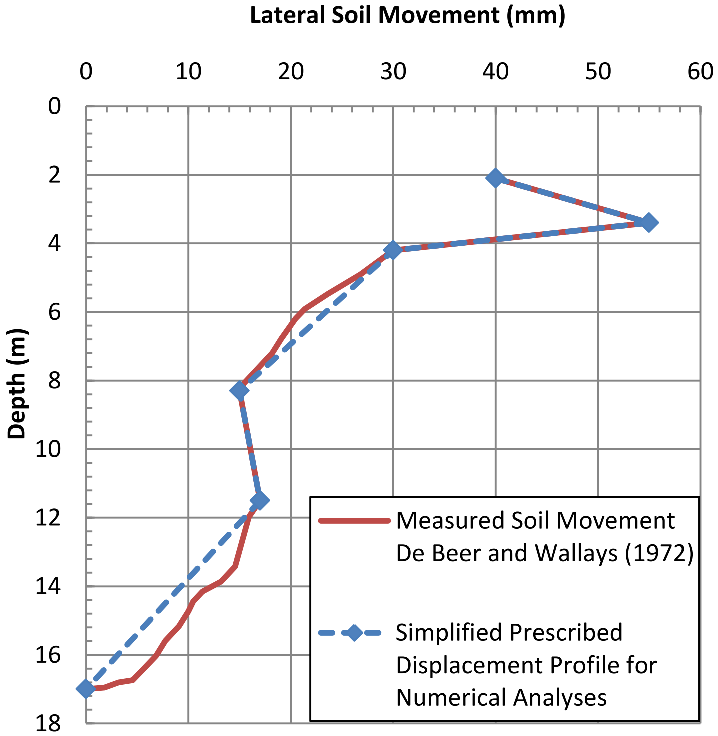

Figure 4.2 Measured and simplified lateral soil movement profiles for case studies of De Beer and Wallays (1972)

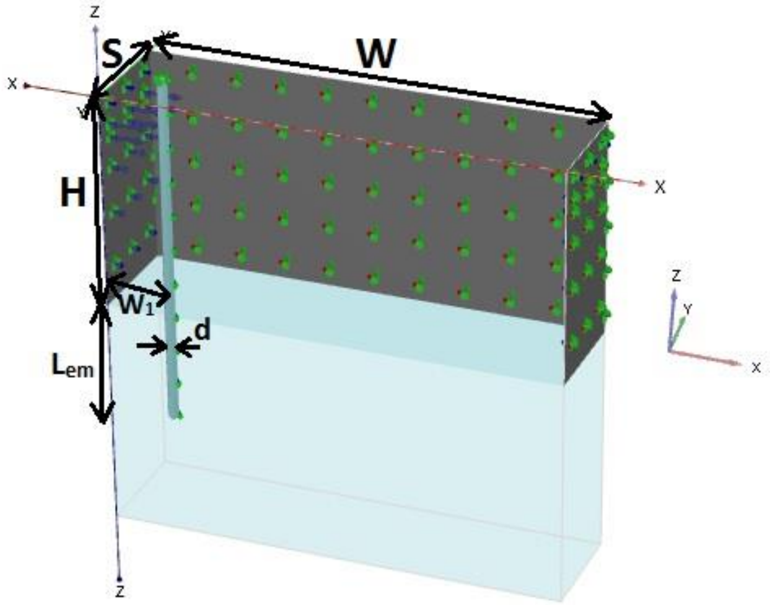

Figure 4.3 Schematic illustration of the model boundary dimensions

Two calculation phases were implemented for the modeling of case studies. First one is initial phase. It includes calculation of initial soil stresses and water pressures if there is any ground water level. In this phase, only assigned soil materials were activated and other structural elements, loads or prescribed movements were deactivated. Second phase was used for the analysis of load and displacement effects on structural elements (Table 4.2).

Table 4.2 Calculation phases for De Beer and Wallays (1972) case studies

Phase name	**Calculation type**	**Activated model properties**
Initial phase	K_0 procedure	Soils
Phase 1	Plastic drained	Soils
		Embedded pile
		Surface displacements
		Point displacements

4.1.1 Case 1. Steel Pipe Pile

Three dimensional model box analyses were conducted for steel pipe pile case according to the given information. However, additional assumptions were made by regarding the approximations of Chen and Poulos (1997). Geometry of the model box, assigned material properties, evaluation and comparison of the results are presented in the following parts.

4.1.1.1 Geometry of the Model

Schematic illustration, values of the model boundary dimensions and surface fixity conditions of the case 1 are presented in Figure 4.3, Table 4.3 and Table 4.4. Mesh generation view of the model is presented in Figure 4.4.

Table 4.3 Model boundary dimensions for case 1 (De Beer and Wallays 1972)

Pile diameter	**Pile length**	**Embedded pile depth into stable layer**	**Unstable soil depth**	**Width of the model**	**Distance btw. prescribed disp. and pile**	**Length of the model**
d (m)	L (m)	L_{em} (m)	H (m)	S=10d (m)	W_1=5d (m)	W=40d (m)
0.9	28	11	17	9	4.5	36

Table 4.4 Surface fixity conditions for case 1 (De Beer and Wallays 1972)

Surface		**x direction**	**y direction**	**z direction**
Unstable ground	Front side	Free	Fixed	Free
	Rear side	Free	Fixed	Free
	Right side	Fixed	Fixed	Free
	Left side	Prescribed displacement (u_x)	Fixed	Free

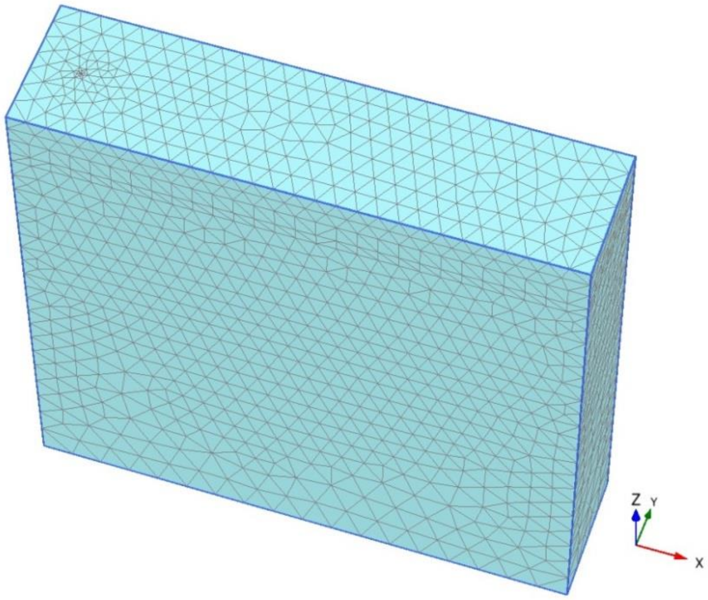

Figure 4.4 Mesh generation for the steel pipe pile case (De Beer and Wallays 1972)

4.1.1.2 Material Properties

Stiffness properties of soil profile and embedded pile were assigned regarding the given information and assumptions of Chen and Poulos (1997). There is no distinction between moving and stationary soil profiles in De Beer and Wallays (1972) cases. Therefore, same materials were used for unstable and stable soils. Assigned material properties for unstable soil, stable soil and embedded pile were listed in Table 4.5 and Table 4.6.

Table 4.5 Material properties of unstable and stable soils for
De Beer and Wallays (1972) cases

Parameter			Value	Unit
General	Material model		Mohr Coulomb	-
	Drainage type		Drained	-
	Unit weight	γ_{unsat}	18.0	kN/m^3
		γ_{sat}	18.5	kN/m^3
Strength parameters	Deformation modulus	E'	30000	kN/m^2
	Poisson's ratio	ν'	0.3	-
	Cohesion	c'	3	kN/m^2
	Internal friction angle	ϕ'	33	°
	Dilatancy angle	Ψ	2	°
	Interface	R_{inter}	0.7	-
Flow parameters	Coefficients of permeability	k_x	0	m/day
		k_y	0	m/day
		k_z	0	m/day

Table 4.6 Material properties of embedded pile for steel pipe pile
(De Beer and Wallays 1972)

Parameter			Value	Unit
Strength parameters	Deformation modulus	E	$210x10^6$	kN/m^2
	Unit weight	γ	27	kN/m^3
	Predefined pile type	Circular tube	-	-
	Pile diameter	d	0.9	m
	Thickness	t	0.015	m
Skin resistance	Maximum traction allowed at the pile top	$T_{top,max}$	200	kN/m
	Maximum traction allowed at the pile bottom	$T_{bot,max}$	200	kN/m
	Base resistance	F_{max}	3000	kN

Maximum traction allowed at the pile top and bottom and base resistance values were decided considering lateral pile capacities and interaction with the surrounding ground.

4.1.1.3 Discussion of Results

Steel pipe pile case reported by De Beer and Wallays (1972) was analyzed by using Plaxis 3D software. Deformed shape of the model is presented in Figure 4.5. Deflection, bending moment and shear force distributions through pile length of case 1 are presented in Figure 4.6.

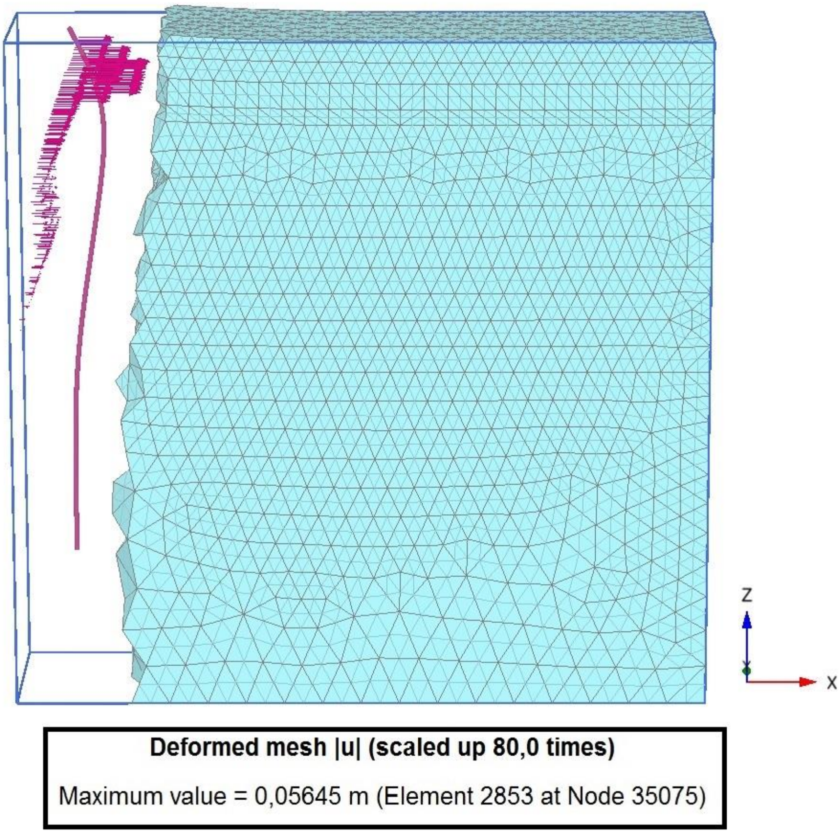

Figure 4.5 Illustration of deformed model view for steel pipe pile case (De Beer and Wallays 1972)

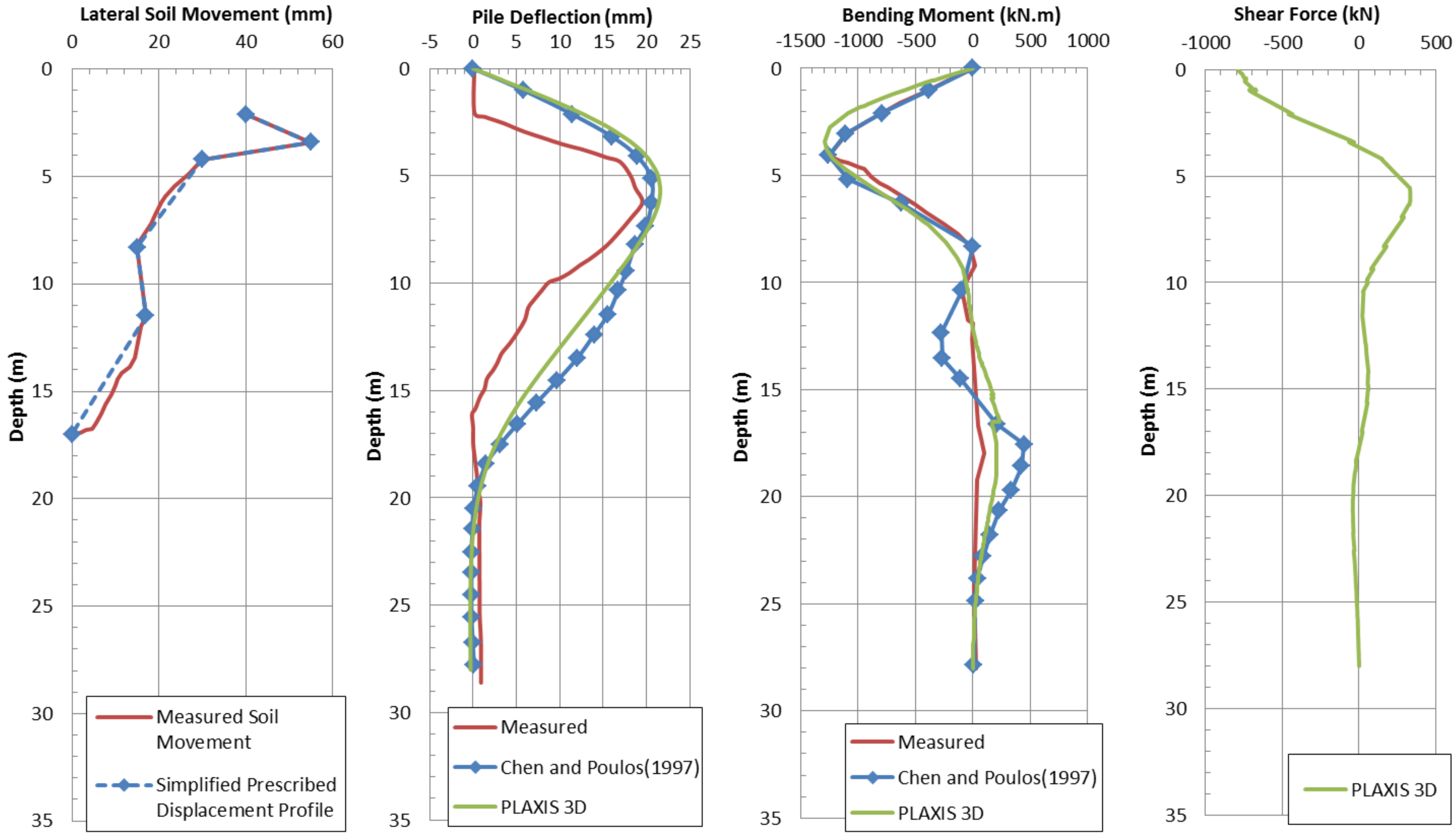

Figure 4.6 Lateral soil movement, pile deflection, bending moment and shear force profiles for steel pipe pile case of De Beer and Wallays (1972)

Deflection profile of steel pipe pile was drawn for the assigned lateral soil displacement after three dimensional analysis (Figure 4.6). Pile deflection showed very similar distribution with the approximation of Chen and Poulos (1997). General behavior through pile length was seen to be overestimated according to the measured field data. However, maximum deflection and its depth were estimated with satisfactory proximity as around 20 mm deflection at 5.5 m depth. In addition, more similar behavior was captured in lower portions of the pile with the measured data with respect to Chen and Poulos (1997).

Bending moment distribution of steel pipe pile was observed to be well predicted by three dimensional analysis. Maximum bending moment was observed as 1300 kN.m at the depth of 3.5 m from ground surface. Maximum value of bending moment and its depth were estimated very similar to the measured data and also Chen and Poulos (1997) approximation. As it can be seen from Figure 4.6, maximum bending moment was observed very close to the depth where maximum lateral soil movement and also pile deflection were occurred as expected. This could be captured with numerical modeling of the field study. In addition, lower portions of the pile obviously showed more similar behavior with the measured data than Chen and Poulos (1997).

After confirmation of pile deformations and structural forces, some illustrations of lateral deformations in the direction of soil movement are presented. Embedded pile cannot be displayed as a structural element in these figures; however deformations of the pile can be seen in visual at locations where the pile is placed. Vertical cross section in a line passing through center of the pile was taken as shown in Figure 4.7. There is no deformation in the top center of the image because lateral deformation of the pile head was restrained in De Beer and Wallays (1972) cases. Deformation of soil from sides of the pile through pile length can be seen in this figure.

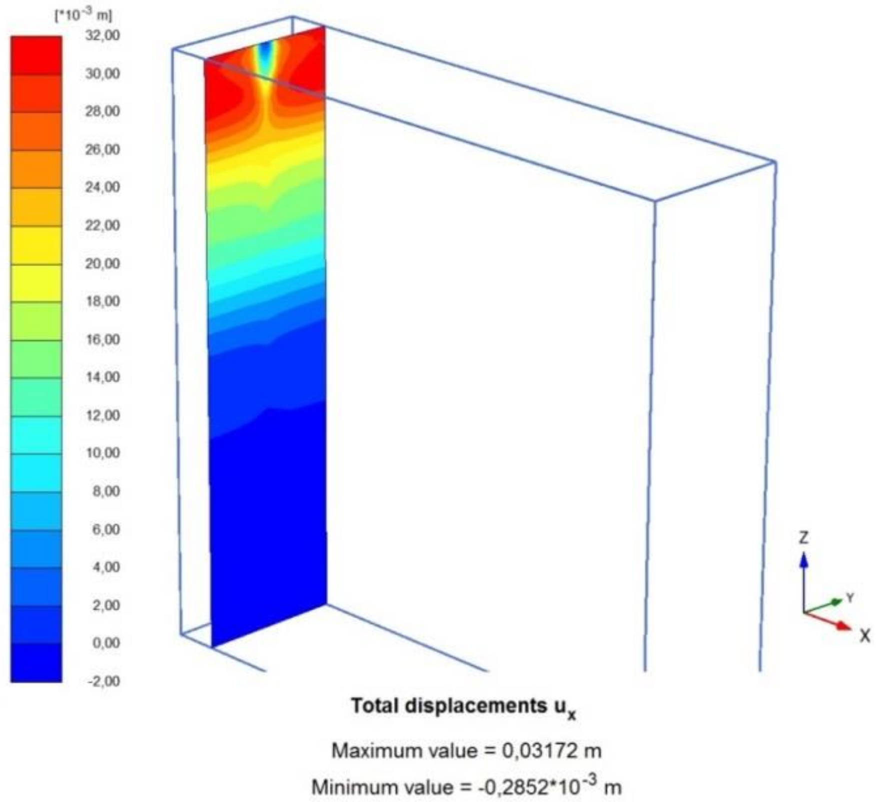

Figure 4.7 Lateral deformation distribution of case 1 in a vertical cross section through center of the pile (De Beer and Wallays 1972)

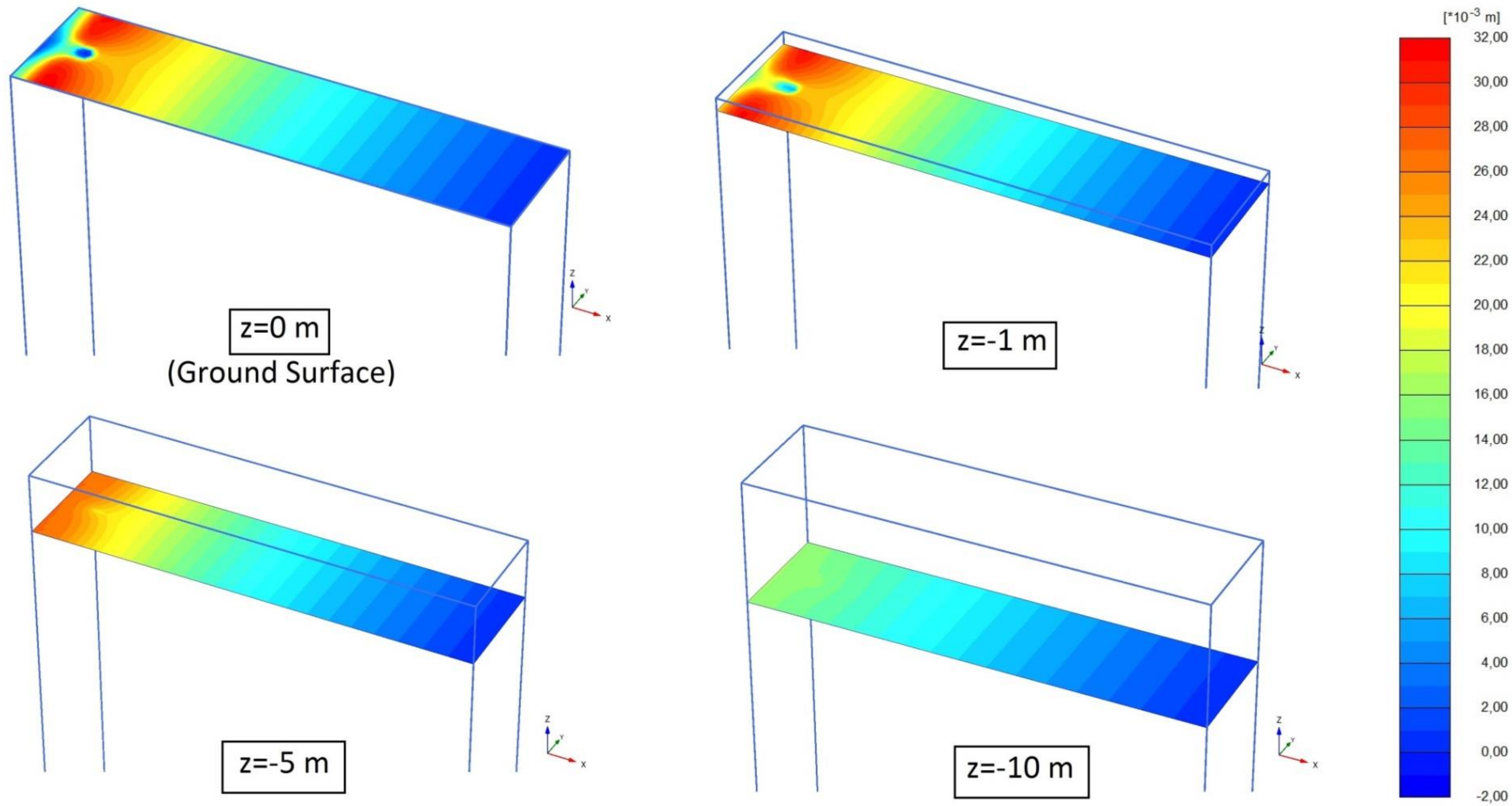

Figure 4.8 Lateral deformation distribution of case 1 for different horizontal cross sections (De Beer and Wallays 1972)

Lateral deformation distributions for different horizontal cross sections were plotted as shown in Figure 4.8. Reductions in lateral deformations through model length for different cross sections can be seen in this figure. Because pile head was restrained to move in lateral directions, pile volume was observed to be stationary and soil moves through sides of the pile in ground surface (z=0). Relative difference between pile and soil displacements was observed to decrease as depth increases.

4.1.2 Case 2. Reinforced Concrete Pile

Reinforced concrete pile case of De Beer and Wallays (1972) was also analyzed by using Plaxis 3D. Three dimensional model was formed by regarding the given information and assumptions of Chen and Poulos (1997) for the missing data. Geometry of the model box, assigned material properties, evaluation and comparison of the results are presented in the following parts.

4.1.2.1 Geometry of the Model

Schematic illustration, values of the model boundary dimensions and surface fixity conditions of the case 2 are presented in Figure 4.3, Table 4.7 and Table 4.8. Mesh generation view of the model is presented in Figure 4.9.

Table 4.7 Model boundary dimensions of case 2 (De Beer and Wallays 1972)

Pile diameter	**Pile length**	**Embedded pile depth into stable layer**	**Unstable soil depth**	**Width of the model**	**Distance btw. prescribed disp. and pile**	**Length of the model**
d (m)	L (m)	L_{em} (m)	H (m)	S=10d (m)	W_1=5d (m)	W=40d (m)
0.6	23.2	6.2	17	6	3	24

Table 4.8 Surface fixity conditions of case 2 (De Beer and Wallays 1972)

Surface		**x direction**	**y direction**	**z direction**
Unstable ground	Front side	Free	Fixed	Free
	Rear side	Free	Fixed	Free
	Right side	Fixed	Fixed	Free
	Left side	Prescribed displacement (u_x)	Fixed	Free

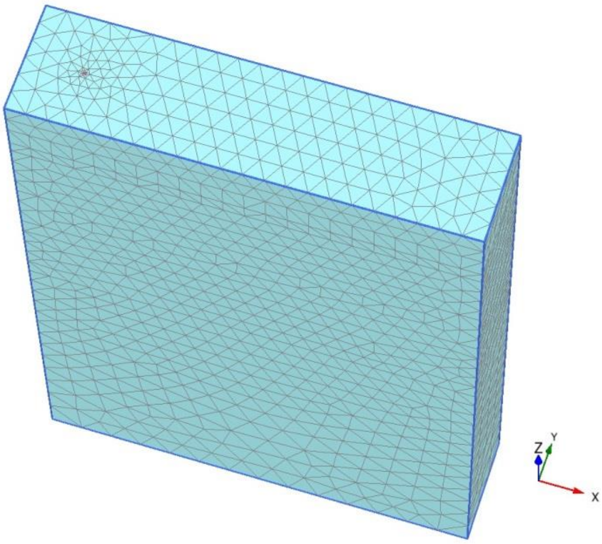

Figure 4.9 Mesh generation for the reinforced concrete pile case of De Beer and Wallays (1972)

4.1.2.2 Material Properties

Material properties for unstable and stable soils were assigned just like steel pipe pile case as shown in Table 4.5. Assigned material properties of reinforced concrete pile are presented in Table 4.9.

Table 4.9 Material properties of embedded pile for reinforced concrete pile case (De Beer and Wallays 1972)

Parameter			Value	Unit
Strength parameters	Deformation modulus	E	$20x10^6$	kN/m^2
	Unit weight	γ	24	kN/m^3
	Predefined pile type	Massive circular pile	-	-
	Pile diameter	d	0.6	m
Skin resistance	Maximum traction allowed at the pile top	$T_{top,max}$	150	kN/m
	Maximum traction allowed at the pile bottom	$T_{bot,max}$	150	kN/m
	Base resistance	F_{max}	1500	kN

4.1.2.3 Discussion of Results

Deformed shape of the reinforced concrete pile and surrounding soil just around the pile are presented in Figure 4.10. Deflection, bending moment and shear force distributions through pile length of case 2 are also presented in Figure 4.11.

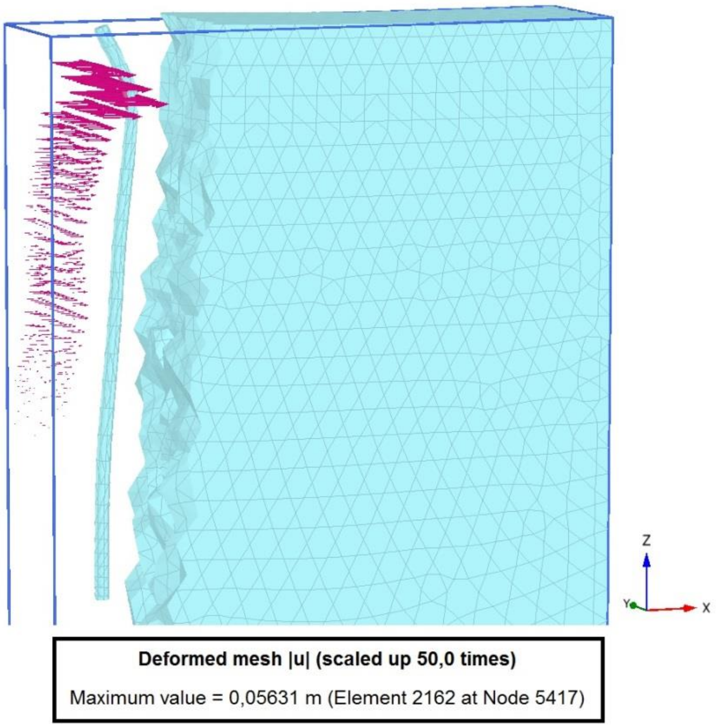

Figure 4.10 Illustration of deformed model view for reinforced concrete pile and surrounding soil (De Beer and Wallays 1972)

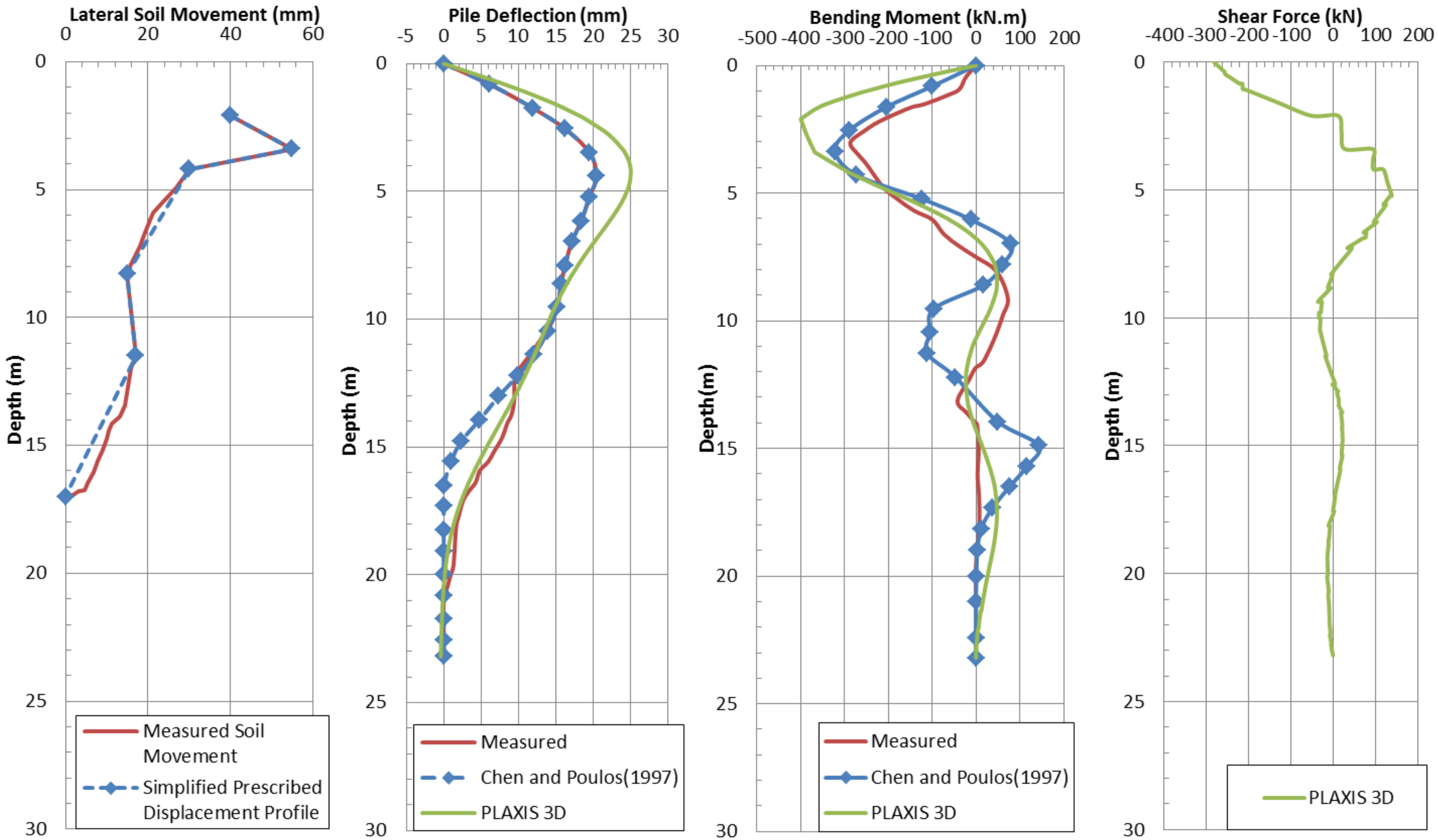

Figure 4.11 Lateral soil movement, pile deflection, bending moment and shear force profiles for reinforced concrete pile case of De Beer and Wallays (1972)

Pile deflection profile of reinforced concrete pile was compared with the measured field data and Chen and Poulos (1997). Maximum pile deflection was observed as 25 mm at 4 m depth from ground surface. As it can be seen from Figure 4.11, the depth maximum deflection occurred was accurately estimated however, value of the maximum pile deflection was overestimated slightly in three dimensional analysis. On the other hand, general pile behavior was seen to be more similar to measured field data than Chen and Poulos (1997) especially in lower portions of the pile just as steel pipe pile case.

Bending moment distribution of reinforced concrete pile was also plotted as a result of numerical analysis. Maximum bending moment was observed as 400 kN.m at 2 m depth. As it is seen in Figure 4.11, this value was overestimated by comparison to the measured field data and also Chen and Poulos (1997) approximation. However, general pile behavior has significantly good agreement with the measured data of De Beer and Wallays (1972). More similar pile response was observed again in lower portions of the pile with the measured data than Chen and Poulos (1997).

Reinforced concrete pile and steel pipe pile cases were modeled according to the information given by De Beer and Wallays (1972) and assumptions of Chen and Poulos (1997) approximation (Table 4.1). However, additional assumptions were made about model boundary conditions and material properties for the necessary input parameters in numerical modeling as presented in previous chapters. Despite all the assumed data, very similar behavior to actual pile response was captured in both steel pipe pile and reinforced concrete pile cases in numerical analyses (Figure 4.6 and Figure 4.11). Maximum deflection and bending moment values were slightly overestimated in reinforced concrete case but the depth where maximum occurs were well predicted.

Chen and Poulos (1997) emphasized that approximations to case studies were developed by matching their predictions about maximum values of the bending moment and deflections with the measured values. Therefore, their approximations are generally well predicted in upper portions of the pile, however discrepancies arise between measured and predicted profiles towards to lower portions of the pile. Closer agreement in lower portions with the measured data was observed for both steel pipe pile and reinforced concrete pile cases in Plaxis 3D analyses. Briefly, three dimensional numerical analyses give satisfactory performance for the evaluation of laterally loaded pile behavior for even piles subjected to non-uniform and complex soil movement profiles. In addition, calculation accuracy of Plaxis 3D for both steel pipe and reinforced concrete pile under soil movement in sandy materials was verified.

Some illustrations of lateral deformations for reinforced concrete pile in the direction of soil movement are presented. Vertical cross section in a line passing through center of the pile was plotted as shown in Figure 4.12. In this figure, middle of the image where pile top is located is seen to be stationary just like steel pipe pile case because of the pile head fixity in lateral directions. Pile movement relative to moving soil through near sides of the pile can be selected. It can be observed that reinforced concrete pile is easier to deform relative to steel pipe pile by comparing vertical cross section through piles (Figure 4.7).

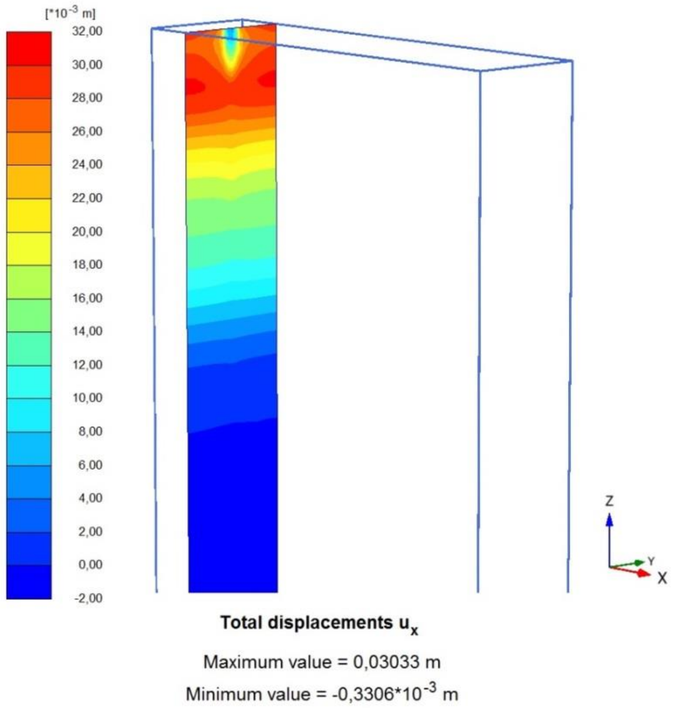

Figure 4.12 Lateral deformation distribution of case 2 in a vertical cross section through center of the pile (De Beer and Wallays 1972)

Lateral deformation of reinforced concrete pile and surrounding soil for cross sections at the ground surface, depths of 1 m, 5 m and 10 m are presented in Figure 4.13. Pile could be seen as stationary in ground surface and relative pile soil displacement decreases with depth. It is harder to separate pile soil relative movement for reinforced concrete pile comparing to steel pipe pile (Figure 4.8) for larger depths than 5 m. This may cause from the stiffness differences of pile materials. Reinforced concrete pile with lower stiffness deforms more than steel pipe pile which subjected to same amount of soil movement at same depth.

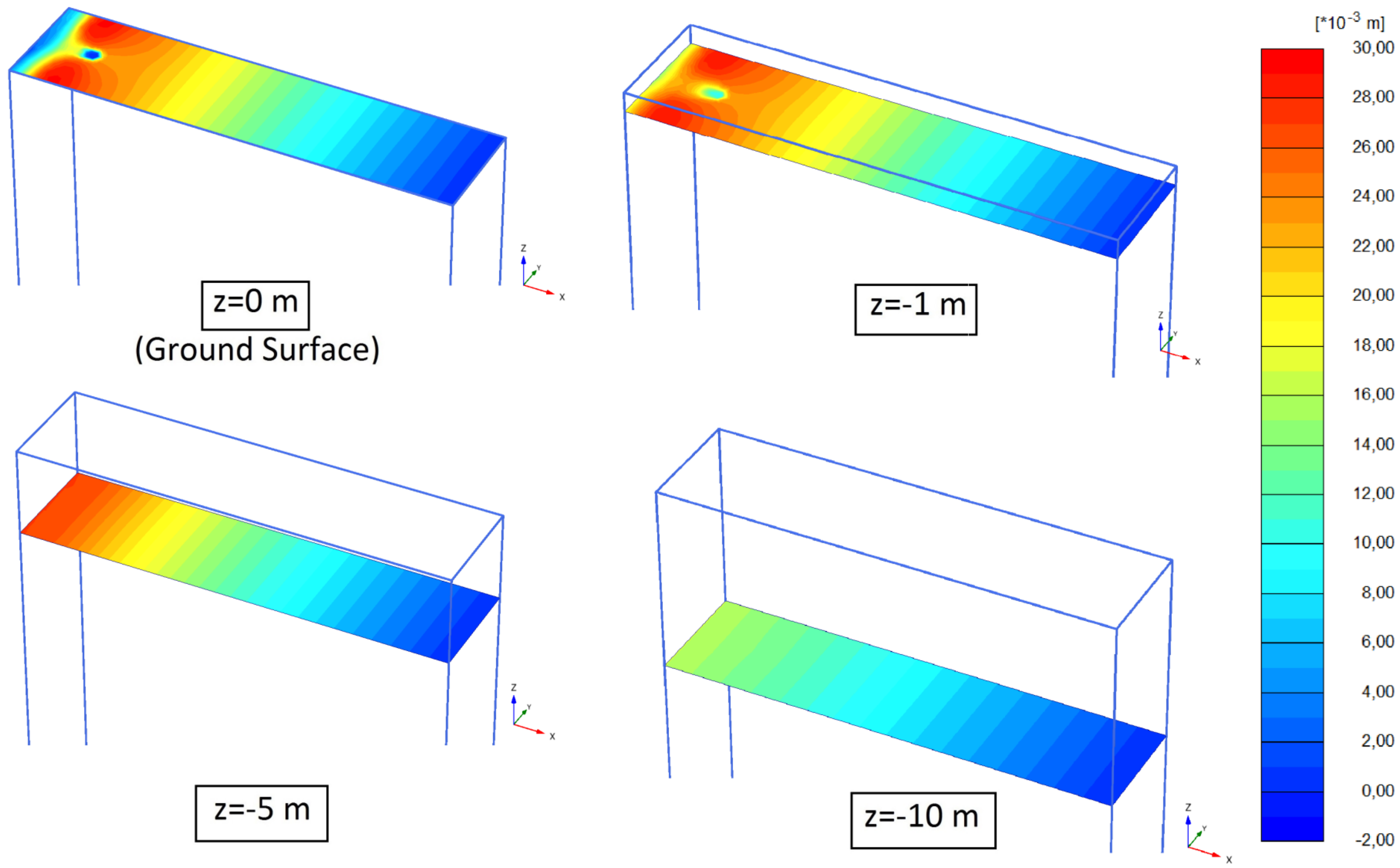

Figure 4.13 Lateral deformation distribution of case 2 for different horizontal cross sections (De Beer and Wallays 1972)

4.2 Esu and D'Elia (1974)

A field case was reported by Esu and D'Elia (1974) in which a free head reinforced concrete pile was placed in a sliding slope. The test pile was 30 m in length, 0.79 m in diameter and had a flexural rigidity (E_pI_p) of 360 MNm^2. Lateral soil movement was reported to take place in upper 7.5 m however, soil movement distribution of unstable soil was not reported. There is not much information given about the stiffness properties of the soil profile however, it was considered to consist mainly from cohesive type of soil materials. Inclinometer measurements were taken from inside of the pile at the center through pile length to obtain deflections and rotations. In addition, pile was instrumented with pressure cells at the depth of 5 m, 10 m and 15 m along its shaft. Bending moment and shear force distributions through pile length were presented in the report.

Magueri and Motta (1992), Chow (1996), Chen and Poulos (1997), Cai and Ugai (2002) investigated Esu and D'Elia (1974) field study for the verification of their proposed methodologies. They used information given by Esu and D'Elia (1974) and made some additional assumptions for the missing data which was required for their solution. Because displacement profile of 7.5 m unstable soil was not reported, it was assumed differently by researchers to match their predictions with the measured field data.

Magueri and Motta (1992) suggested that undrained shear strength (c_u) of the clay in site might be 40 kPa and yield soil pressure (p_u) can be estimated as $p_u=3c_u$ for the upper unstable soil layer and $p_u=8c_u$ for the lower stable soil.

Chow (1996) developed a numerical solution which models the pile using beam elements, soil behavior with subgrade reaction solution and pile soil interaction with the theory of elasticity. Proposed hybrid method of analysis was used for the prediction of Esu and D'Elia (1974) case study. For the missing data, Chow (1996) used suggestion of Magueri and Motta (1992) for the undrained shear strength (c_u=40 kPa). Deformation modulus of clay was assumed to be ($E_s=200c_u$) and constant with depth. Sliding soil movement profile was assumed as 110 mm uniformly distributed through 7.5 m unstable soil layer.

Chen and Poulos (1997) used simplified boundary element method to analyze case study of Esu and D'Elia (1974). In addition, maximum bending moment and pile deflection values were predicted by using design chart estimation. Design charts developed for linearly increasing soil stiffness and uniform soil movement profile were used for this purpose. Chen and Poulos (1997) used suggestion of Magueri and Motta (1992) for undrained shear strength and yield soil pressure values. Soil deformation modulus was estimated to increase linearly from zero at the ground surface and 16 MPa at the level of the pile base. Sliding soil movement profile was assumed as 110 mm uniformly distributed through 7.5 m unstable soil layer.

Cai and Ugai (2003) used subgrade reaction solution for the estimation of pile response for the case study. Stiffness properties of the clay were taken same as Chow (1996) assumptions which undrained shear strength of soil is c_u=40 kPa and deformation modulus is E_s=200c_u. However, lateral movement of sliding soil was considered as 137 mm at the ground surface and 40 mm at the sliding surface (88.5 mm in average).

Information given by Esu and D'Elia (1974) about the case study and additional assumptions of Chow (1996), Chen and Poulos (1997) and Cai and Ugai (2003) were summarized in Table 4.10.

Table 4.10 Given information and some assumptions about the case study of Esu and D'Elia (1974)

	Soil properties	Pile properties	Lateral soil movement
Information given by Esu and D'Elia (1974)	*- Soil profile consists of mainly clayey materials.*	*- 30 m length* *- 0.79 m diameter* *- Pile rigidity* E_pI_p=858 MN.m^2 *- Pile head is free to move in lateral directions* *- Bending moment shear force and pile deflection distributions were presented*	*- Depth of sliding soil is 7.5 m.* *- Lateral soil displacement profile was not reported.*
Assumptions of Chow (1996)	*- Undrained shear strength* (c_u=40 kPa) *- Deformation modulus* (E_s=200c_u=8000 kPa) *uniformly distributed and constant with depth*	-	*- 110 mm uniform lateral soil movement was assumed in unstable soil*
Assumptions of Chen and Poulos (1997)	*- Undrained shear strength* (c_u=40 kPa) *- Yield soil pressure* (p_u) p_u=3c_u *for the upper unstable soil layer* p_u=8c_u *for the lower stable soil. (Magueri and Motta 1992)* *- Linearly increasing deformation modulus* E_s=0 *at the ground surface* E_s=16 MPa *at the level of the pile tip*	-	*- 110 mm uniform lateral soil movement was assumed in unstable soil*
Assumptions of Cai and Ugai (2003)	*- Undrained shear strength* (c_u=40 kPa) *- Deformation modulus* (E_s=200c_u=8000 kPa) *uniformly distributed and constant with depth*	-	*-Lateral movement of sliding soil was considered as 137 mm at the ground surface and 40 mm at the sliding surface (88.5 mm in average).*

Case study of Esu and D'Elia (1974) was investigated by using three dimensional finite element analysis software Plaxis 3D. Reinforced concrete pile was modeled as single isolated pile with free head.

Because there is not much information about the geometry of the site, model sizes were selected large enough so that boundary conditions do not influence the results of the pile, soil deflections and structural forces. It was observed that enough accuracy was obtained by choosing model dimensions and surface fixity conditions same as indicated in Chapter 3.3 in also Esu and D'Elia (1974) case.

4.2.1 Geometry of the Model

Schematic illustration, values of the model boundary dimensions and surface fixity conditions of the Esu and D'Elia (1974) case is presented in Figure 4.3, Table 4.11 and Table 4.12. Mesh generation view of Esu and D'Elia (1974) case model is presented in Figure 4.15.

Table 4.11 Model boundary dimensions for case study of Esu and D'Elia (1974)

Pile diameter	**Pile length**	**Embedded pile depth into stable layer**	**Unstable soil depth**	**Width of the model**	**Distance btw. prescribed disp. and pile**	**Length of the model**
d (m)	L (m)	L_{em} (m)	H (m)	S=10d (m)	W_1=5d (m)	W=40d (m)
0.79	30	22.5	7.5	8	4	32

Table 4.12 Surface fixity conditions for case study of Esu and D'Elia (1974)

Surface		**x direction**	**y direction**	**z direction**
Unstable ground	Front side	Free	Fixed	Free
	Rear side	Free	Fixed	Free
	Right side	Fixed	Fixed	Free
	Left side	Prescribed displacement (u_x)	Fixed	Free

Because displacement profile of upper 7.5 m unstable soil was not reported, it was assumed as shown in Figure 4.14 to approximate numerical analysis results to the measured field data.

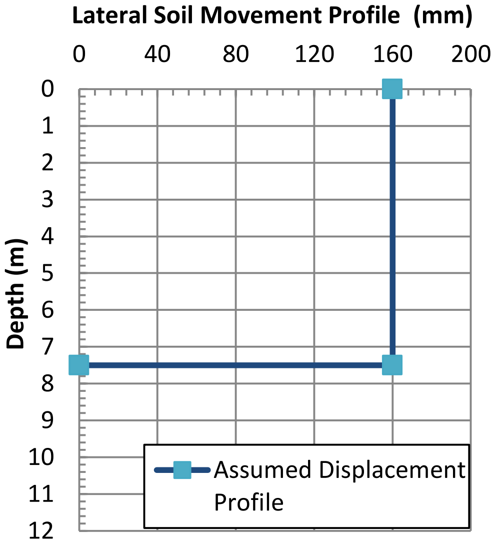

Figure 4.14 Assumed displacement profile for numerical analysis of Esu and D'Elia (1974) case study

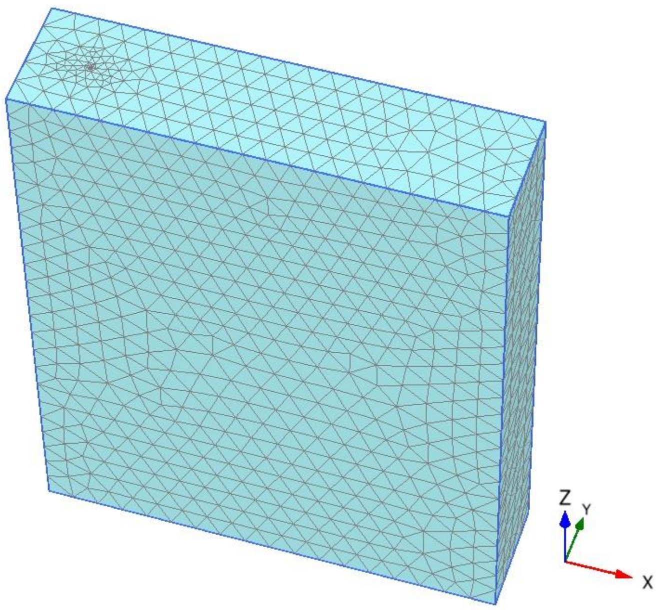

Figure 4.15 Mesh generation for case study of Esu and D'Elia (1974)

Calculation phases implemented for the modeling of the case study are presented in Table 4.13.

Table 4.13 Calculation phases for numerical analysis of Esu and D'Elia (1974) case study

Phase name	**Calculation type**	**Activated model properties**
Initial phase	K_0 procedure	Soils
Phase 1	Plastic	Soils
		Embedded pile
		Surface displacements

4.2.2 Material Properties

Stiffness properties of soil profile and embedded pile were assigned considering the given information and assumptions of some researchers (Chow 1996, Chen and Poulos 1997, Cai and Ugai 2003). Same material properties were used for unstable and stable soils because no distinction was indicated between moving and stationary soils. Assigned material properties for unstable soil, stable soil and embedded pile were listed in Table 4.14 and Table 4.15.

Table 4.14 Material properties of unstable and stable soils for Esu and D'Elia (1974) case study

Parameter			**Value**	**Unit**
General	Material model		Mohr Coulomb	-
	Drainage type		Undrained (C)	-
	Unit weight	γ_{unsat}	18.5	kN/m^3
Strength parameters	Deformation modulus	E_u	8000	kN/m^2
	Poisson's ratio	ν_u	0.495	-
	Cohesion	c_u	40	kN/m^2
	Internal friction angle	ϕ_u	0	°
	Dilatancy angle	Ψ	0	°
	Interface	R_{inter}	0.7	-
Flow parameters	Coefficients of permeability	k_x	0	m/day
		k_y	0	m/day
		k_z	0	m/day

Undrained analysis was carried out for cohesive type of soil material in case study. Plaxis 3D offers several options for adjusting stiffness properties according to the drainage type of soil materials. In undrained (C) option, total stress analysis is conducted by using undrained stiffness and strength parameters. Undrained material parameters were assigned to the soil for this reason. Poisson's ratio for fully undrained material should be theoretically 0.5; however, assignment of this value is not possible because it causes to singularity of the stiffness matrix. Instead, very close value to 0.5 was selected as 0.495.

Table 4.15 Material properties of embedded pile for Esu and D'Elia (1974) case study

Parameter			**Value**	**Unit**
Strength parameters	Deformation modulus	E	$20x10^6$	kN/m^2
	Unit weight	γ	24	kN/m^3
	Predefined pile type	Massive circular pile	-	-
	Pile diameter	d	0.79	m
Skin resistance	Maximum traction allowed at the pile top	$T_{top,max}$	300	kN/m
	Maximum traction allowed at the pile bottom	$T_{bot,max}$	800	kN/m
	Base resistance	F_{max}	1500	kN

4.2.3 Discussion of Results

Three dimensional numerical analysis was conducted for the case study of Esu and D'Elia (1974). Assumed soil movement profiles; deflection, bending moment and shear force distributions through pile length are presented in Figure 4.16.

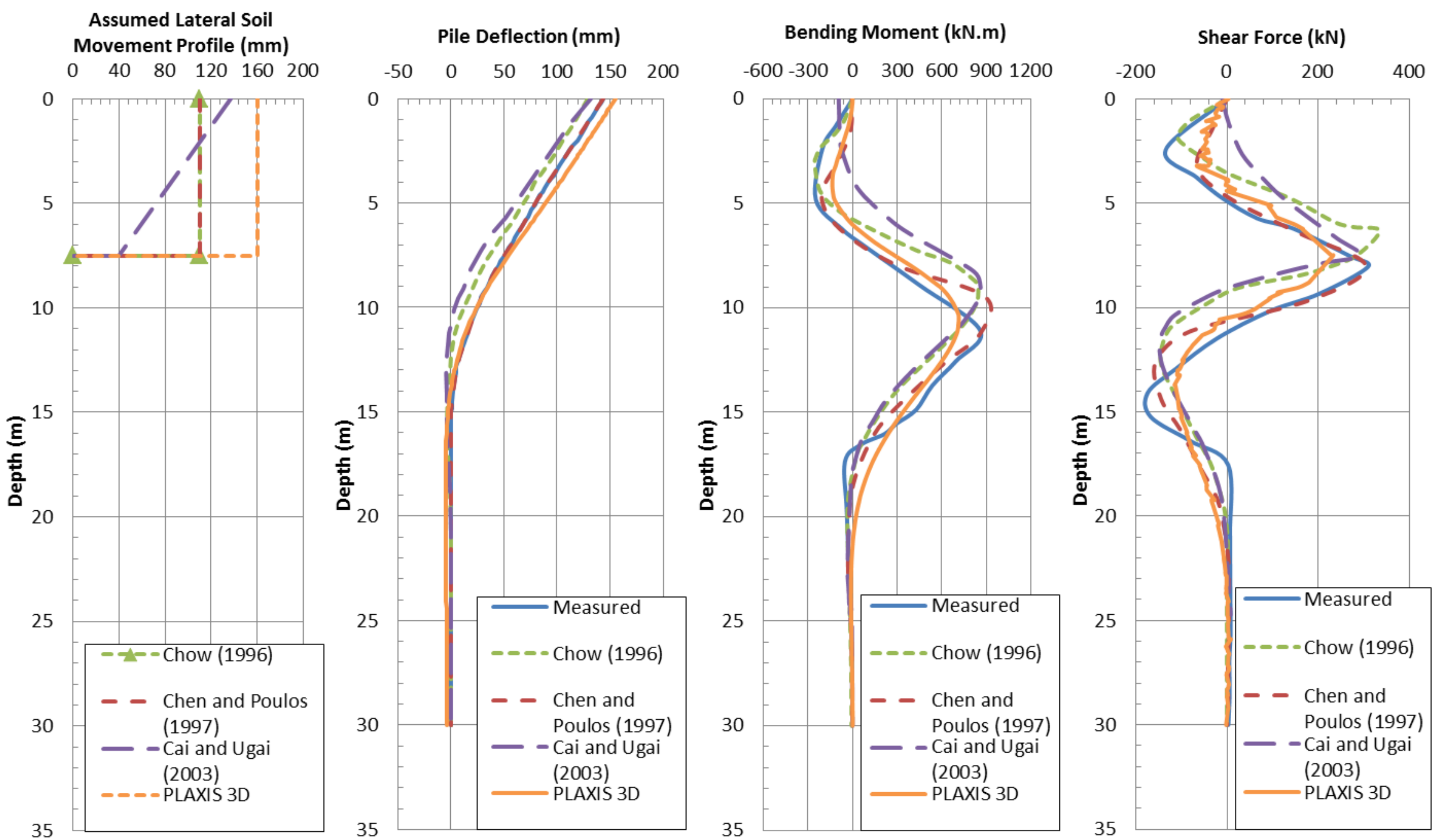

Figure 4.16 Lateral soil movement, pile deflection, bending moment and shear force profiles for case study of Esu and D'Elia (1974)

Lateral soil movement profile in case study was assumed differently by several researchers to match their predictions about pile deflections and forces with the measured field data. For the same reason, uniform distribution of 160 mm soil displacement from ground surface down to the sliding surface was assumed in numerical analysis. This value is higher than the assumptions of other researchers (Chow 1996, Chen and Poulos 1997, Cai and Ugai 2003). This indicates that higher amount of soil movement was required in numerical analysis respect to other approaches to match the same amount of structural forces for relatively same soil properties.

Pile deflection profile of numerical analysis was compared with the measured field data and other approximations. Maximum pile deflection was observed around 150 mm at the ground surface. This value is very similar to the measured field data (Figure 4.16).

Bending moment distribution of case study as a result of numerical analysis was plotted with the actual field data and other approaches. Maximum bending moment was observed as 715 kN.m at 11 m depth. As it can be seen in Figure 4.16, maximum value was underestimated by 15 %; however, the depth where maximum bending moment occurred was accurately predicted. In addition, general bending moment distribution through pile length shows good agreement with the measured field data.

Shear force distribution acting on the pile shaft is also presented in Figure 4.16. The depth maximum shear force developed was well predicted as 7.5 m; however, value of the maximum was underestimated by 20 %. Maximum shear force was observed as 235 kN at the level of sliding surface.

Distribution of lateral deformations in the direction of soil movement is presented for the case study. Deformation distributions for different horizontal cross sections were plotted in Figure 4.17. Vertical cross section in a line passing through center of the pile was plotted as shown in Figure 4.18.

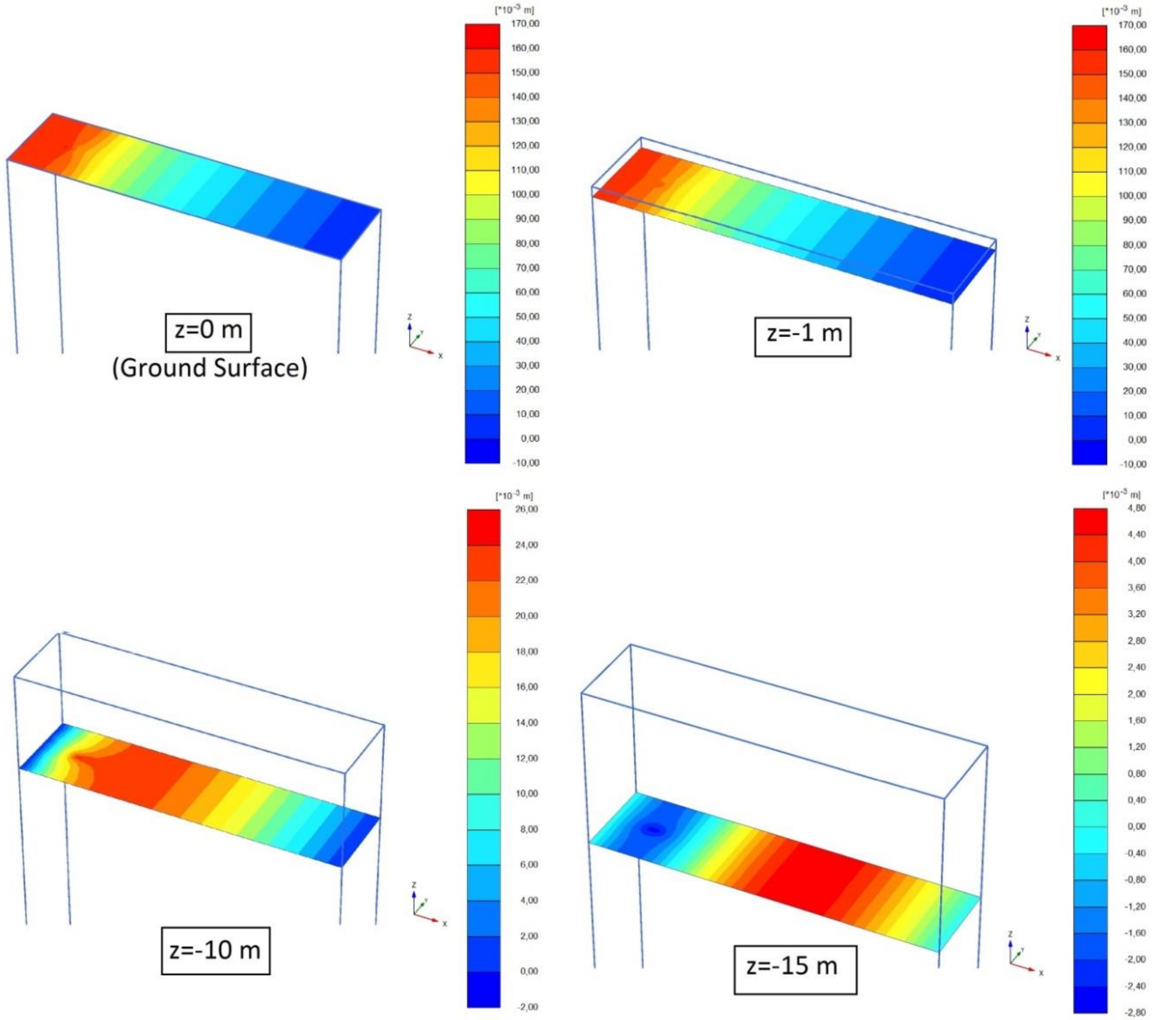

Figure 4.17 Lateral deformation distribution of Esu and D'Elia (1974) case study for different horizontal cross sections

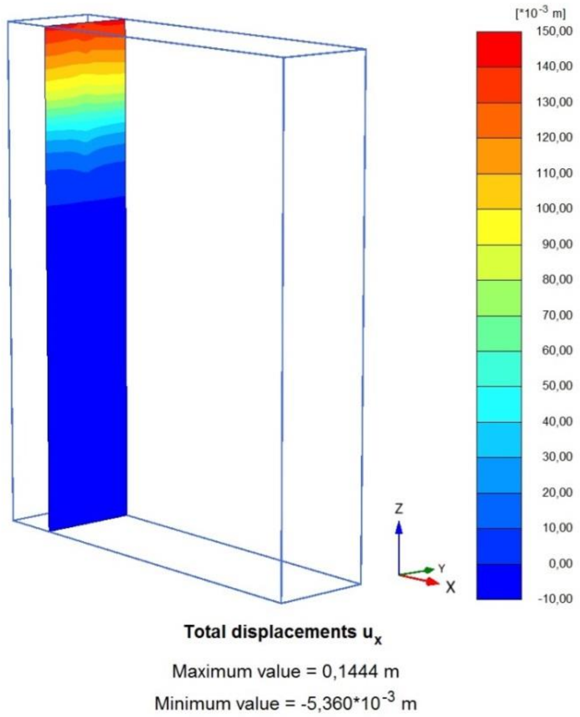

Figure 4.18 Lateral deformation distribution for Esu and D'Elia (1974) case study in a vertical cross section through center of the pile

Analyses were conducted without matching purpose of force and displacement values of a specific point with the experimental data. Numerical analysis provides continuous calculation of forces and displacements on both structural elements and soil formations. Yet, magnitude and distribution of pile deflections, bending moments and shear forces were estimated with satisfactory accuracy.

In conclusion, three dimensional numerical analysis with finite element method is capable of predicting actual passive pile response in laterally moving slopes. Although other approaches used in this manner are consistent with the measured field data, their methodologies are far more complex. In addition, they include some preconditions and assumptions in their method of analysis about homogeneity of the soil profile or pile flexibility. However, pile soil interaction behavior can be modeled as appropriate to the complexity of the problem by 3D numerical analysis. All kinds of model geometries, non-homogenous soil stratigraphy with varying material properties can be introduced for simulating the true nature of the problem. In addition, soil arching behavior could be captured with three dimensional analyses unlike the other methods. For this reason, assumption of larger soil movement was required respect to the other approaches to match same amount of structural forces and displacements in case study of Esu and D'Elia (1974).

CHAPTER 5

PARAMETRIC STUDY

Variations in the factors affecting the passive pile behavior were investigated in series of parametric analyses for both cohesive and granular materials. After verification of the finite element solution in case studies, numerical models were developed to evaluate relationship between the factors that affect the design of piles for slope stabilization works. There are several factors and parameters affecting the slope stabilizing pile response as some of them are summarized in Table 2.3. In the scope of this parametric study, effect of pile embedment depth, strength ratio of unstable and stable soils, unstable soil properties, pile spacing and amount of lateral soil movement on passive pile response were studied by systematically changing the related parameters.

5.1 Description of Simplified Models

Unstable soil thicknesses of 5 m and 10 m were used in parametric analyses. These values were considered to be common slide thickness for landslide cases of shallow and intermediate scale. Sliding of upper unstable soil above a stable ground was sustained by assigning predefined deformations in shear box models by using Mohr Coulomb material model as explained in Chapter 3.2.

Two sets of analyses were conducted for the investigation of parameters. In first series, determination of pile embedment depth and the effect of the strength ratio between unstable and stable soils were studied in a 10 m sliding soil. Reinforced concrete single piles in a row were used for this purpose. Appropriate embedment depth of pile into a stationary layer was investigated for different unstable and stable ground stiffness alternatives. In second series, effect of pile spacing was investigated with the variation of unstable soil properties and amount of lateral soil movement. In the scope of analyses, three reinforced concrete piles in a row were socketed into a very stiff stationary rock with different spacings. Unstable soil thickness of 5 m was used for the investigation of pile spacing effect.

Boundary fixity conditions were assumed same as in Chapter 3.3 for all of the parametric analyses. Model dimensions for single pile analyses are presented in Table 5.1.

In analyses for the determination of pile spacing effect (three piles in a row), width of the model was selected as three times of pile spacing (Figure 5.1). Pile spacing ratio (s/d) alternatives of 2, 4, 6, 8, 10 and 20 were used in analyses. Selected boundary dimensions according to the pile spacing variations are presented in Table 5.2.

Table 5.1 Model boundary dimensions for single pile analyses

Pile diameter	Unstable soil depth	Width of the model	Distance btw. prescribed disp. and pile	Length of the model
d (m)	H (m)	S=10d (m)	W_1=5d (m)	W=40d (m)
1	10	10	5	40

Table 5.2 Model boundary dimensions for analyses with three piles in a row

Pile spacing/pile diameter	Pile diameter	Unstable soil depth	Width of the model	Distance btw. prescribed disp. and pile	Length of the model
s/d	d (m)	H (m)	S=3s (m)	W_1=5d (m)	W=40d (m)
20	1	5	60	5	40
10	1	5	30	5	40
8	1	5	24	5	40
6	1	5	18	5	40
4	1	5	12	5	40
2	1	5	6	5	40

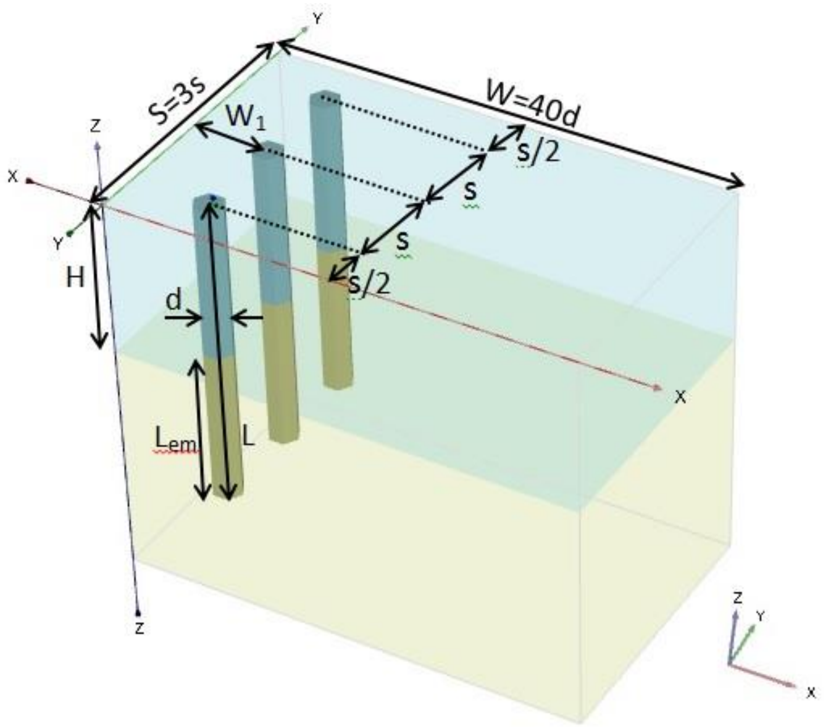

Figure 5.1 Model view of the analyses with three piles in a row

Medium type of mesh was selected for general mesh element size in all analyses. 6 edged cylindrical soil volume having the same properties with the surrounding ground was defined also in parametric analyses (Figure 5.1). Local fineness just around the embedded piles was obtained in this way.

5.2 Material Properties

Cohesive and granular type of soil materials were studied in parametric models as unstable and stable soils. Determination of appropriate pile embedment depth mainly depends on the strength ratio between stable and unstable soils. Therefore, stable soil parameters were selected as the strength of the stable layer would be the positive multitudes of the unstable soil strength. Because strength ratio can be defined as undrained shear strength ratios of stable and unstable soils for cohesive materials (Equation 5.1), undrained behavior of soft, medium and stiff clayey soils was investigated as sliding material for simplicity in pile embedment depth analyses.

$$\text{Strength ratio (SR)} = \frac{c_{u(stable)}}{c_{u(unstable)}} \tag{5.1}$$

Ultimate soil pressures for undrained cohesive materials are expressed in terms of undrained shear strength of that soil such as P_u=N_p.c_u where N_p is a dimensionless coefficient. Therefore definition of strength ratio indicates ultimate soil pressure ratios of related soils as well.

Strength ratios of 1, 3 and 5 were considered in analyses for the determination of stable soil strength parameters for soft, medium and stiff clay type of unstable soils. Material properties of unstable ground for the determination of pile embedment depth are presented in Table 5.3.

Drained analyses of granular materials were conducted for both sliding and stable layers in pile spacing analyses. Three piles in a row with different pile spacings were embedded in a very stiff rock. Unstable cohesionless materials of loose silty sand and dense sand having a sliding thickness of 5 m were selected for investigation. Thus, clear visualization of relative pile soil displacement was obtained that is required for the evaluation of soil arching. Material properties of unstable and stable soils for pile spacing analyses are presented in Table 5.4.

Same pile properties were used in all of the analyses as presented in Table 5.5.

Table 5.3 Material properties of unstable soil for the analyses of pile embedment depth

Unstable soil type	Material properties							
	General			Strength parameters				
	Material model	Drainage type	Unit weight, γ_{unsat} (kN/m^3)	Undrained shear strength, c_u (kN/m^2)	Deformation modulus, E_u (kN/m^3)	Poisson's ratio, ν_u	Internal friction angle, ϕ_u	Dilatancy angle, Ψ
Soft clay	Mohr Coulomb	Undrained	17.0	20	4000 ($200c_u$)	0.495	0	0
Medium clay	Mohr Coulomb	Undrained	18.0	50	12500 ($250c_u$)	0.495	0	0
Stiff clay	Mohr Coulomb	Undrained	18.5	100	30000 ($300c_u$)	0.495	0	0

Table 5.4 Material properties of unstable and stable soils for the analyses of pile spacing

		Material properties							
		General			Strength parameters				
		Material model	Drainage type	Unit weight, γ (kN/m^3)	Undrained shear strength, c' (kN/m^2)	Deformation modulus, E (kN/m^3)	Poisson's ratio, ν	Internal friction angle, ϕ'	Dilatancy angle, Ψ
Unstable soil	Loose silty sand	Mohr Coulomb	Drained	17.5	3	40000	0.3	20	2
	Dense sand	Mohr Coulomb	Drained	18.0	3	120000	0.3	35	2
Stable soil	Stiff rock	Mohr Coulomb	Drained	20.0	50	$1*10^6$	0.25	45	5

Table 5.5 Material properties of embedded pile for all analyses

Parameter			Value	Unit
Strength parameters	Deformation modulus	E	$20x10^6$	kN/m^2
	Unit weight	γ	24	kN/m^3
	Predefined pile type	Massive circular pile	-	-
	Pile diameter	d	1	m
Skin resistance	Maximum traction allowed at the pile top	$T_{top,max}$	500	kN/m
	Maximum traction allowed at the pile bottom	$T_{bot,max}$	500	kN/m
	Base resistance	F_{max}	5000	kN

5.3 Parametric Analyses

Two series of analyses were conducted by Plaxis 3D for the investigation of interrelation between the parameters. In the first one, embedment depth of pile into a stable layer and effect of stiffness ratio between the stable and unstable ground were investigated for different soils. In the second part, the effect of pile spacing on passive pile response was studied with the variation of material properties of unstable ground and amount of lateral soil movement.

5.3.1 Pile Embedment Depth and Effect of the Stable Soil Strength

Appropriate embedment depth of pile into a stationary layer was studied with the variation of strength ratio between unstable and stable soils for different sliding ground materials. For this purpose, single reinforced concrete piles were socketed into a stable layer in different lengths. Pile embedment depths were considered in terms of the multitudes of unstable soil thickness (H). Soft, medium and stiff clay materials were considered as unstable soil. Material properties of stationary soil were decided according to the strength ratio values of 1, 3 and 5 for each unstable ground material.

Analyses were performed for 5 cm lateral movement of 10 m thick unstable soil on a stable ground. Variation of parameters for the analysis of pile embedment depth is listed in Table 5.6.

Table 5.6 Variation of pile embedment depth, strength ratio and unstable soil type for analyses

Unstable soil type	Strength parameters of unstable soil		Strength ratio (SR)	$c_{u(stable)}$ (kPa)	Unstable soil depth, H (m)	Pile embedment depth, L_{em} (m)	Pile length, L (m)	Lateral prescribed movement	
	c_u (kPa)	E_u (kPa)	$\frac{c_{u(stable)}}{c_{u(unstable)}}$					ε=u/D	u_x (cm)
Soft clay	20	4000 ($200c_u$)	1	20	10	0.25H=2.5	12.5	0.05	5
						0.5H=5	15		
						1.0H=10	20		
						1.5H=15	25		
			3	60	"	0.25H=2.5	12.5		
						0.5H=5	15		
						1.0H=10	20		
						1.5H=15	25		
			5	100	"	0.25H=2.5	12.5		
						0.5H=5	15		
						1.0H=10	20		
						1.5H=15	25		
Medium clay	50	12500 ($250c_u$)	1	50	"	0.25H=2.5	12.5	"	"
						0.5H=5	15		
						1.0H=10	20		
						1.5H=15	25		
			3	150	"	0.25H=2.5	12.5		
						0.5H=5	15		
						1.0H=10	20		
						1.5H=15	25		
			5	250	"	0.25H=2.5	12.5		
						0.5H=5	15		
						1.0H=10	20		
						1.5H=15	25		
Stiff clay	100	30000 ($300c_u$)	1	100	"	0.25H=2.5	12.5	"	"
						0.5H=5	15		
						1.0H=10	20		
						1.5H=15	25		
			3	300	"	0.25H=2.5	12.5		
						0.5H=5	15		
						1.0H=10	20		
						1.5H=15	25		
			5	500	"	0.25H=2.5	12.5		
						0.5H=5	15		
						1.0H=10	20		
						1.5H=15	25		

Note:
**All models were also analyzed for no pile conditions*
**Single pile models were used in analyses*

Analyses for the investigation of sufficient embedment depth were conducted for 5 cm lateral movement of unstable soil material as explained before (Table 5.6). This value was chosen because resultant bending moment and forces occurred in the pile shaft should not reach or exceed the ultimate pile capacity values in practical slope stabilization works. Additionally, further analyses concluded that different lateral movement values cause variations in bending moment and shear force results; however, it does not create significant influence on the required embedment depth evaluation without exceeding pile capacities.

Shear force, bending moment, horizontal deflection values and distributions through pile shaft were evaluated for the analyses which parameter variations are shown in Table 5.6. Maximum shear force values for different unstable soil materials and strength ratio values are presented in Figure 5.2. Bending moment distributions for soft medium and stiff type of unstable soils are presented in Figure 5.3, Figure 5.4 and Figure 5.5. Pile deflection profiles for unstable soil of medium clay are presented in Figure 5.6.

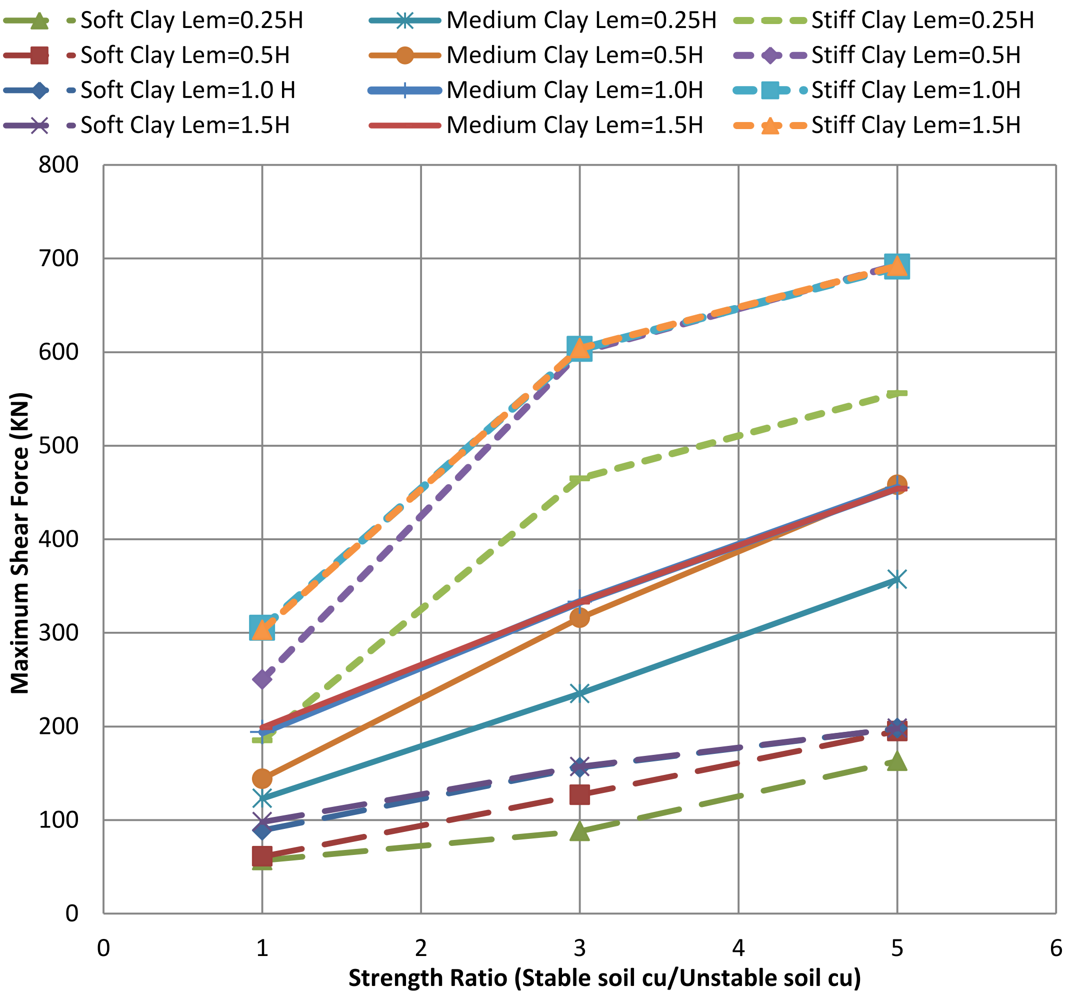

Figure 5.2 Maximum shear force developed in pile shaft for soft, medium, stiff clay type of unstable soils and strength ratio variations of 1, 3, 5
(lateral soil movement, u_x=5 cm; unstable soil thickness H=10 m)

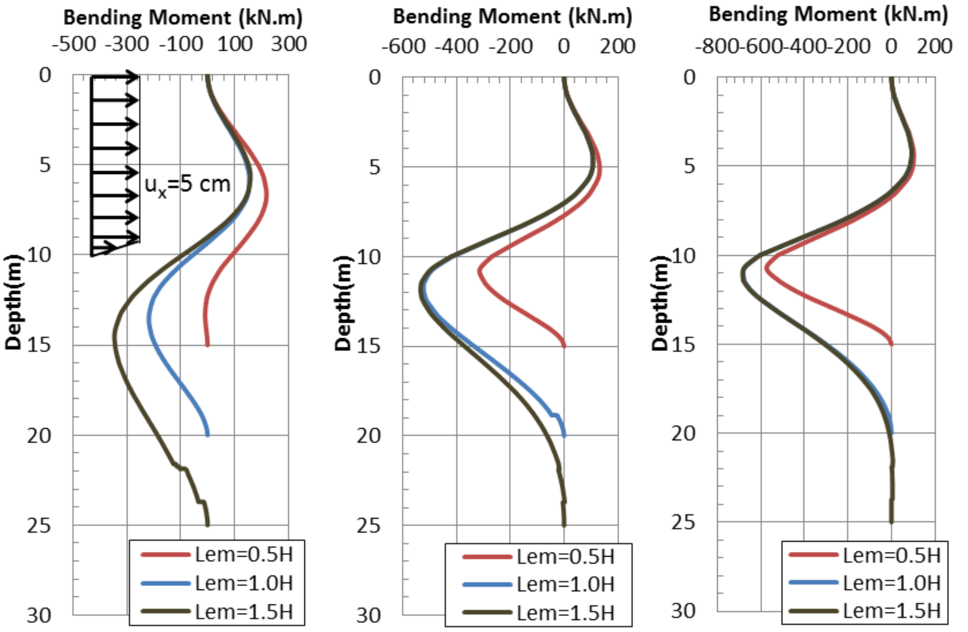

Strength Ratio, (SR)=1 Strength Ratio, (SR)=3 Strength Ratio, (SR)=5

Figure 5.3 Bending moment distributions for unstable soil of soft clay (piles were embedded in stable soils which strength properties determined by strength ratio of 1,3 and 5)

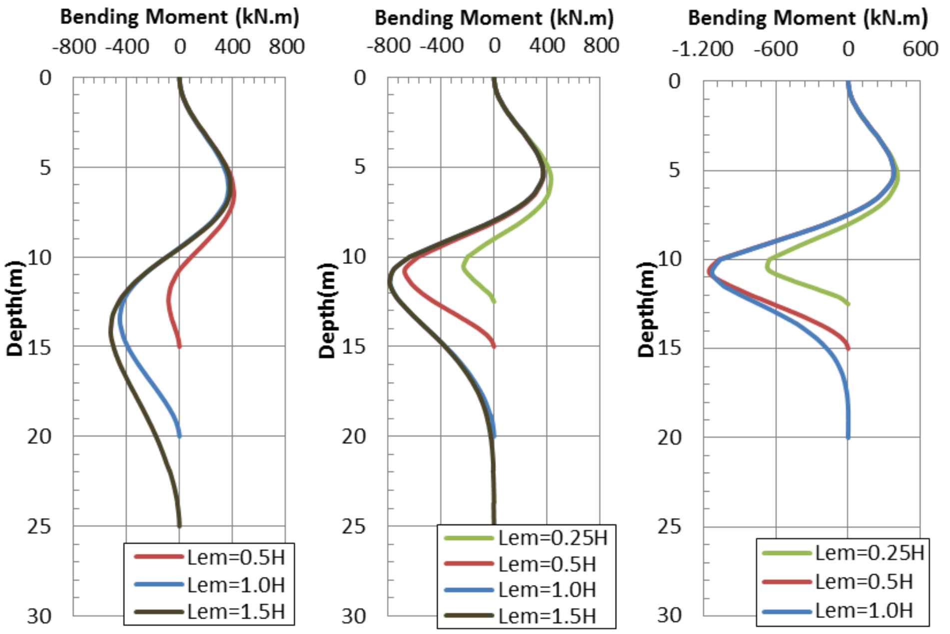

Strength Ratio, (SR)=1 Strength Ratio, (SR)=3 Strength Ratio, (SR)=5

Figure 5.4 Bending moment distributions for unstable soil of medium clay (piles were embedded in stable soils which strength properties determined by strength ratio of 1,3 and 5)

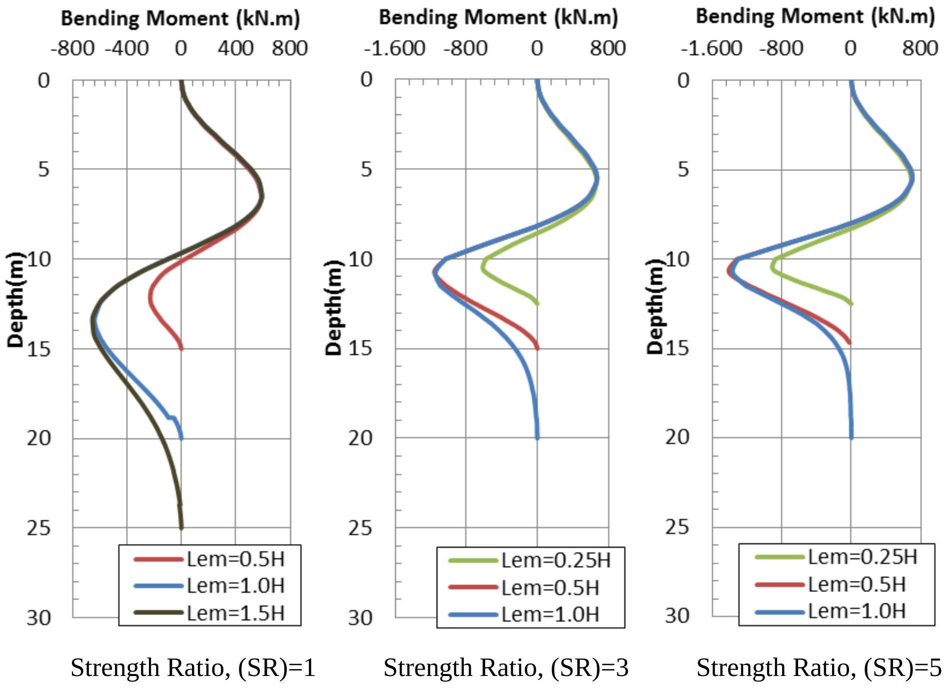

Figure 5.5 Bending moment distributions for unstable soil of stiff clay (piles were embedded in stable soils which strength properties determined by strength ratio of 1,3 and 5)

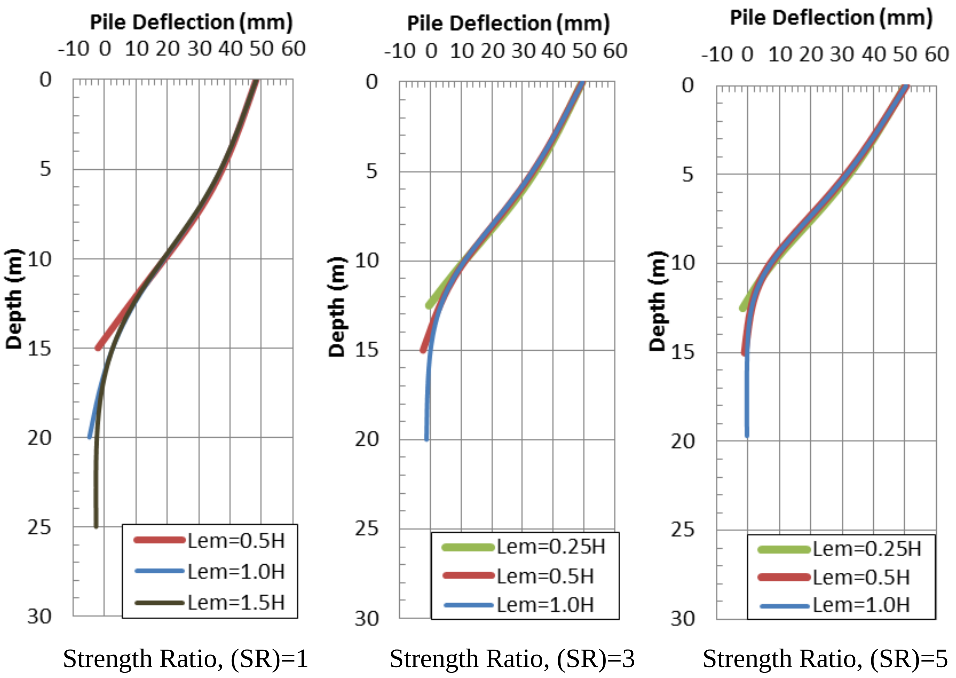

Figure 5.6 Pile deflection distributions for unstable soil of medium clay (piles were embedded in stable soils which strength properties determined by strength ratio of 1,3 and 5)

It was observed that maximum shear force values were developed in the depth of sliding zone between unstable and stable soils as expected. Therefore, these values can also be treated as pile resistance force occurred in the pile shaft because of the lateral loading of unstable soil thickness.

Increase in stable soil strength for the same unstable ground material type cause increase in horizontal force exerted by soil. As shown in figure 5.2, increase in strength ratio has more dramatic effect on the horizontal force for stiff clay type of unstable soils.

Horizontal soil force exerted on pile increases as pile embedment depth into a stable layer increases for all type of unstable and stable soil strength variations (Figure 5.2). There is a critical embedment depth providing sufficient pile end fixity condition (flexural bending rather than rigid body rotation). Beyond this critical embedment depth, pile force exerted by soil remains constant for longer embedment depths for same amount of loading condition.

As sliding soil strength increases (soft clay to stiff clay) horizontal force exerted by soil on pile also increases. However, strength ratio between stable and unstable soils, strength ratio (SR), has more effect on the resultant pile force for all soil types as it can be seen in Figure 5.2. Therefore strength ratio is an important factor for the determination of sufficient embedment depth of pile into stable layer. However, only strength ratio may not be adequate for the determination of the critical pile embedment depth. Stable, unstable soil properties and amount of their strength values should be also considered besides their ratio. Therefore, critical embedment depths were evaluated separately for soft, medium and stiff clay type of unstable soils.

As ratio between unstable and stable soils (SR) increases, critical embedment depth decreases for all soil types. This is expected because increase in strength ratio means increase in strength and stiffness properties of stable ground where main pile resistance develop from. Thus, shorter pile embedment could create sufficient pile resistance with stiffer stable soils.

Amount of critical embedment depth could be determined by the evaluation of pile deflection, shear force and bending moment developed in the pile shaft. In pile deflection evaluation, end of the pile should be fixed for economical slope stabilizing pile designs. Pile should be long enough to prevent bottom of the pile to move or rotate because of the force exerted by soil movement. Rigid body rotation causes short pile failure which is attributed to insufficient pile embedment length. Pile deflection profiles for unstable soil of medium clay are presented in Figure 5.6. Longer embedment depths cause flexural bending of the pile with end of the pile is stationary as it can be seen in the figure. This evaluation gives an idea about the required critical embedment depth. Similar pile deflection graphs were obtained for all unstable soil types.

Briefly, critical depth for pile embedment can be determined from pile deflection graph satisfying flexural bending of the pile shaft while end of the pile is stationary. Besides, bending moment and shear force distributions for different embedment depths is another important evaluation parameter. Bending moment and shear force values reaches their maximum at a depth near the slip plane and remains constant for longer embedment depths than a certain critical embedment for a specific loading condition (Figure 5.3, Figure 5.4 and Figure 5.5). Beyond this critical embedment depth longer pile embedments do not create additional pile resistance (Figure 5.2).

Ranges of critical pile embedment for different unstable soils and stable strength variations were determined considering above parameters. First, unstable soil of soft clay was evaluated for different strength ratio variations (Figure 5.2 and Figure 5.3). If both unstable and stable soil materials consists of soft clay (SR=1), embedment depth which is 1.5 times of unstable soil thickness (L_{em}=1.5H) is not sufficient to create enough pile resistance and pile fixity. Therefore, deeper pile embedments than L_{em}=1.5H should be applied to uniform soft clay soil formations. In the case of SR=3 and SR=5 for unstable soft clay material, same amount of maximum bending moment and shear force values were obtained for L_{em}=1.5H and L_{em}=1.0H (Figure 5.2 and Figure 5.3). Differences may start to occur in values when L_{em}=0.5H. Therefore, critical pile embedment should be in the range of $L_{em(critical)}$=1.0H-0.50H. Exact value of the critical embedment depth approaches to 0.5H from 1.0H as strength ratio gets increase (SR=3 to SR=5) for soft clay.

Ranges of critical embedment depths were also determined by using the same evaluation method for medium and stiff clay type of unstable soil materials as shown in Table 5.7.

Table 5.7 Range of critical embedment depths for different unstable soil materials and strength ratio variation (H=unstable soil thickness)

Strength ratio, (SR) $\frac{c_{u(stable)}}{c_{u(unstable)}}$	**Unstable soil materials**		
	Soft clay	**Medium clay**	**Stiff clay**
SR=1	>1.5H	1.5H-1.0H	1.0H-0.5H
SR=3	1.0H-0.5H	1.0H-0.5H	0.5H-0.25H
SR=5	1.0H-0.5H	0.5H-0.25H	0.5H-0.25H

Kourkoulis et al. (2011) found that critical embedment depth of pile into a stable layer could be range from $L_{em(critical)}=1.5H_u$ for $P_{u(stable)}=P_{u(unstable)}$ to $L_{em(critical)}=0.7H_u$ for $P_{u(stable)}=3P_{u(unstable)}$ where; H_u is the thickness of unstable soil layer, $P_{u(stable)}$ and $P_{u(unstable)}$ are ultimate passive soil pressures provided by stable and unstable layers. Ranges of critical embedment depth for different unstable soil materials presented in Table 5.7 show good agreement with the findings of Kourkoulis et al. (2011).

5.3.2 Effect of Pile Spacing

Effect of pile spacing on pile response was evaluated by shear box models with the variation of unstable soil properties and amount of lateral soil movement. Unstable soil thickness (H) was selected as 5 m and analyses were conducted for three piles in a row embedded in a very stiff rock (Table 5.2). Pile embedment depth was selected as the thickness of unstable soil layer (L_{em}=H) to guarantee full pile end fixity conditions.

Drained analyses were applied for two types of granular soils namely; loose silty sand and dense sand. Unstable soil movements of u_x=5 cm and u_x=10 cm were assigned for both loose silty sand and dense sand. Pile response was evaluated for pile spacing (s/d) alternatives of 2, 4, 6, 8, 10 and 20. Variation of parameters for the analyses of pile spacing effect was summarized in Table 5.8.

Table 5.8 Variation of the parameters for the analyses of pile spacing effect

Unstable soil		**Stable soil parameters**	**Unstable soil depth, H (m)**	**Pile embedment depth, L_{em} (m)**	**Pile spacing (s/d)**	**Lateral prescribed movement**	
Type	**Parameters**					**ε=u/D**	**u_x (cm)**
Loose silty sand	c'= 3 kPa ϕ'=20° E'=40000 kPa Ψ=2°	c'= 50 kPa ϕ'=45° E'=1x10^6 kPa Ψ=2°	5	H=5	20	0.05	5
						0.10	10
					10	0.05	5
						0.10	10
					8	0.05	5
						0.10	10
					6	0.05	5
						0.10	10
					4	0.05	5
						0.10	10
					2	0.05	5
						0.10	10
Dense sand	c'= 3 kPa ϕ'=35° E'=120000 kPa Ψ=2°	c'= 50 kPa ϕ'=45° E'=1x10^6 kPa Ψ=2°	5	H=5	20	0.05	5
						0.10	10
					10	0.05	5
						0.10	10
					8	0.05	5
						0.10	10
					6	0.05	5
						0.10	10
					4	0.05	5
						0.10	10
					2	0.05	5
						0.10	10

Pile spacing is an important design parameter for the slope stabilization works with piles. Selection of appropriate pile spacing provides an economic and efficient design. Therefore, studies on this topic are mainly focused on the determination of suitable pile spacing. There are two main considerations in pile design that are most affected from the spacing between the piles. These are soil arching and group action reduction.

Development of strong soil arching is crucial and one of the fundamental purposes of slope stabilization with piles. Soil arching could be defined as the stress transfer between a yielding part of a soil mass and a less yielding or stationary parts of soil masses. Degree of arching could be estimated from the ratio of u_{ip}/u_p (Figure 5.7); where, u_{ip} is interpile ground displacement (horizontal soil displacement in the middle, between the piles) and u_p is the displacement of the pile head (Kourkoulis 2011). This approximation gives an idea about the relative pile soil displacement which is most critical at the ground surface for free headed piles. It can also be observed in general model view and vertical cross section passing through pile heads that are presented in Figure 5.8 and Figure 5.9.

Low values of u_{ip}/u_p indicates strong soil arching which means relative movement of soil between the piles is low and the stability could be achived. On the other hand, higher values of u_{ip}/u_p indicates that soil between the piles plastically flow and the piles behave ineffectively in terms of slope stabilization.

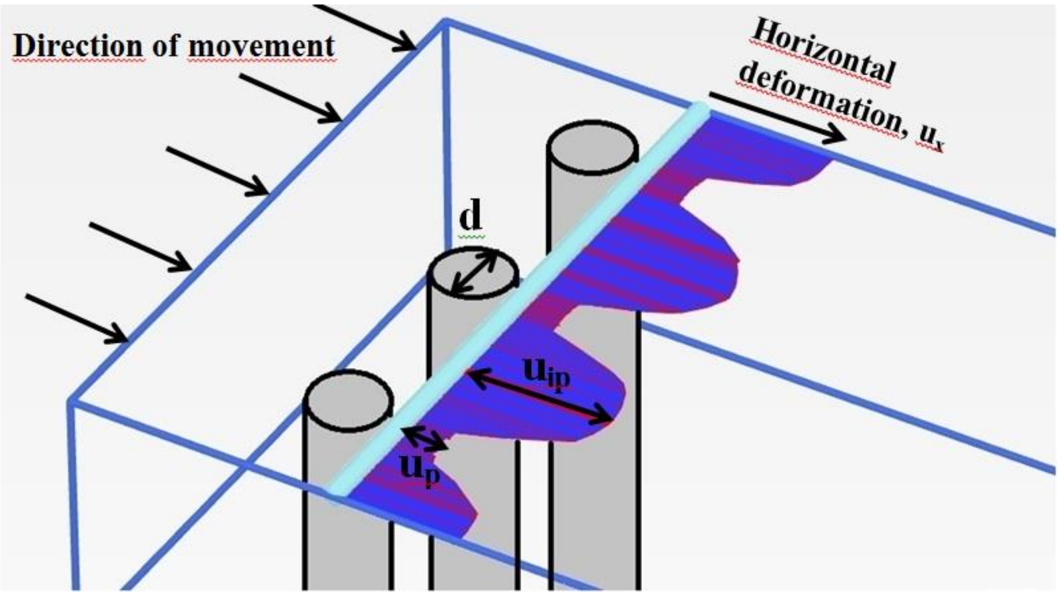

Figure 5.7 Horizontal deformation distribution in a line passing through the heads of the piles

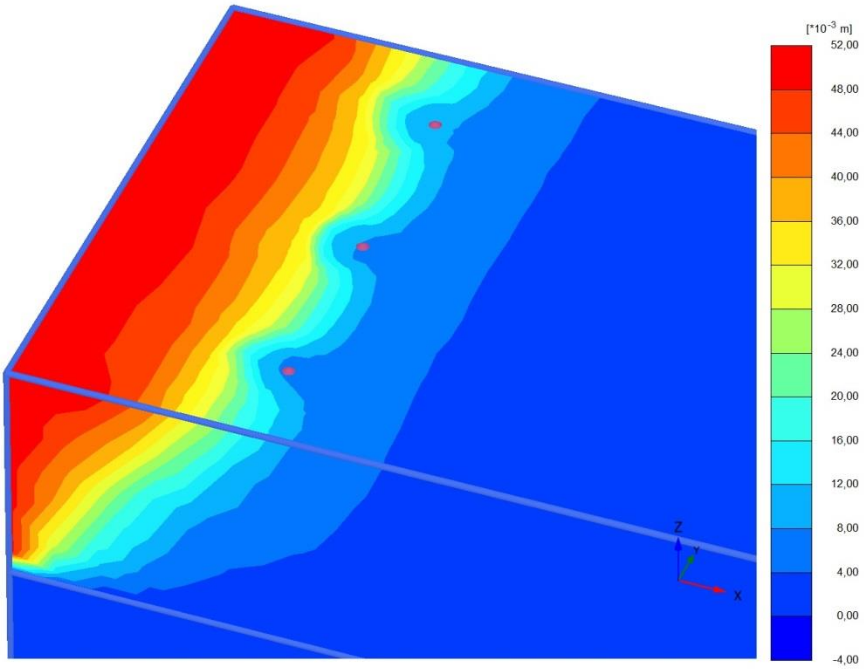

Figure 5.8 General model view for horizontal deformation distribution in multiple piles in a row

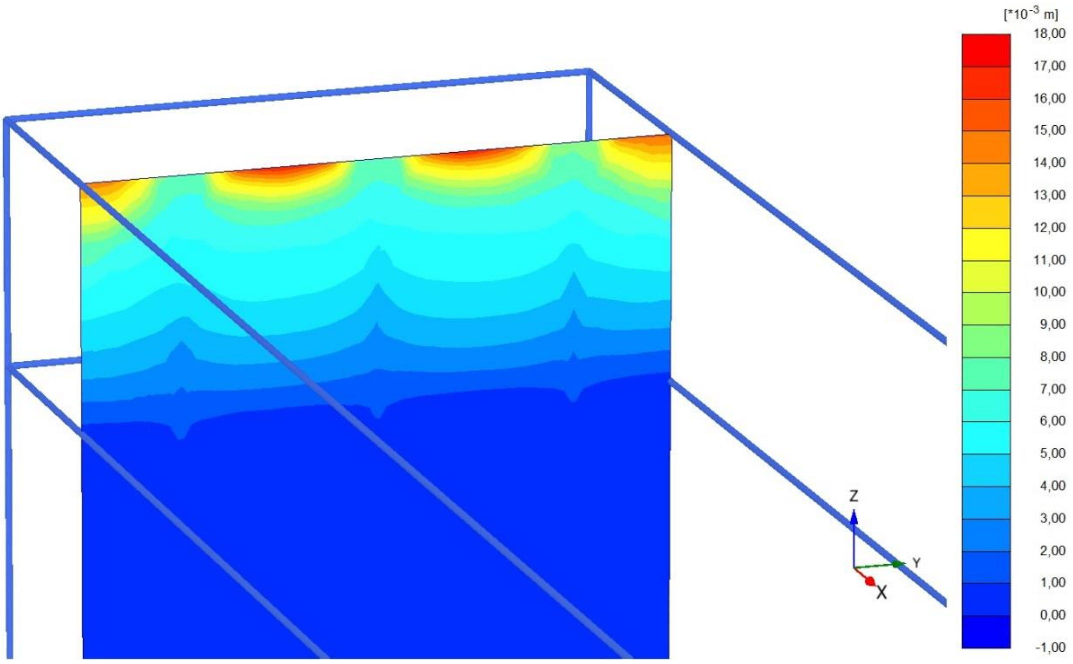

Figure 5.9 Horizontal deformation distribution in a vertical cross section passing through the pile heads in multiple piles in a row

Lateral load exerted to a pile in a group of piles could be significantly less than the load on an individual pile. Possible reductions because of the group behavior is defined as group action reduction. Pile spacing is the most important factor affecting this phenomena. Group reductions should be controlled with spacing between the piles for an effective design.

Consequently, Influence of pile spacing on soil arching and group action reduction were evaluated for the optimum pile spacing determination. For this purpose different pile spacing alternatives were analyzed with the variation of unstable soil properties and the amount of lateral soil movement as it can be seen in Table 5.8.

Relative pile soil displacement (u_{ip}/u_p) variation at the pile head with different pile spacing alternatives is plotted in Figure 5.10 according to the analysis results. In addition, average maximum soil force and average maximum bending moment per pile are plotted for the variation of pile spacing as presented in Figure 5.11 and 5.12.

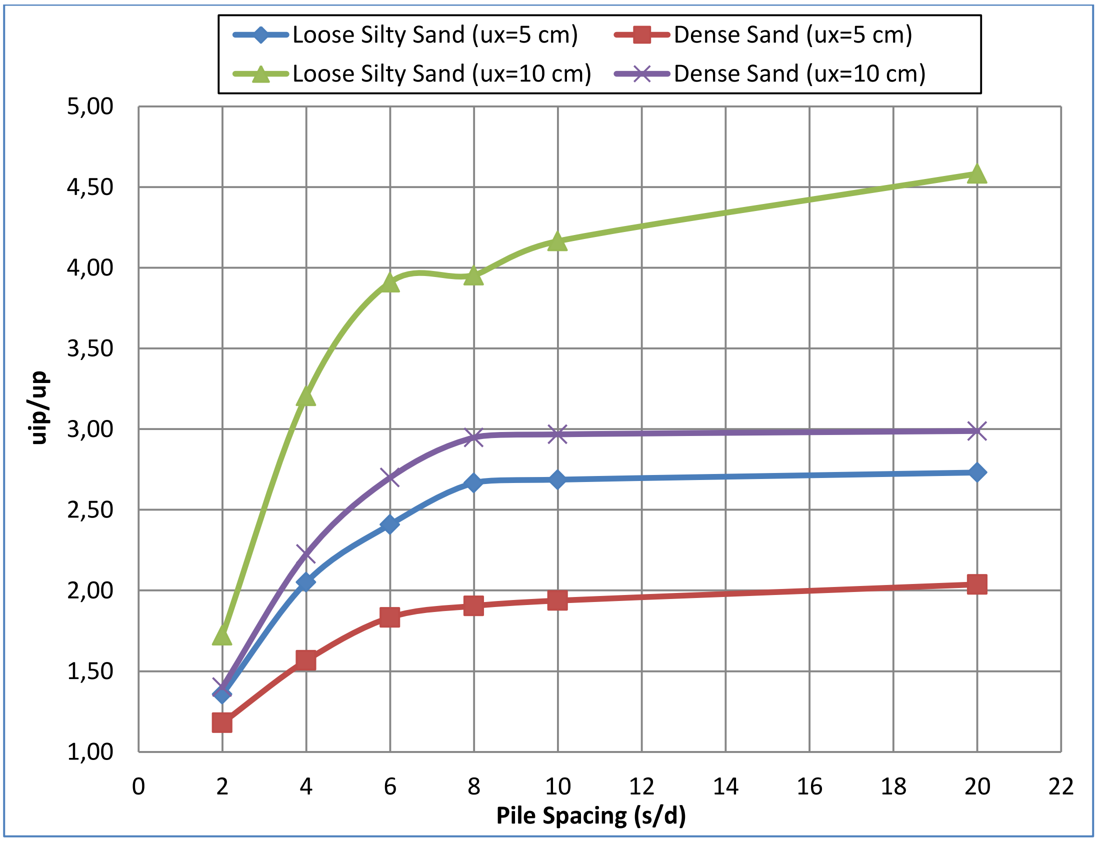

Figure 5.10 Ratio of soil displacement (in the middle between piles) to pile head displacement (u_{ip}/u_p) with the variation of pile spacing for loose silty sand and dense sand for two different lateral soil movement alternatives, u_x=5 cm and u_x=10 cm

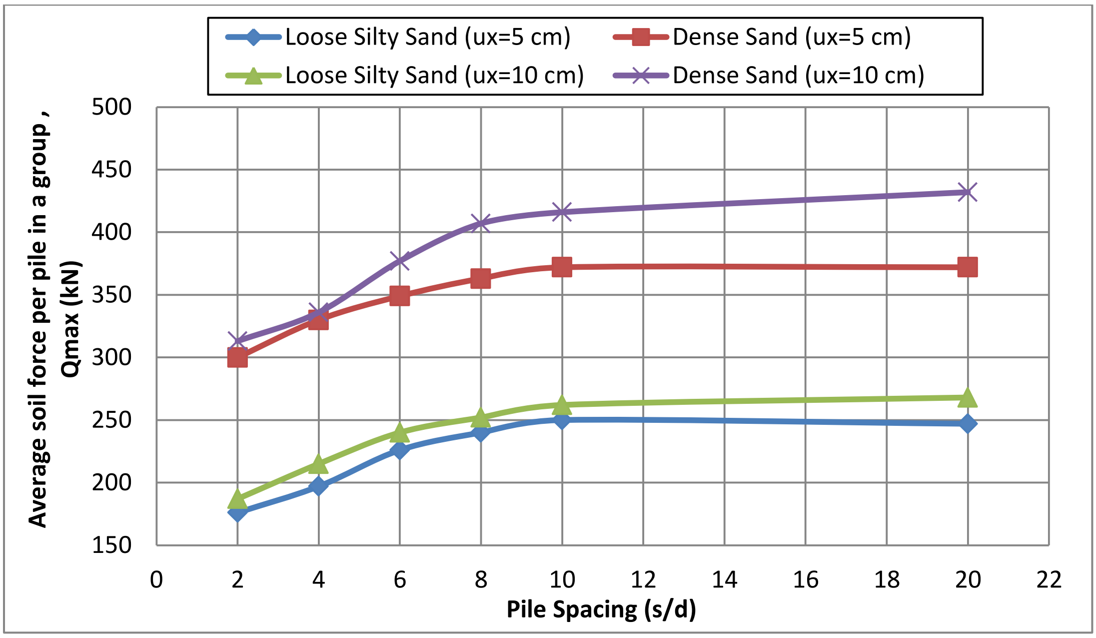

Figure 5.11 Average soil force per pile in a group with the variation of pile spacing for loose silty sand and dense sand for two different lateral soil movement alternatives, u_x=5 cm and u_x=10 cm

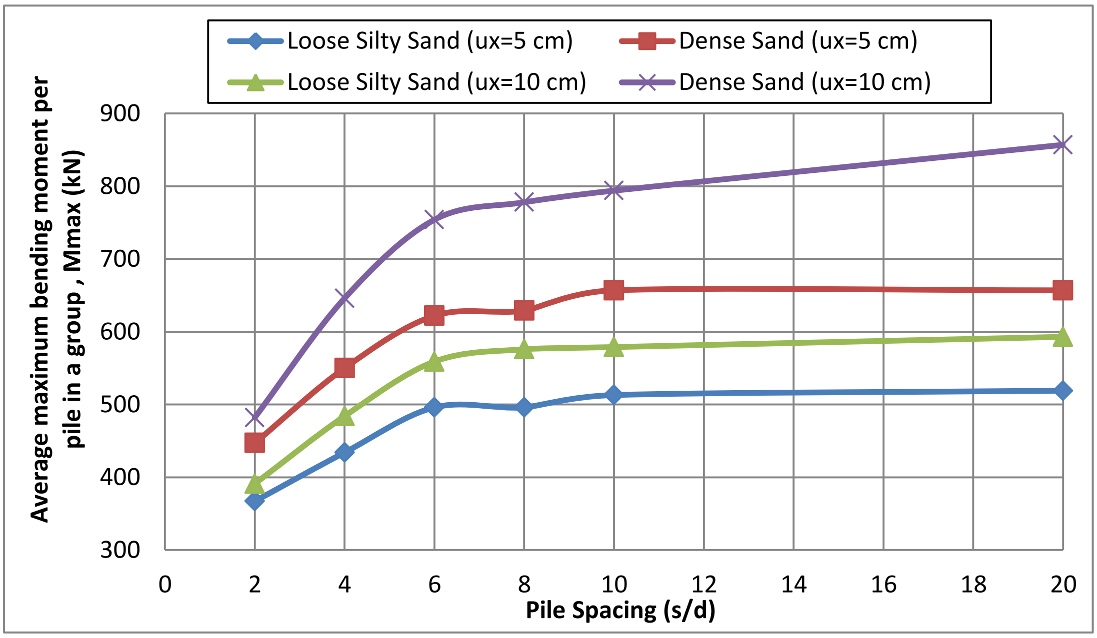

Figure 5.12 Average maximum bending moment per pile in a group with the variation of pile spacing for loose silty sand and dense sand for two different lateral soil movement alternatives, u_x=5 cm and u_x=10 cm

As explained before increase in the value of the ratio between soil and the pile head displacement (u_{ip}/u_p) means decrease in soil arching. In other words, sliding soil flows between the piles. On the other hand, strong soil arching develops for the low values of the relative pile soil displacement (u_{ip}/u_p). As shown in Figure 5.10, value of the relative pile soil displacement, u_{ip}/u_p increases with the increase of the spacing between the piles. Therefore, it can be concluded that amount of soil arching decreases with the increase of pile spacing.

Value of the u_{ip}/u_p is below 2 in all of the cases when pile spacing (s/d) is equal to 2. Pile and soil deforms together and strong soil arching develops in close pile spacings. In addition, different unstable soil materials and lateral soil movement have relatively less effect on the development of soil arching in closely spaced piles. However, as pile spacing increases relative pile soil movement thereby soil arching gets more open to affect from other factors (Figure 5.10).

Increase in the stiffness properties of the unstable ground material has positive effect for the development of soil arching. As shown in Figure 5.10, more soil arching develops in dense sand comparing to loose silty sand for the same pile spacing and lateral soil movement values. This is expected because higher stiffness properties of ground material prevent soil from deforming too much between the piles.

Amount of lateral soil movement is also important for the development of soil arching. Higher soil movement causes middle soil to deform more and that increases relative pile soil displacement. Consequently, stronger soil arching develops for lower lateral soil movement values for the same pile spacing and unstable material properties.

Average soil force and maximum bending moment per pile in a group were plotted against pile spacing in Figure 5.11 and Figure 5.12. Increase in the stiffness properties of unstable ground material and amount of lateral soil movement cause to increase resultant pile force and bending moment values for the same pile spacing as clearly seen in the figures.

Maximum bending moment and shear force values developed in piles within a group also increases as pile spacing increases for the same unstable soil material and same amount of lateral soil movement in all cases. Simply, pile spacing increase cause pile forces to increase. However, amount of soil forces and moments gets constant after a critical pile spacing and further pile spacing increase does not affect the development of shear force and bending moment values (Figure 5.11 and Figure 5.12). Similar behavior is also observed in soil arching evaluation (Figure 5.10). After a critical pile spacing relative pile soil displacement ratio gets constant and further pile spacing increase does not create any significant effect on it. This indicates that group effect disappears and single pile behavior starts beyond a specific pile spacing.

For drained cohesionless materials, arching effect significantly decreases for higher pile spacings than s/d=6 for all cases as it can be seen in Figure 5.10, Figure 5.11 and Figure 5.12. Piles within a group start to behave like singular piles when pile spacing is around s/d=8. However, in the case of loose silty sand with high lateral soil movement, development of arching seems to be more problematic. Closer pile spacings should be preferred for loose soils having relatively high lateral soil movement profile.

Variation of average pile force and maximum bending moment values with different pile spacings were used for the evaluation of group action reduction. As pile spacing increases, forces exerted on the piles in group also increase until a critical pile spacing ratio (≈s/d=8). Forces are not significantly different from each other for pile spacings larger than s/d=8. In group reduction analyses, forces and bending moments were taken as single pile values for pile spacing ratio which is equal to s/d=20. Reduction values for each pile spacing were calculated accordingly by Equation 5.1 and Equation 5.2.

$$\%\, Group\ Reduction\ (Q) = \left(\frac{Q_{single\ pile} - Q}{Q_{single\ pile}}\right) * 100 \qquad 5.1$$

$$\%\, Group\ Reduction\ (M) = \left(\frac{M_{single\ pile} - M}{M_{single\ pile}}\right) * 100 \qquad 5.2$$

Where;

$Q_{single\ pile}$ = Average pile force exerted on a singular pile (for pile spacing s/d=20)

Q = Average pile force for related pile spacing ratio

$M_{single\ pile}$= Maximum bending moment exerted on a singular pile (for pile spacing s/d=20)

M = Maximum bending moment for related pile spacing ratio

Percent of group reduction values of different pile spacing variations for loose silty sand and dense sand are presented in Table 5.9. Group reduction percentages for all cases and reductions for both pile force and bending moment values are approximately consistent. It can be seen in the table that significant group reduction starts to develop for larger pile spacing ratios than s/d>6. As piles are closely spaced reduction percentages dramatically increase. In average, 8 % reduction for s/d=6, 18 % reduction for s/d=4 and 31 % reduction for s/d=2 were observed in pile forces within a group.

It can be concluded that there is an opposite relationship between soil arching and resultant pile forces caused by the moving soil. Decrease of pile spacing ratio (s/d) causes stronger soil arching but it also causes the development of group reduction in pile forces. Therefore, optimum pile spacing should be selected for an economical and effective design. In drained sandy materials, strong soil arching development can be observed for pile spacing ratios (s/d) between 2 and 4 (Figure 5.10). However, reduction (≈30 %) in forces when pile spacing is s/d=2 may significantly decrease group efficiency and also design could be uneconomical. Even though there is an 18 % reduction in pile forces for pile spacing ratio of s/d=4, sufficient soil arching is still sustained. Therefore, spacing ratio of s/d=4 is seem to be more optimum value for an effective pile design. However, sliding cases having very soft unstable soil materials or having excessive lateral soil movements should be specifically investigated by considering soil arching and group action reduction phenomena.

Findings in this thesis study about pile spacing have good agreement with the conclusions of other researchers as some of them were quoted in Table 2.3 (Chen 2001, Liang and Zeng 2002, Kahyaoğlu et al. 2009, Liang and Yamin 2009, Kourkoulis et al. 2011).

Table 5.9 Group reduction values according to the variation of pile spacings for loose silty sand and dense sand for lateral soil movements of u_x=5 cm and u_x=10 cm

Unstable soil type	**Lateral soil movement, u_x (cm)**	**Pile spacing (s/d)**	**u_{ip}/u_p**	**Average force per pile in group**		**Average maximum bending moment per pile in group**	
				Q_{max} (kN)	**Group reduction, (%)**	**M_{max} (kN.m)**	**Group reduction (%)**
Loose silty sand	5	2	1.36	176	**30**	367	**29**
		4	2.05	197	**21**	434	**16**
		6	2.41	226	**10**	496	**4**
		8	2.67	240	**4**	496	**4**
		10	2.69	250	**0**	513	**1**
		20	2.73	247	**0**	519	**0**
	10	2	1.72	187	**30**	391	**34**
		4	3.21	215	**20**	484	**18**
		6	3.91	240	**10**	559	**6**
		8	3.95	252	**6**	576	**3**
		10	4.17	262	**2**	579	**2**
		20	4.58	268	**0**	593	**0**
Dense sand	5	2	1.18	300	**19**	447	**32**
		4	1.57	330	**11**	550	**16**
		6	1.83	349	**6**	622	**5**
		8	1.90	363	**2**	629	**4**
		10	1.94	372	**0**	657	**0**
		20	2.04	372	**0**	657	**0**
	10	2	1.40	313	**28**	482	**44**
		4	2.23	336	**22**	646	**25**
		6	2.70	377	**13**	754	**12**
		8	2.95	407	**6**	778	**9**
		10	2.97	416	**4**	794	**7**
		20	2.99	432	**0**	857	**0**

CHAPTER 6

SUMMARY AND CONCLUSIONS

6.1 Summarized Points and Conclusions

Some of the important results and conclusions of this study are given below:

1) <u>Three dimensional finite element solution for laterally loaded passive piles: selection of the geometry/dimensions, boundary conditions and mesh size</u>

Three dimensional shear box models were used for the simulation of laterally loaded passive pile behavior. Proposed methodology provided more efficient use of calculation time in hundreds of analyses. In addition, number of variables and the effect of uncertain parameters such as slope angle, direction and amount of ground movement, interface properties were tried to be controlled with this way. Sliding of unstable layer was provided by using predefined displacements on the left side surface of the box model. Piles were embedded in a stationary layer and lateral loading of piles were sustained with this way.

Analyses results indicated that boundary sizes, surface fixities and mesh generation have significant effect on the variation of pile forces and moments. Therefore, boundaries should be large enough that no stress-strain distributions are affected from it. For this purpose, boundary sizes of the models were controlled for the minimum dimensions that deflections and forces are not affected or interrupted. Effect of mesh generation was also evaluated and three dimensional medium type of mesh generation was seen to provide sufficient accuracy for the scope of this study.

2) <u>Verification of the proposed shear box models with case studies</u>

Three case studies were analyzed to investigate calculation accuracy of three dimensional finite element solution with shear box models. Three full scale field experiments, two of them were reported by De Beer and Wallays (1972) and one of them by Esu and D'Elia (1974), were used for this purpose. Steel pipe pile and reinforced concrete pile were subjected to non-uniform lateral soil movements in drained sandy soil in De Beer and Wallays (1972) cases. On the other hand, uniform lateral soil movement of undrained cohesive clay was exerted to reinforced concrete pile in Esu and D'Elia (1974) case. Analyses results show satisfactory agreement with the measured field data in pile deflection, bending moment and shear forces of the reported cases. It was concluded that three dimensional finite element solution with PLAXIS 3D can accurately calculate the measured data in the field. Therefore it is a good tool to estimate passive pile behavior for different variations of pile materials, soil properties and lateral soil movement, provided that the properties of the soil are accurately represented and the soil movement is correctly inputted.

3) <u>Embedment depth of pile</u>

Parametric analyses were conducted to find required embedment depth of pile into a stationary layer. Most important factors affecting the embedment depth are unstable soil properties and strength ratio between unstable and stable soils. Therefore, analyses were carried out with the variation of these parameters. Single reinforced concrete piles were socketed into a stable layer in different lengths. Undrained soft, medium and stiff clay materials were considered as unstable soils.

According to the analyses results, there is a critical embedment depth providing sufficient resistance and pile end fixity condition (flexural bending rather than rigid body rotation). Beyond this critical embedment depth, pile forces (shears and moments) exerted by soil movement remains constant for longer embedment depths for the same amount of loading condition. Ranges of critical embedment depths were determined according to the strength ratio of stable soil to unstable soil alternatives for soft, medium and stiff clay type of unstable materials as shown in Table 6.1.

Table 6.1 Range of critical embedment depths for different unstable soil materials and strength ratio variation (H=unstable soil thickness)

Strength ratio, (SR) $\frac{c_{u(stable)}}{c_{u(unstable)}}$	**Unstable soil materials**		
	Soft clay	**Medium clay**	**Stiff clay**
SR=1	>1.5H	1.5H-1.0H	1.0H-0.5H
SR=3	1.0H-0.5H	1.0H-0.5H	0.5H-0.25H
SR=5	1.0H-0.5H	0.5H-0.25H	0.5H-0.25H

Some conclusions are made from the evaluation of bending moment, shear force and pile deflection distributions of different embedment depth alternatives:

- Increase in unstable soil properties cause increase in horizontal force exerted by soil for the same amount of lateral movement. However, strength ratio of stable soil to unstable soil ($SR = \frac{c_{u(stable)}}{c_{u(unstable)}}$) has more significant effect on the development of pile forces and also determination of pile embedment depth.

- Pile forces because of lateral soil movement increase as embedment depth increases until a certain critical depth. Beyond this, pile forces remain constant for longer pile embedment depths.
- As strength ratio of stable soil to unstable soil (SR) increases, critical embedment depth providing sufficient resistance for pile stability decreases for all soil types.

4) Pile spacing

Different pile spacing alternatives were analyzed with the variation of unstable soil properties and amount of lateral soil movement to evaluate the effect of pile spacing on passive pile response. Piles were embedded in a very stiff stationary layer with sufficient embedment depth.

Pile spacing evaluation was made according to two main considerations in pile design that are most affected from the spacing between piles. These are soil arching and group reduction. Degree of arching was measured from the ratio of u_{ip}/u_p; where, u_{ip} is interpile ground displacement (horizontal soil displacement in the middle, between the piles) and u_p is the displacement of the pile head. This method of analysis uses the consideration of relative pile soil displacements. Difference between pile and soil displacements was more clearly observed in sandy materials in 3D analyses. Therefore, drained analysis of cohesionless soil materials were used as unstable and stable soils. In addition, variation of average pile force and maximum bending moment values with different pile spacings were used for the evaluation of group action reduction.

Some conclusions are made from the results of analyses:

- Soil arching is most critical at the ground surface for free headed piles where maximum relative pile soil displacement occurs.
- Low values of u_{ip}/u_p indicates strong soil arching which means relative movement of soil between piles is low and the stability could be achived. On the other hand, higher values of u_{ip}/u_p indicates that soil between piles plastically flow and piles behave ineffectively in terms of slope stabilization.
- It can be concluded that amount of soil arching decreases with the increase of pile spacing.
- Increase in the stiffness properties of the unstable ground material has positive effect for the development of soil arching. Dense materials have more soil arching for the same pile spacing and same lateral soil movement distribution.

- Increase in the stiffness properties of unstable ground material and amount of lateral soil movement cause to increase resultant pile force and bending moment values for the same pile spacing.

- For drained sandy materials, arching effect significantly decreases for higher pile spacings than s/d=6 for all cases. Piles within a group start to behave like singular piles when pile spacing is approximately around s/d=8.

- Decrease of pile spacing ratio (s/d) causes stronger soil arching but it also causes the development of group reduction. There is an opposite relationship between soil arching and resultant pile forces caused by the moving soil. Therefore, optimum pile spacing should be selected for an economical and effective design.

- As piles are closely spaced reduction percentages dramatically increase. In average, 8 % reduction for s/d=6, 18 % reduction for s/d=4 and 31 % reduction for s/d=2 were observed in pile forces within a group.

- Pile spacing ratio of s/d=4 is seem to be an optimum value for pile design in aspect of soil arching and group action reduction for sandy materials.

It should be noted that elastic-perfectly plastic Mohr Coulomb failure criterion was used in all of the analyses in this study as the material constitutive model. Although it is well known that, the more advanced soil constitutive models can capture the nonlinear stress-strain behavior of soils more accurately, they also require significant number of material model parameters to be input. Therefore Mohr-Coulomb model is considered to be adequate for the content of this parametric study.

It should also be noted that in all of the analyses in this study pile heads are free. In real project of slope stabilization by piles, typically a pile cap can be used. Pile cap is considered not to provide any fixity at the pile head.

6.2 Future Work and Recommendations

1. Although there are studies that compare two dimensional and three dimensional solution differences, investigation in this area can be increased. Parameters that are most sensitive to the 2D-3D effect can be determined.

2. Effect of some other factors (such as variation of unstable soil thicknesses, rate of soil movement, ground water conditions) on pile embedment depth, pile spacing, soil arching and group action reduction can be investigated in further studies. Factors affecting the design of passive piles such as optimum location of piles in the slope, effect of pile rigidity, effect of different pile head fixity conditions and pile materials are some of the topics that need more investigation.

3. Landslide cases having very soft unstable soil materials or having excessive lateral soil movements should be specifically investigated by considering soil arching and group action reduction phenomena.

4. In order to see the effect on soil arching and group reduction an advanced soil constitutive model can be used and compared with Mohr Coulomb material model results.

5. Soil arching and group reduction phenomena should also be studied for undrained behavior of cohesive soils.

6. More laboratory or field cases measuring the movement of the soil before and after installation of the pile and movement of the pile, stresses on the pile should be performed. These studies should also try to quantify group reduction and soil arching by laboratory and field measurements. The laboratory and field measurements are invaluable resources to verify the accuracy of numerical methods.

REFERENCES

PLAXIS 3D Version 2010 (Computer Software), P.O. Box 572, 2600 AN Delft, The Netherlands

PLAXIS 3D Manuals 2010, P.O. Box 572, 2600 AN Delft, The Netherlands

Abraham, L. W., Lee, T.S., Sharma, S., Boyce, G.M. (1995). “Slope Stability and Stabilization Methods.” John Wiley & Sons, Inc.

Albataineh, N., (2006). “ Slope Stability Analysis using 2D and 3D methods.” M.S. Thesis, The Graduate Faculty of University of Akron, Ohio, U.S.A

Banerjee, P. K. and Davies, T. G. (1978). “The behaviour of axially and laterally loaded single piles embedded in non-homogeneous soils.” Geotechnique, Vol. 21, No. 3, pp. 309-326.

Begemann, H. K. S. PH. and E. H. De leeuw (1972). “ Horizontal earth pressures on foundation piles as a result of nearby soil fills.” Proc. 5th. European Conf. Soil. Mech. and Found. Eng. Madrid. Vol.1. pp.3-10

Bertini, T., Cugusi, F., D'Elia, B., & Rossi-Doria, M. (1984). “Climatic conditions and slow movements of colluvial covers in central Italy. ” *Proc. IV Int. Symp. on landslides, Toronto.* Toronto.

Brinch Hansen (1961). “Ultimate Resistance of Rigid Piles Against Transversal Forces.” Bulletin of the Danish Geotechnical Intstitude, No:12

Broms, B.B. (1964). “Lateral Resistance of Piles in Cohesionless Soil. ” Journal of Soil Mechanics and Foundations Division, Vol. 90(3), pp. 123-156.

Broms, B.B. (1964). “Lateral Resistance of Piles in Cohesive Soil.” Journal of Soil Mechanics and Foundations Division, Vol. 90 (2), pp. 237-263.

Bransby, M. F. and Springman, S. (1994). “ Selection of load transfer functions for passive lateral loading of pile groups. ” Computers and Geotechnics, Vol. 24, pp. 155-184

Cai, F. and Ugai, K. (2003). “Response of flexible piles under laterally linear movement of the sliding layer in landslides.” Canadian Geotechnical Journal, 2003, 40(1): 46-53

Chen, C. Y. (2001). “ Numerical Analysis of Slope Stabilization Concepts using piles.” PhD. Thesis in Civil Engineering, University of Southern California, California, U.S.A.

Chen, L.T. and Poulos, H.G. (1993). "Analysis of pile-soil interaction under lateral loading using infinite and finite elements." Computer and Geotechnics, Vol. 15, pp. 189-220.

Chen, L.T., and Poulos, H.G. (1997). "Piles subjected to lateral soil movements." Journal of Geotechnical and Geoenvironmental Engineering, Vol. 123, No. 9, pp. 802-811.

Chow, Y.K. (1996). "Analysis of Piles for Slope Stabilization," International Journal for Numerical and Analytical Methods in Geomechanics", Vol. 20,pp. 635-646.

Craig, R. F. (2004). Craig's Soil Mechanics. London: Spon Press.

Cruden, D. M., & Varnes, D. J. (1996). Landslide types and processes. *In: Turner, K.A., Schuster, R.L. (Eds.), Landslides :investigation and mitigation, 247,* 36-75.

Dağistani, I. (1992). "Model Study of Lateral Earth Pressure Distribution Developed on a Rigid Passive Pile." M.S. Thesis in Civil Engineering, Middle East Technical University, Ankara, Turkey.

Dao, T. P. T. (2011). "Validation of PLAXIS Embedded Piles for Lateral Loading." M.S. Thesis in Faculty of Civil Engineering and Geosciences, Section of Geo-Engineering, Delft University of Technology, Netherlands.

De Beer, E. (1977). "Piles subjected to static lateral loads." Proceedings, 9^{th} I.C.S.M.F.E., Specialty Session 10, Tokyo

De Beer, E. E., and Wallays, M. (1972). "Forces induced in piles by unsymmetrical surcharges on the soil around the piles." Proc., 5th Eur. Conf. on Soil Mech. and Found. Engrg., Vol. 1,325-332.

Ergun, M. U., (2000). "Stabilization of Landslides Using Piles." 8th International Symposium on Landslides-Landslides in Research, Theory and Practice, Vol 1 pp. 513-18, Thomas Telford Pub. Co.,London.

Esu, F., and D'Elia, B. (1974). "Interazione terreno-struttura in un palo sollecitato dauna frana tipo colata." Rivsita Italiana di Geotechica,Vol:8, pp:27-38

Finno, R J., Lawrence, S. A., Allawh, N. F., and Harahap, I. S. (1991). "Analysis of performance of pile groups adjacent to deep excavation." *J. Geotech. Engrg.,* ASCE, 117(6), 934-955.

Fukumoto, Y. (1975). "Experimental study on the behavior of lateral resistance of piles against a Landsliding." Journal of Landslides, Vol. 12(1), pp. 20-24.

Fukuoka, M. (1977). "The Effects of Horizontal Loads on Piles due to Landslides." Proceedings, 9th I.C.S.M.F.E., Specialty Session 10, Tokyo.

Gilson, G. J., Marcos, A. S., Murray F. (2008). “Three-dimensional analysis of the lodalen landslide.” GeoCongress 2008, New Orleans, LA, USA

Hassiotis, S., Chameau, J. L., and Gunaratne, M. (1997). “Design method for stabilization of slopes with piles.” J. Geotech. Geoenviron. Eng., 123(4), 314–323.

Hetenyi, M. (1946). “Beams on Elastic Foundation” The University of Michigan Press, Ann Arbor, 255 pp.

Ilyas,T., Leung, C., Chow, Y., Budi, S. (2004). “Centrifuge model study of laterally loaded pile groups in clay.” Journal of. Geotechnical and Geoenvironmental Engineering., ASCE, Vol. 130, No. 3, p. 274-283.

Ingold, T.S. (1977). “A field study of laterally loaded piles.” Proceedings, 9th I.C.S.M.F.E., Specialty Session 10, Tokyo.

Ito, T., Matsui, T. (1975). “Methods to estimate lateral force acting on stabilizing piles.” Soils and Foundations, Vol. 15, No.4, 43-59.

Ito, T., Matsui, T., and Hong, W. P. (1981). “Design method for stabilizing piles against landslide-one row of piles.” Soils and Foundations, March, Vol.21, No.1, pp. 21-37

Ito, T., Matsui, T., and Hong, W. P. (1982). “Extended design method for multi-row stabilizing piles against landslide.” Soils and Found., 22. 1-13.

Kahyaoğlu, M.R., Kayalar, A.Ş., İmançlı, G., Özden, G. (2009). “ Computational 3D finite element analyses of model passive piles.” Computational Materials Science (July 2009), Vol. 46 (1), pg. 193-202

Kalteziotis, N., Zervagiannis, F.R., Seve, G., and Berche, J.C. (1993). “Experimental study of landslide stabilization by large diameter piles.” Proc. Int. Symp. on Geotechnical Engineering of Hard Soils-Soft Rock, Vol.2, Athens.

Kelesoglu, M. K., and Cinicioglu, S.F. (2009). “Soil stiffness degradation in the design of passive piles.” 2nd International Conference on New Developments in Soil Mechanics and Geotechnical Engineering, 28-30 May 2009. Pp. 194-197. North Cyprus.

Kın, Y. (1993). “Effect of Penetration Depth and Soil Stiffness on Behavior of a Rigid Pile.” M.S. Thesis in Civil Engineering, Middle East Technical University, Ankara, Turkey.

Kourkoulis, R., Gelagoti, F., Anastasopoulos, I., and Gazetas, G. (2011). “Slope stabilizing piles and pile-groups: Parametric study and design insights.” J. Geotech. Geoenviron. Eng., 137(7), 663–678.

Kourkoulis, R., Gelagoti, F., Anastasopoulos, I., and Gazetas, G. (2012). “Hybrid method for analysis and design of slope stabilizing piles.” J. Geotech. Geoenviron. Eng., 138(1), 1–14.

Liang, R. Y., and Yamin, M. M. (2009). “Three-dimensional finite element study of arching behavior in slope/drilled shafts system.” Int. J. Numer. Anal. Methods Geomech., 34(11), 1157–1168

Liang, R. Y., and Zeng, S. (2002). “Numerical study of soil arching mechanism in drilled shafts for slope stabilization.” Soils Found., 42(2), 59.

Magueri, M., and Motta E. (1992). “Stresses on Piles Used to Stabilize Landslides,” Proceedings, 6th International Symposium on Landslides, pp.785-790, Christchurch, New Zeland.

Marche, R. and Chapuis, R. (1973). “Contrôle de la stabilité des remblais par la mesure des déplacements horizontaux.” Département de Génie Civil, Ecole Polytechnique de Montréal. Section de Mécanique des soils, juillet.

Mindlin, R.D. (1936). “Force at a point in the interior of a semi-infinite solid.” Physics, Vol.7, pp.195-202

Nakamura, H., (1984). “Design of rigid dowel piles for landslide control.” 4th International Symposium on Landslides, Vol.2, pp. 149-154.

Nalçakan, M.S. (1999). “Stabilization of Landslides by Piles in Cohesive Soils with Special Reference to Group Action,” PhD. Thesis in Civil Engineering, Middle East Technical University, Ankara, Turkey.

Oteo, C. S. (1977). “Horizontally loaded piles. Deformation influence” Proceedings, 9th I.C.S.M.F.E., Specialty Session 10, Tokyo.

Öztürk, Ş. (2009). “Distribution of Bending Moments in Laterally Loaded Passive Pile Groups a Model Study” Ms. Thesis in Civil Engineering, Middle East Technical University, Ankara, Turkey.

Pan, J. L., Goh, A. T. C., Wong, K. S. and Selby, A. R. (2002). “Three-dimensional analysis of single pile response to lateral soil movements.” Int. J. Numer. Anal. Meth. Geomech., 26: 747–758.

Poulos, H.G. (1973). “Analysis of Piles in Soil Undergoing Lateral Movement,” A.S.C.E, Journal of the SMFE, Vol. 99(5), pp. 391-406.

Poulos, H.G., and Davis, E.H. (1980). “Pile Foundation Analysis and Design,” John Wiley and Sons, Inc.

Poulos, H. G. (1999). “Design of slope stabilizing piles.” Slope stability engineering, J. C. Jiang, N. Yagi, and T. Yamagami, eds., Balkema, Rotterdam, Netherlands.

Reese, L. C., and Van Impe, W. F. (2001). “Single piles and pile groups under lateral loading.” Balkema, Rotterdam, Netherlands.

Reese, L. C., Wang, S. T., and Fouse, J. L. (1992). “Use of drilled shafts in stabilizing a slope.” Proc., Specialty Conf. on Stability and Performance of Slopes and Embankments II (GSP 31), Vol. 2, ASCE, New York, 1318–1332.

Rowe, K. and Poulos, H.G. (1979). “A method for predicting the effect of piles on Slope behavior.” University of Sydney, School of Civil Engineering, Research Report, R340.

Sommer, H. (1977). “Creeping slope in a stiff clay.” Proceedings, 9th I.C.S.M.F.E., Specialty Session 10, Tokyo.

Stewart, D.P. (1992). “Lateral loadings of pile bridge due to embankment construction.” PhD thesis, University of Western Australia.

Vesic, A.S. (1975). Principles of Pile Foundation Design. Soil Mechanics Series No.38. School of Engineering, Duke University, Durham, NC.

Viggiani, C. (1981). “Ultimate Lateral Loads on Piles Used to Stabilize Landslides.” Proceedings, 10th I.C.S.M.F.E., Vol. 3, pp. 555-560, Stockholm.

Wang, W. L., and Yen, B.C. (1974). “Soil arching in slopes.” Journal of the Geotechnical Engineering Division, Vol. 100, No. 1, pp. 61-78

Wei, W. B., (2008). “ Three Dimensional Slope Stability and Failure Mechanism.” PhD. Thesis in Department of Civil and Structural Engineering, Hong Kong Polytechnic University, Hong Kong

Yamagami, T., Suzuki, H. and Yamakawa, O., (1992). “A simplified estimation of the stabilizing effect of piles in a landslide slope applying the Janbu Method.” Proceedings, 6th International Symposium on Landslides, pp. 613-618. Christchurch, New Zealand.

APPENDIX A

ILLUSTRATIONS FOR CASE HISTORIES

A.1 De Beer and Wallays (1972)

Additional model illustrations of case studies of De Beer and Wallays (1972) and Esu and D'Elia (1974) were prepared from calculation results of Plaxis 3D analyses. Displacements and cartesian effective stresses in the direction of movement are presented from different views and cross sections.

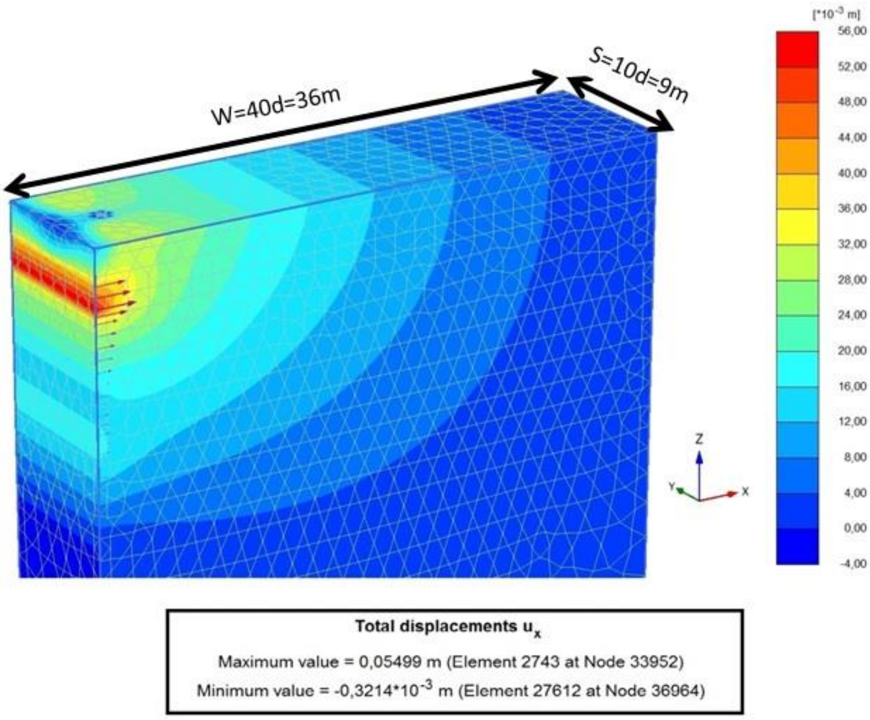

Figure A.1 Overall view for displacements in the direction of soil movement for steel pipe pile case

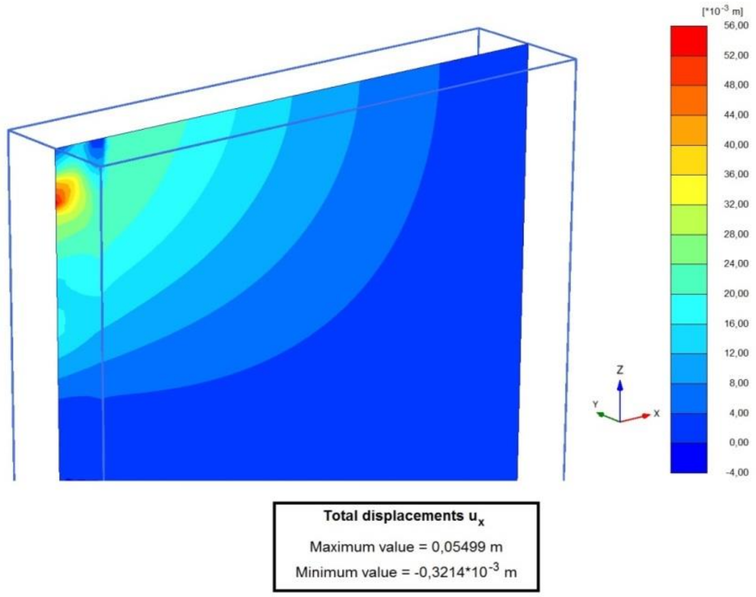

Figure A.2 Vertical cross section through model length passing by pile center for displacements in the direction of soil movement for steel pipe pile case

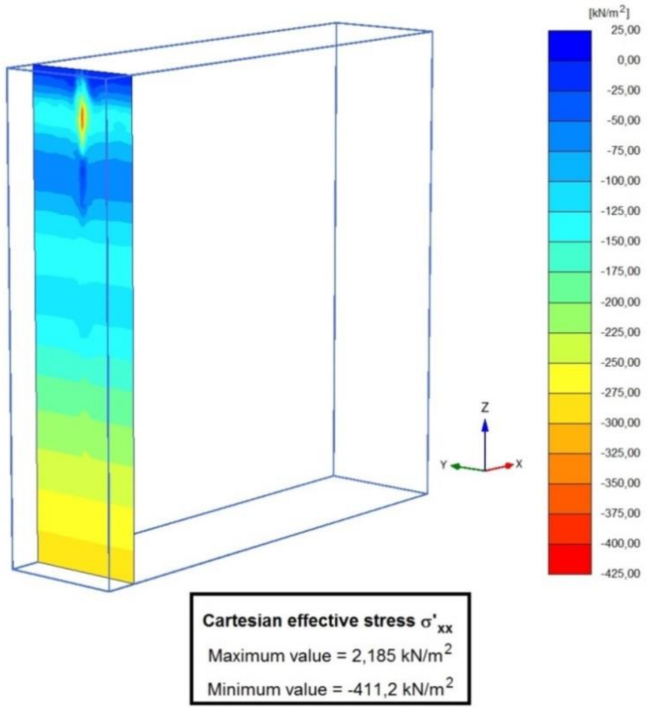

Figure A.3 Vertical cross section through model width passing by pile center for cartesian effective stresses in the direction of soil movement for steel pipe pile case

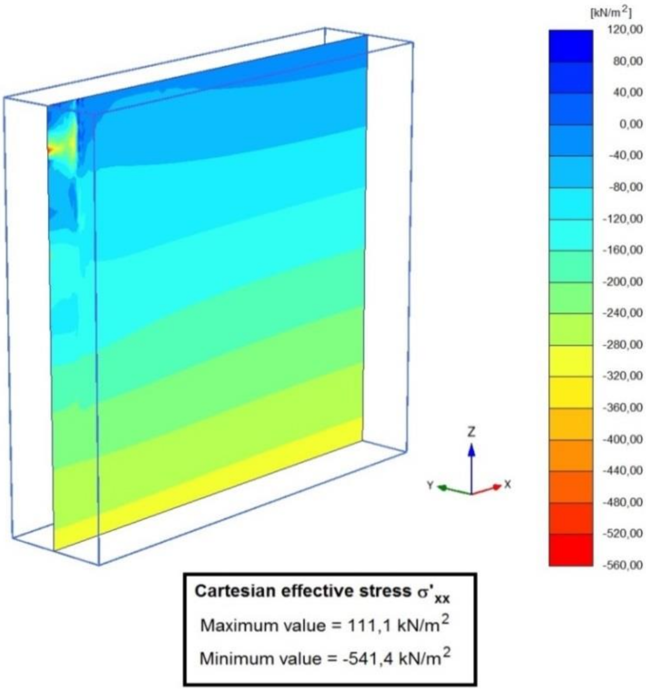

Figure A.4 Vertical cross section through model length passing by pile center for cartesian effective stresses in the direction of soil movement for steel pipe pile case

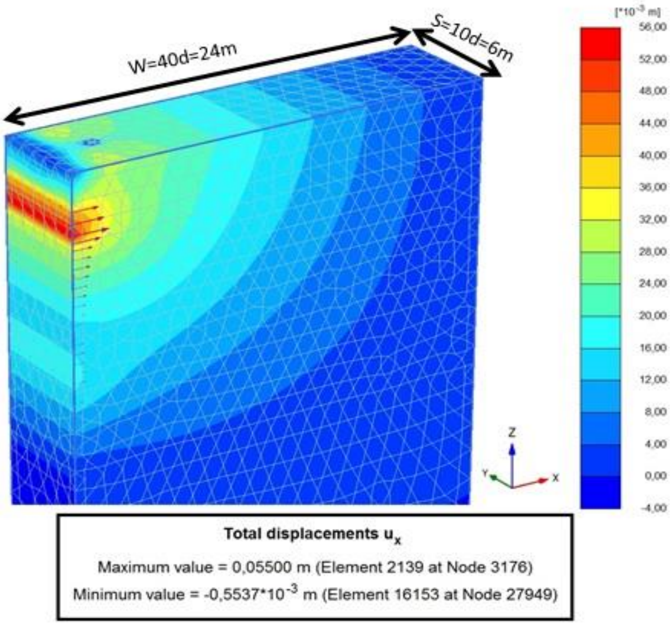

Figure A.5 Overall view for displacements in the direction of soil movement for reinforced concrete pile case

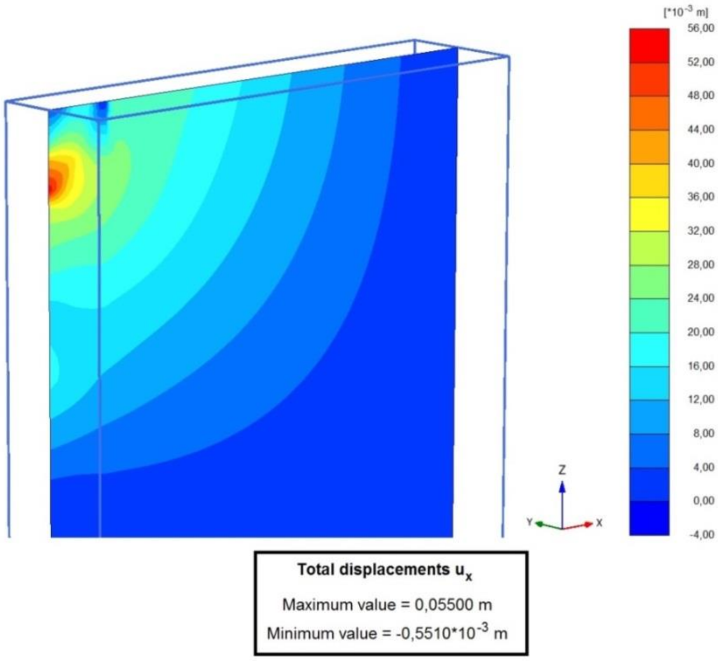

Figure A.6 Vertical cross section through model length passing by pile center for displacements in the direction of soil movement for reinforced concrete pile case

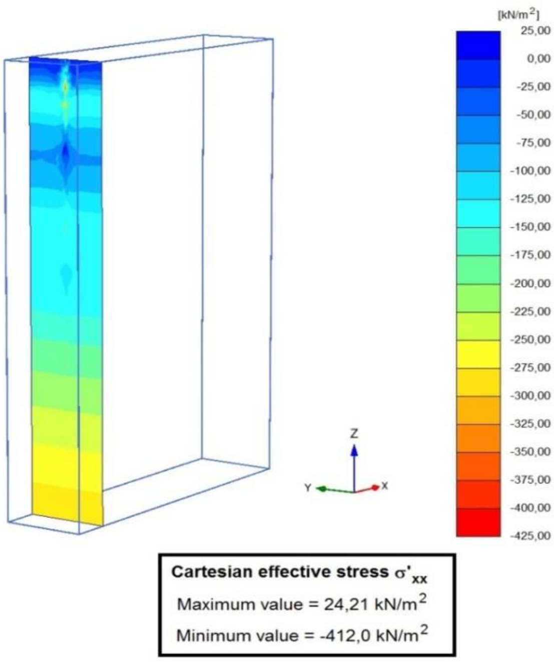

Figure A.7 Vertical cross section through model width passing by pile center for cartesian effective stresses in the direction of soil movement for reinforced concrete pile case

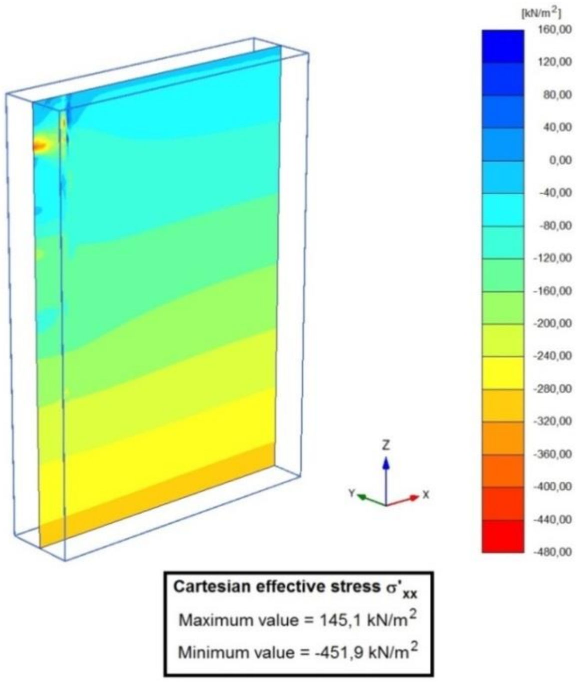

Figure A.8 Vertical cross section through model length passing by pile center for cartesian effective stresses in the direction of soil movement for reinforced concrete pile case

A.2 Esu and D’Elia (1974)

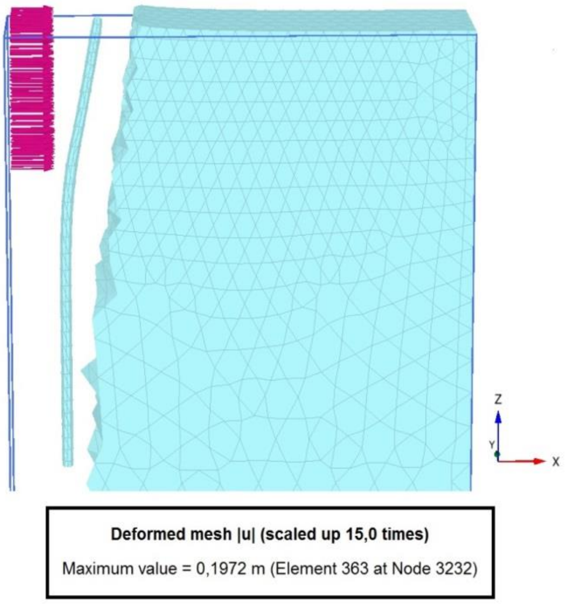

Figure A.9 Illustration of deformed model view for embedded pile and surrounding soil for Esu and D’Elia (1974) case study

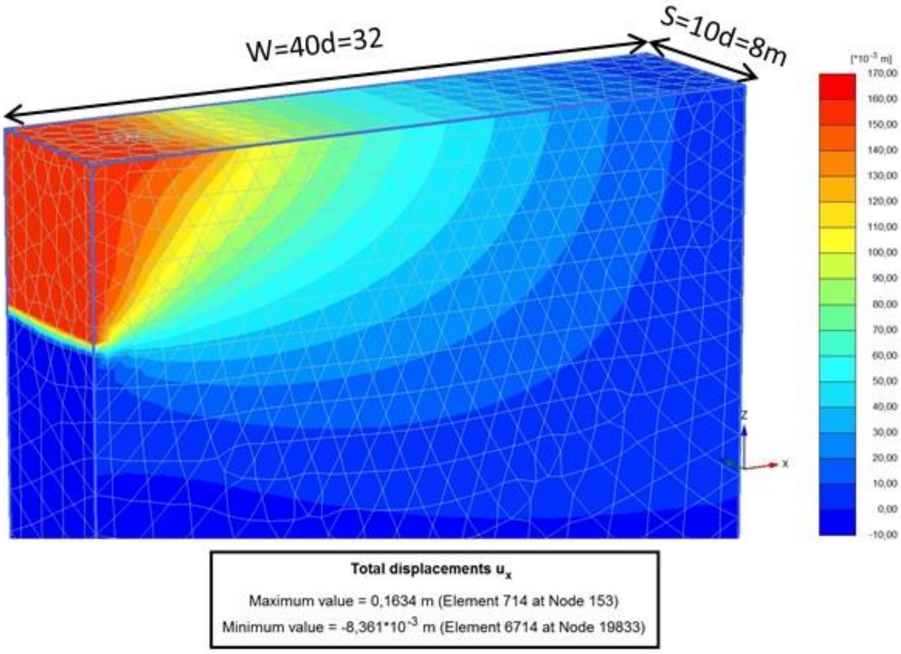

Figure A.10 Overall view for displacements in the direction of soil movement for Esu and D'Elia (1974) case study

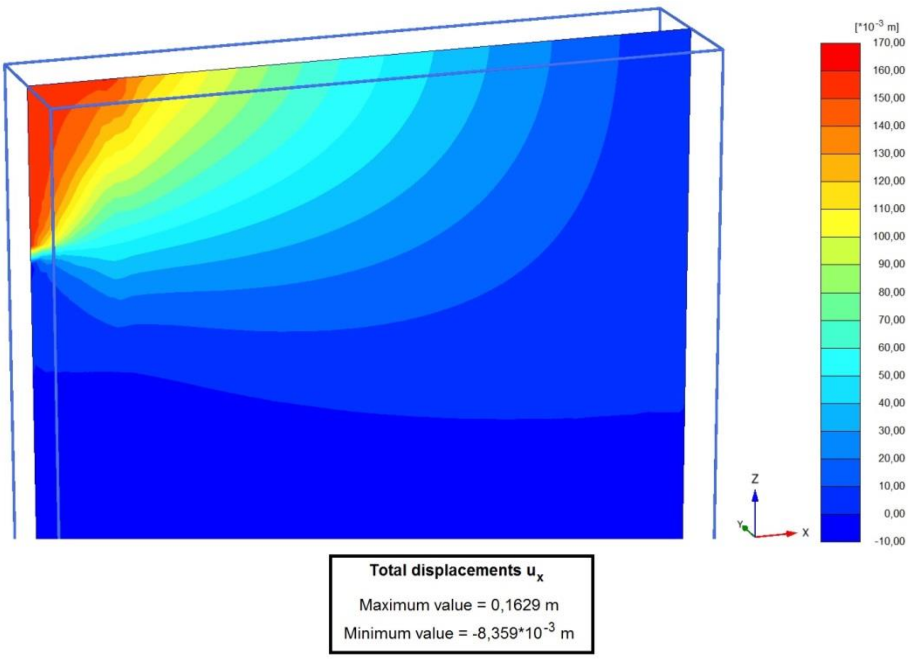

Figure A.11 Vertical cross section through model length passing by pile center for displacements in the direction of soil movement for Esu and D'Elia (1974) case study

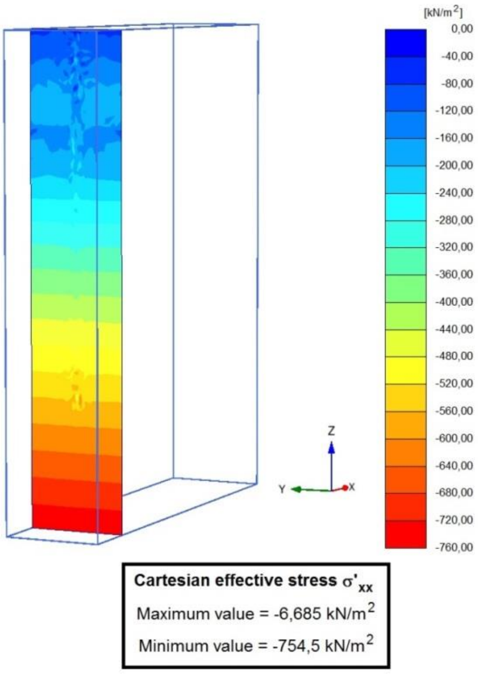

Figure A.12 Vertical cross section through model width passing by pile center for cartesian effective stresses in the direction of soil movement for Esu and D’Elia (1974) case study

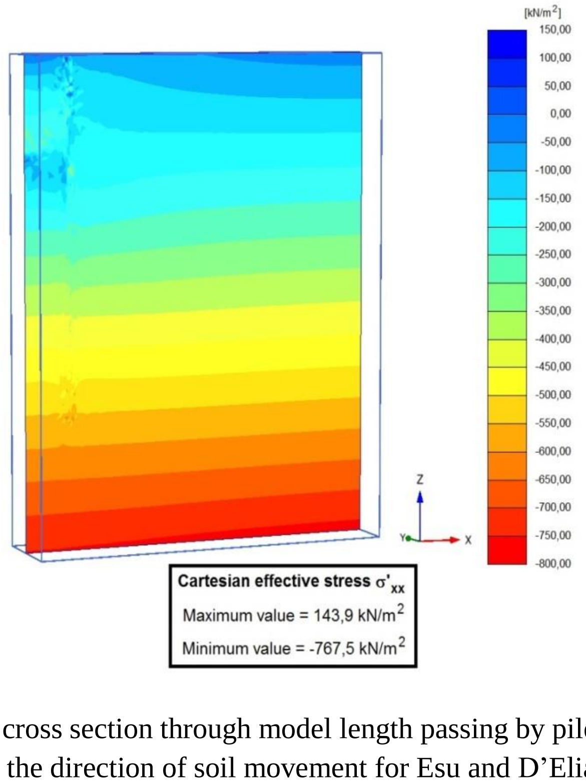

Figure A.13 Vertical cross section through model length passing by pile center for cartesian effective stresses in the direction of soil movement for Esu and D’Elia (1974) case study

APPENDIX B

ILLUSTRATIONS FOR PARAMETRIC ANALYSES

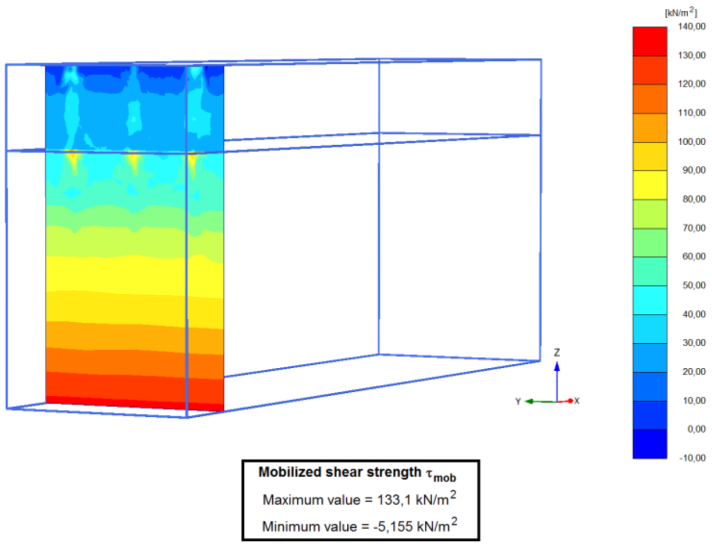

Figure B.1 Vertical cross section through model width passing just in front of piles for mobilized shear stresses (for loose sand, u_x=5cm, s/d=4)

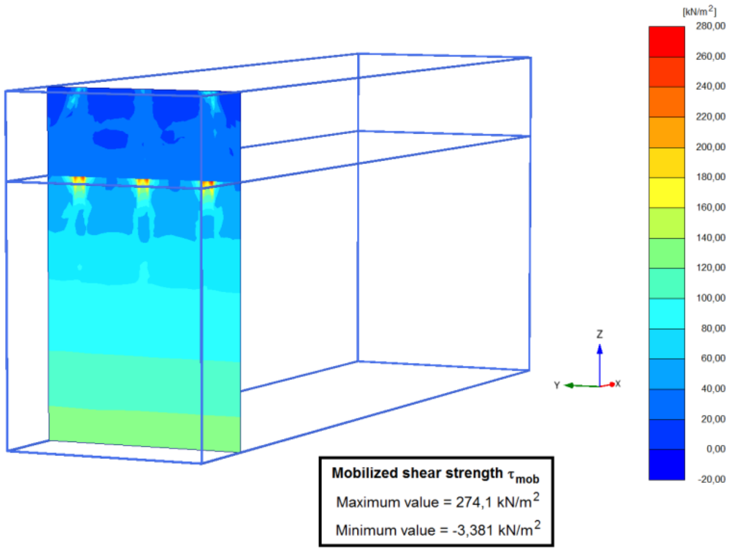

Figure B.2 Vertical cross section through model width passing by center of the piles for mobilized shear stresses (for loose sand, u_x=5cm, s/d=4)

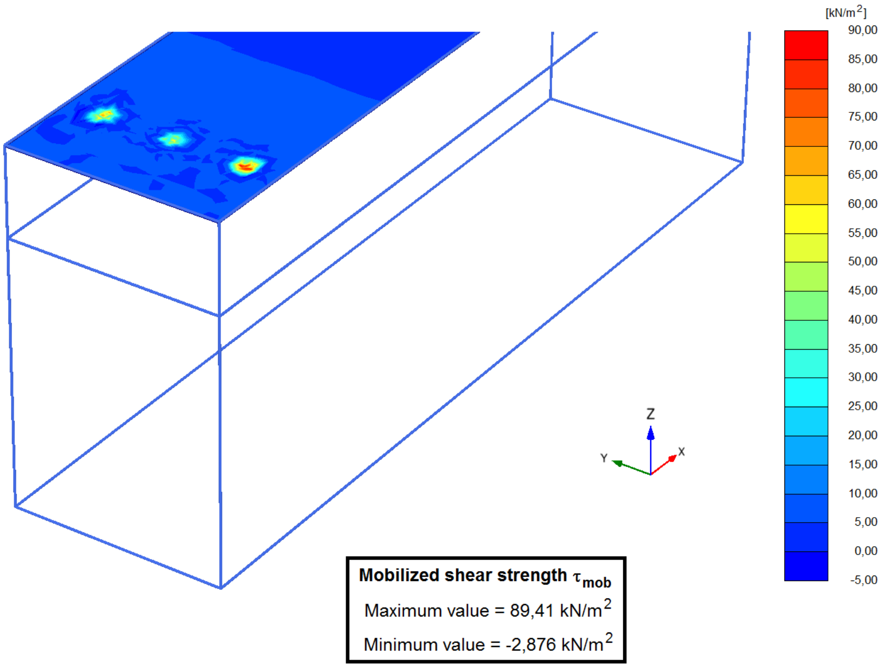

Figure B.3 Horizontal cross section in ground surface for mobilized shear stresses (for loose sand, u_x=5cm, s/d=4)

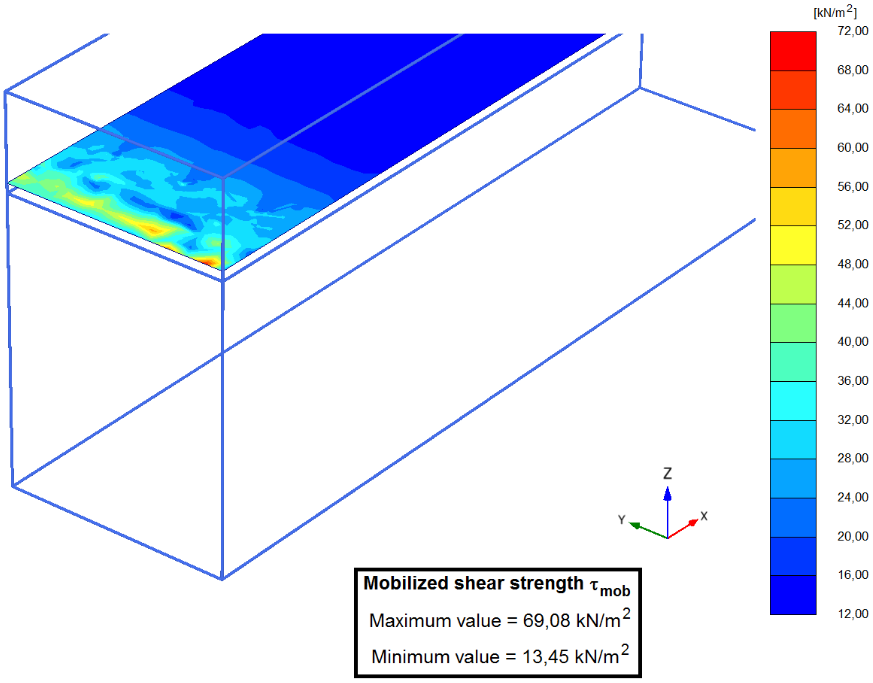

Figure B.4 Horizontal cross section just above the sliding surface for mobilized shear stresses (for loose sand, u_x=5cm, s/d=4)

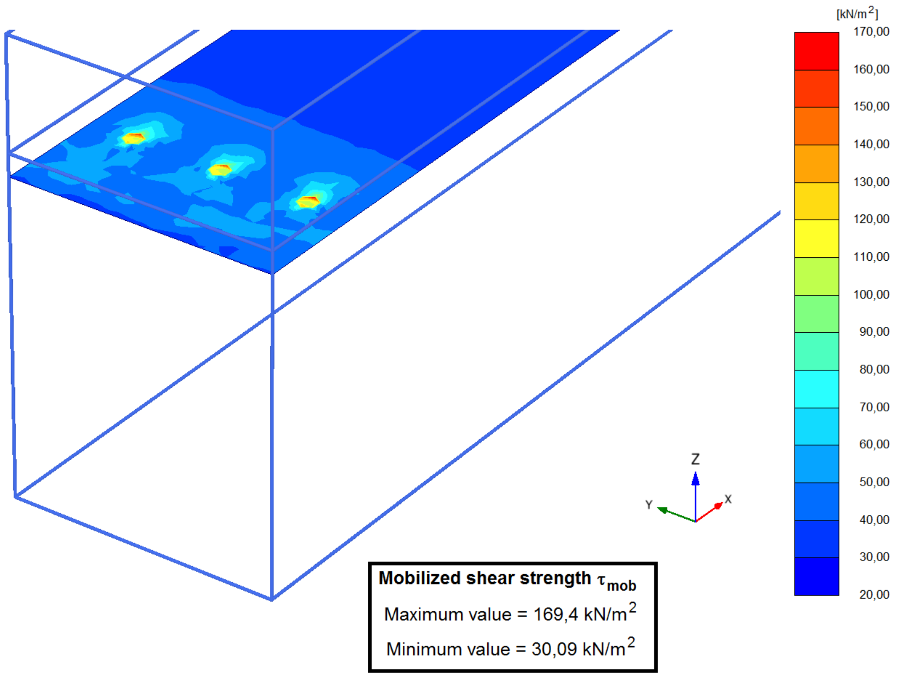

Figure B.5 Horizontal cross section just below the sliding surface for mobilized shear stresses (for loose sand, u_x=5cm, s/d=4)

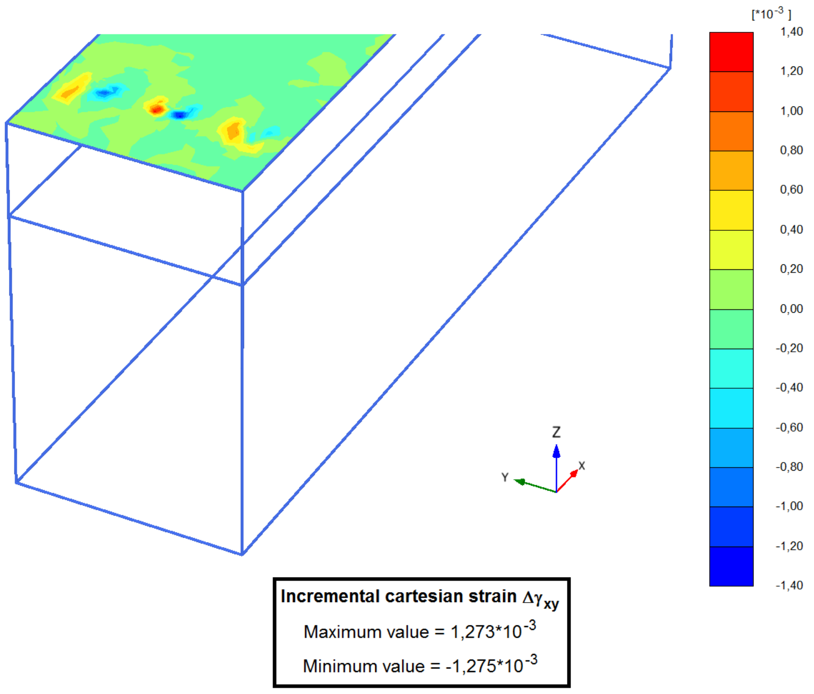

Figure B.6 Horizontal cross section in ground surface for incremental cartesian strain ($\Delta\gamma_{xy}$) (for loose sand, u_x=5cm, s/d=4)